



Spring 2000

A Systematic Study of the Correlations Between Meteorite Impacts and Soot Formation

Susanna L. Widicus '00
Illinois Wesleyan University

Follow this and additional works at: https://digitalcommons.iwu.edu/chem_honproj



Part of the [Chemistry Commons](#)

Recommended Citation

Widicus '00, Susanna L., "A Systematic Study of the Correlations Between Meteorite Impacts and Soot Formation" (2000). *Honors Projects*. 7.
https://digitalcommons.iwu.edu/chem_honproj/7

This Article is protected by copyright and/or related rights. It has been brought to you by Digital Commons @ IWU with permission from the rights-holder(s). You are free to use this material in any way that is permitted by the copyright and related rights legislation that applies to your use. For other uses you need to obtain permission from the rights-holder(s) directly, unless additional rights are indicated by a Creative Commons license in the record and/ or on the work itself. This material has been accepted for inclusion by faculty at Illinois Wesleyan University. For more information, please contact digitalcommons@iwu.edu.

©Copyright is owned by the author of this document.

A Systematic Study of the Correlations Between Meteorite Impacts and Soot Formation

Susanna L. Widicus

Chemistry Honors

Spring 2000

Committee:

Dr. Rebecca Roesner

Dr. Wendy Wolbach

Dr. Ram Mohan

Dr. Brian Hatcher

Table of Contents

Abstract	Page 2
Background	Pages 3 - 13
Theory	Pages 14 - 19
Procedure.....	Pages 20 - 34
Raw Data	Page 35, Appendices 5 - 9
Calculated Data	Pages 35 - 37, Appendices 10 - 14
Sample Calculations	Page 34, Appendix 15
Discussion	Pages 38 - 51
Ongoing and Future Work	Pages 52-56
Appendix 1. Heavy Liquid Density Separations	Page 57
Appendix 2. Correction Factor for Leaching of Glass Tubes	Page 58
Appendix 3. Correction for Significant Minerals in Post-Oxidation Residue	Pages 59 - 61
Appendix 4. Estimation of Soot Fraction Using SEM Data	Pages 62 - 63
Appendix 5. Raw Data for Berwind, Colorado	Page 64
Appendix 6. Raw Data for Madrid, Colorado	Pages 65 - 66
Appendix 7. Raw Data for DSDP Core 465-A	Pages 67 - 68
Appendix 8. Raw Data for the Sudbury Impact Structure, Canada	Pages 69 - 70
Appendix 9. Raw Data for the Gardnos Impact Structure, Norway	Pages 71 - 78
Appendix 10. Calculated Data for Berwind, Colorado.....	Pages 79 - 80
Appendix 11. Calculated Data for Madrid, Colorado	Pages 81 - 83
Appendix 12. Calculated Data for DSDP Core 465-A	Pages 84 - 87
Appendix 13. Calculated Data for the Sudbury Impact Structure, Canada	Pages 88 - 89
Appendix 14. Calculated Data for the Gardnos Impact Structure, Norway	Pages 90 - 101
Appendix 15. Sample Calculations	Pages 102 - 113
Acknowledgements	Page 114
References	Pages 115 - 116

Abstract:

A massive extinction of more than 50 percent of existing life forms on Earth occurred 65 million years (Ma) ago. This event is marked in the geological record by the Cretaceous-Tertiary (KT) boundary and corresponds to the Chicxulub meteorite impact in the Yucatan Peninsula. Since 1985, large quantities of reduced elemental carbon in the form of characteristic spheroidal clusters of soot have been found in twelve KT boundary sites from across the globe. Because of the wide geographic distribution of these sites, the data was interpreted to indicate that deposition of soot was a global phenomenon. The source of this global soot layer is suspected to be eolian (airfall) deposition of fine-grained particles resulting from widespread wildfires. A global soot concentration of 2.2 ± 0.7 mg/cm² has been estimated from these studies.

As a systematic study of the correlation between meteorite impact and soot formation, five sedimentary sequences of meteorite impact-related samples were analyzed for the presence of elemental carbon in the form of soot. Two KT boundary sedimentary sequences from the Berwind, Colorado, and Madrid, Colorado sites were analyzed as continuations of previous KT boundary studies. Soot concentrations of 3000 ± 0 parts per million (ppm) and 780 ± 90 ppm, respectively, were found in the KT boundary sediments of these sequences. These concentrations are similar to those found in previous KT boundary studies and further refine the KT boundary global soot concentration value.

Likewise, samples from Deep Sea Drilling Project (DSDP) Core 465-A were analyzed as a determination of the global nature of the soot layer. A soot concentration of 550 ± 750 ppm was found, again similar to those found in previous KT boundary studies. The mid-Pacific location of Core 465-A rules out the possibility of soot deposition from groundwater runoff and indicates that eolian transport is the most probable mechanism for soot deposition. Therefore, the presence of soot in boundary sediments in DSDP Core 465-A supports the theory that the KT boundary soot layer is global.

In addition, samples related to two other impact events of differing size and age were analyzed for evidence of wildfires. In the first study, samples were analyzed from the Sudbury, Ontario impact structure. This structure is the result of an impact similar in size to the Chicxulub event occurring 1850 Ma ago. These sediments were found to contain soot similar in concentrations to those found in KT boundary studies, ranging from 2300 ± 200 ppm soot to 3000 ± 300 ppm soot across the post-impact sedimentary sequence. The presence of soot in these sediments further strengthens the correlation between meteorite impact and soot formation.

In a second study, samples were analyzed from the Gardnos impact structure, Norway. This structure is the result of an impact at least one order of magnitude smaller than the Chicxulub event occurring between 900 and 400 Ma ago. No appreciable amounts of soot were found in sediments directly related to the impact event. The absence of soot in Gardnos samples suggests that an impact event of this size is below the impact threshold required for ignition of soot-producing wildfires.

Background:

A massive extinction of more than 50 percent of existing life forms on Earth occurred 65 million years (Ma) ago. This event is marked in the geological record by the Cretaceous-Tertiary (KT) boundary and corresponds to the impact of the approximately 10-kilometer Chicxulub meteorite in the Yucatan Peninsula, Mexico [1, 2]. The unusually dark appearance of the KT boundary at several sites led to analysis of carbonaceous residues from these sites. Since 1985, large quantities of reduced elemental carbon in the form of characteristic spheroidal clusters of soot have been found in twelve KT boundary sites from across the globe [3-5]. The global soot concentration estimated from these sites is $2.2 \pm 0.7 \text{ mg/cm}^2$, and the source of this global soot layer is suspected to be eolian deposition of fine-grained particles resulting from widespread wildfires [3, 4, 5, 6]. High concentrations of iridium, a rare earth element and common geochemical signature of extra terrestrial origin, have also been found in KT boundary sediments, indicating that the wildfires were most likely triggered by the Chicxulub impact event [1, 2]. Close correlation between soot and iridium concentrations across several well-preserved KT boundary sites indicates that the soot circled the globe, mixing with fine-grained impact ejecta prior to deposition [4, 5]. Because of the wide geographic distribution of the sites analyzed, these data were interpreted to indicate that deposition of soot was a global phenomenon.

Since the discovery of the correlation between soot and the KT boundary impact event, researchers have continued to analyze KT boundary samples for evidence of wildfires. For this study, two suites of samples from the North American Western Interior at 65 Ma were obtained for further KT boundary investigations. These sample suites,

from the Berwind, Colorado, and Madrid, Colorado, sites, are parts of a series of Western Interior KT boundary sample suites analyzed for the presence of soot. At 65 Ma, the Western Interior of the North American continent was a large inland swamp [8]. This anaerobic, reducing environment favored preservation of carbonaceous material. The data obtained for the soot concentration in these samples would therefore be useful as comparison to other KT boundary sites. The relative location of the Western Interior to the Chicxulub Impact Structure is shown in Figure 1. Detailed descriptions of the Berwind and Madrid samples are given in Tables 1 and 2.

Figure 1. Location of the North American Western Interior Sites

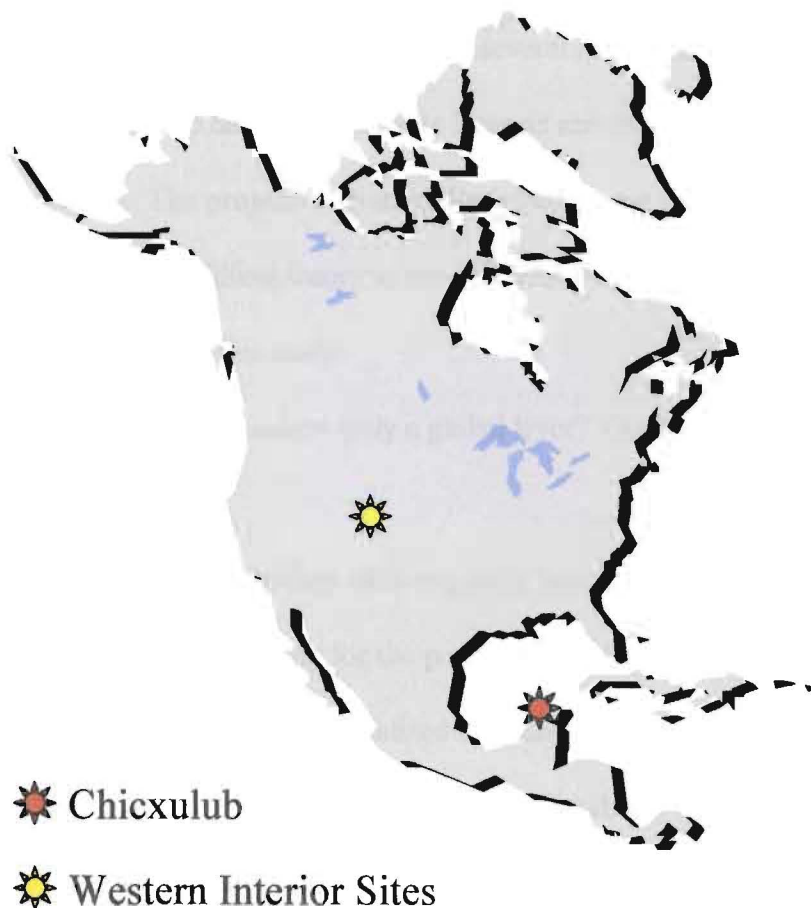


Table 1. Sample Descriptions for Berwind, Colorado.

Sample	Location (relative to KT Boundary)	Description
Berwind 1	10.0 cm above	Post-Impact Sediments
Berwind 2	20.0 cm above	Post-Impact Sediments
Berwind 3	5.0 cm below	Pre-Impact Sediments
Berwind 4	KT Boundary Layer	KT Boundary Layer

Table 2. Sample Descriptions for Madrid, Colorado.

Sample	Location (relative to KT Boundary)	Description
Madrid 1	8.0 cm above	Post-Impact Sediments
Madrid 2	1.0 - 3.0 cm above	Post-Impact Sediments
Madrid 3	KT Boundary Layer	KT Boundary Layer
Madrid 4	1.0 – 2.0 cm below	Pre-Impact Sediments
Madrid 5	8.0 cm below	Pre-Impact Sediments

In addition to further KT boundary studies, several questions have been raised about the general relationship between meteorite impacts and resultant combustion of carbonaceous materials. The projects stemming from these questions test the extension of the meteorite impact-related wildfires theory to non-KT boundary studies. Of these questions, the following are dealt with in this study:

1. Is the soot layer at the KT boundary truly a global layer? Could it be the result of runoff from localized fires?

Each of the twelve KT boundary sites originally analyzed was located on a continent or continental shelf, allowing for the possibility of deposition from stream and groundwater runoff. This possibility of localized soot deposition was not considered until recently. If soot deposition was concentrated on or near land, the KT soot layer might not be truly global. Therefore the amount of soot estimated to have been produced from

wildfires and thus the magnitude of the fires themselves might have been drastically overestimated. The only mechanism for soot deposition in the deep ocean is via air transport and eolian deposition [6]. Thus, the presence of significant quantities of soot in samples from the deep ocean would strongly support the existence of a global soot layer.

To test whether the soot layer is truly global, samples were obtained from five Pacific basin Deep Sea Drilling Project (DSDP) Cores containing sediments from 65 Ma ago. Four of these sets of core samples are from oxidizing environments and contain little to no carbonaceous residue. However, one of these sets of core samples, from Core 465-A, was deposited in a reducing environment, which favors preservation of the carbonaceous components. Because this core is far removed from a continent or continental shelf, evidence of soot found in these samples would confirm the global soot layer due to the necessity of eolian transport of soot to this location. The relative location of Core 456-A to other KT Boundary sites is shown in Figure 2. Detailed descriptions of the samples analyzed from this core are given in Table 3.

Figure 2. KT Boundary Sites Analyzed to Date



Table 3. Sample Descriptions for Deep Sea Drilling Project Core 465-A

Sample	Core Section	Sample Depth within Core Section (centimeters)	Description
Core 1	4	137-139	Pre-Impact Rock
Core 2	4	36-38	Pre-Impact Rock
Core 3	2	132-134	Post-Impact Sediments
Core 4	2	88-90	Post-Impact Sediments
Core 5	2	14-16	Post-Impact Sediments
Core 6	3	24-25	Post-Impact Sediments
Core 7	3	47-49	Post-Impact Sediments
Core 8	3	75-77	Post-Impact Sediments
Core 9	3	95-97	Post-Impact Sediments
Core 10	3	114-116	Post-Impact Sediments
Core 11	3	130-132	KT Boundary Layer

2. Is there a correlation between meteorite impact and soot formation found at other impact sites? If so, is there a correlation between the size of the impactor and the amount and distribution of soot generated?

The investigation of the correlation between meteorite impact and soot formation at non-KT boundary sites includes the systematic analysis of several suites of impact-related sedimentary sequences. Samples from two meteorite impact sites obtained for this purpose are included in this study. The first of these suites of samples was obtained from the Sudbury, Canada, impact structure. The Sudbury structure is the result of an impact similar in size to the Chicxulub event occurring 1850 Ma ago [9]. The presence of soot in Sudbury samples would strengthen the correlation between meteorite impact and soot formation. In addition, the distribution of soot due to the Sudbury impact event in comparison to that of the KT boundary event could offer clues to combustion rates and

sedimentation rates for impactors of this size. The location of the Sudbury impact structure is shown in Figure 3. Detailed descriptions of the samples analyzed from the Sudbury impact structure are given in Table 4.

Figure 3. Location of the Sudbury Impact Structure, Canada



Table 4. Sample Descriptions for the Sudbury Impact Structure, Canada.

Sample	Depth (meters)	Description
Sudbury 22	56.0	Crater Fill Sediments
Sudbury 20	59.0	Crater-Fill Sediments / Contact Unit
Sudbury 16	64.0	Contact Unit
Sudbury 12	68.5	Contact Unit
Sudbury 1	69.0	Contact Unit / Basement Rock
Sudbury 7	71.4	Basement Rock

The second of these suites of impact-related samples was obtained from the Gardnos impact structure, Norway. The Gardnos structure is the result of an impact at least one order of magnitude smaller than the Chicxulub event occurring between 900 and 400 Ma ago [10]. The presence of soot in Gardnos samples would likewise strengthen the correlation between meteorite impact and soot formation. In addition, because Gardnos is

a much smaller impact structure than the Chicxulub or Sudbury structures, its soot concentrations offer possible lower limits of impactor size linked to soot production. The location of the Gardnos impact structure is shown in Figures 4 and 5 [11]. Detailed descriptions of the samples analyzed from the Gardnos impact structure are given in Table 5. A schematic cross-section diagram of this structure showing the relative locations of these samples is shown in Figure 6.

Figure 4. Location of the Gardnos Impact Structure, Norway

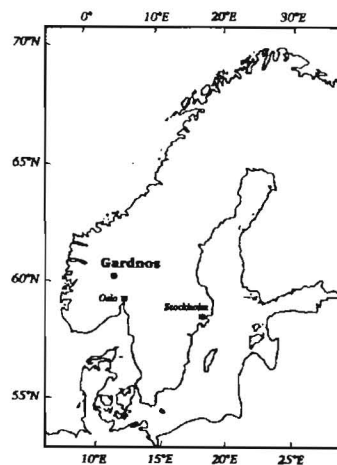


Figure 5. Structure of the Gardnos Impact Structure, Norway

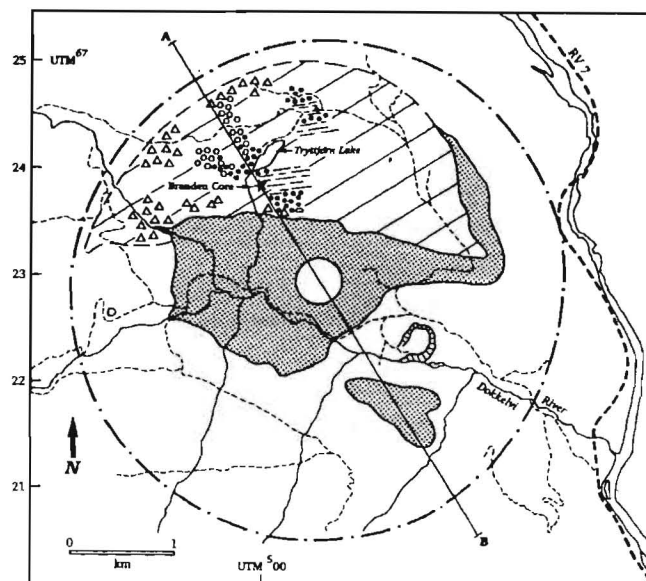


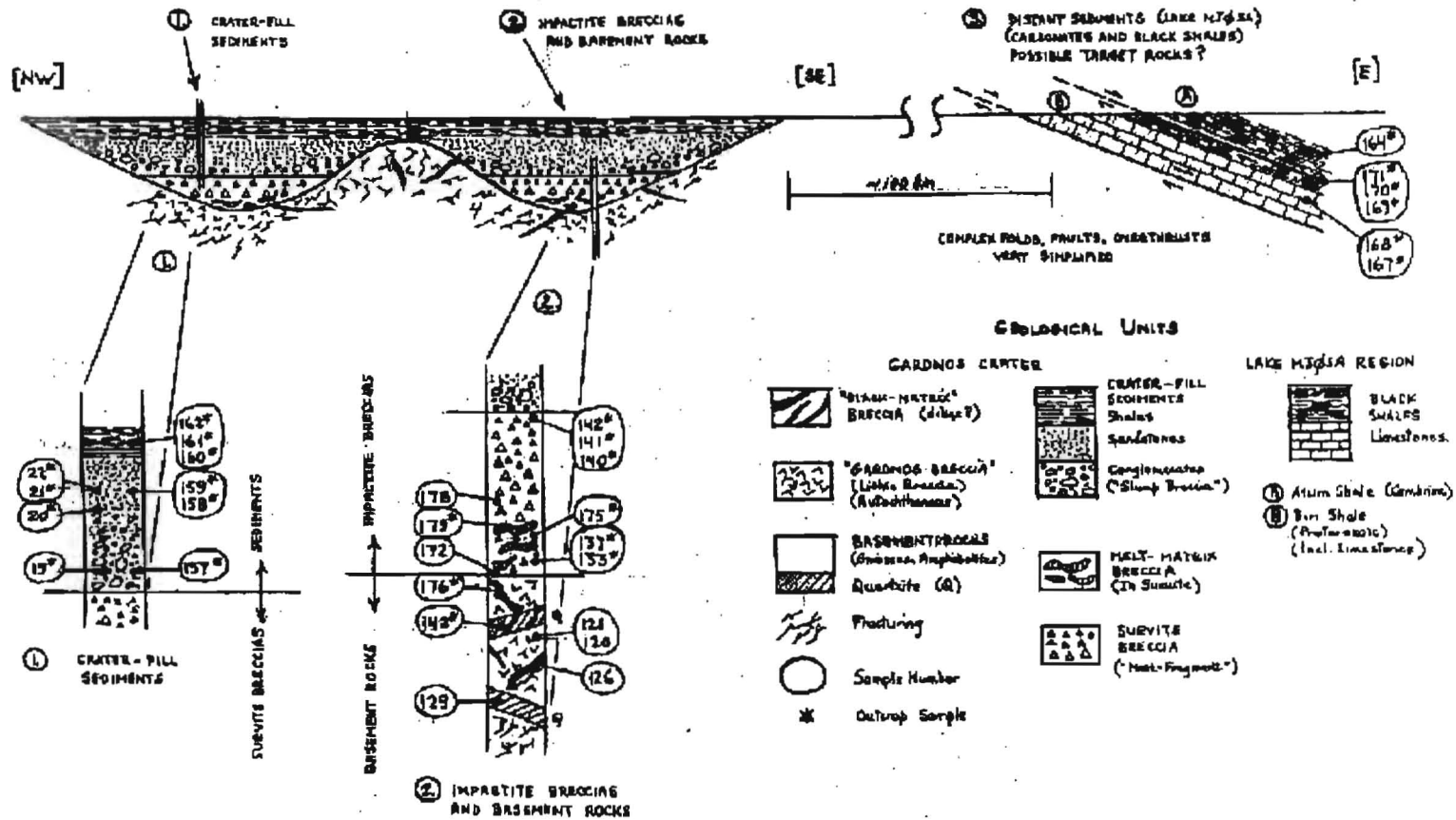
Table 5. Sample Descriptions for the Gardnos Impact Structure, Norway.

Sample	Description
Gardnos 19	Crater Fill Sediments
Gardnos 20	Crater Fill Sediments
Gardnos 21	Crater Fill Sediments
Gardnos 22	Crater Fill Sediments
Gardnos 157	Crater Fill Sediments
Gardnos 158	Crater Fill Sediments
Gardnos 159	Crater Fill Sediments
Gardnos 160a	Crater Fill Sediments
Gardnos 160b	Crater Fill Sediments
Gardnos 161a	Crater Fill Sediments
Gardnos 161b	Crater Fill Sediments
Gardnos 162a	Crater Fill Sediments
Gardnos 162b	Crater Fill Sediments
Gardnos 162c	Crater Fill Sediments
Gardnos 129	Basement Rocks
Gardnos 126	Basement Rocks
Gardnos 120	Basement Rocks
Gardnos 121	Basement Rocks
Gardnos 143	Basement Rocks
Gardnos 176	Basement Rocks
Gardnos 172	Contact Unit
Gardnos 179	Contact Unit
Gardnos 178	Contact Unit
Gardnos133	Contact Unit
Gardnos 137	Contact Unit
Gardnos 175	Contact Unit
Gardnos 137 B	Contact Unit
Gardnos 140	Contact Unit
Gardnos 141	Contact Unit
Gardnos 142	Contact Unit
Gardnos 164	Distant Sediments
Gardnos 171	Distant Sediments
Gardnos 170	Distant Sediments
Gardnos 169	Distant Sediments
Gardnos 168	Distant Sediments
Gardnos 167	Distant Sediments

Figure 6.

SCHEMATIC CROSS SECTION OF GARDNOS IMPACT STRUCTURE, NORWAY

SHOWING RELATIVE LOCATIONS OF ANALYZED SAMPLES



3. Under what conditions will a meteorite impact result in the formation of soot? Could soot formation be affected by local environmental conditions (i.e., type of biomass undergoing combustion, temperature of the fire, target rock composition, atmospheric oxygen concentration, and wetness of vegetation) at the time of the impact?

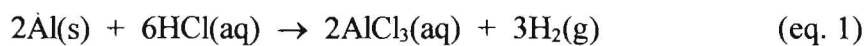
Sudbury is a prime candidate for the study of localized environmental effects on the production of soot by meteorite impact events because it is similar in size to the Chicxulub impact event. If soot is present in Sudbury samples, its size, concentration, and distribution can be directly compared to KT boundary values. Conclusions can then be drawn about the relationship between environmental effects and soot production based on the known similarities and differences between the Sudbury and Chicxulub events. Since the Sudbury impact occurred before significant vegetation on Earth, the presence of soot in these samples would also raise questions about carbonaceous fuel sources for soot formation in conjunction with impact events. The presence of soot in Sudbury impact samples would indicate the ignition of carbonaceous materials in either the impactor or the target rock.

In addition to the further implications of Sudbury results, Gardnos soot concentrations would offer possible insight into the mechanisms of meteorite impact and resultant soot formation. Because of its small size relative to the Chicxulub and Sudbury impact events, a wildfire triggered by the Gardnos impact event would likely be much different in nature (i.e. temperature and duration) than those triggered by the other impacts. Gardnos soot found to be similar in size and distribution to that of characteristic KT boundary soot would indicate that soot formation is independent of environmental conditions.

These five sites -- Berwind, Colorado; Madrid, Colorado; DSDP Core 465-A (North Central Pacific); Sudbury, Canada; and Gardnos, Norway -- offer valuable insight into the relationship between meteorite impact and soot formation. This study analyzes the soot concentration profiles found at each of these sites. From these data, relationships both among these sites and between these sites and previous KT boundary investigations are formulated in an attempt to answer some, if not all, of the questions raised above. These relationships will form the foundations for future studies into the correlations between meteorite impact and soot formation.

Theory:

Due to the similarities in bulk sample compositions (mainly carbonates, silicates, and chemically reduced carbon), it was assumed that techniques for the separation and identification of elemental carbon from sedimentary rocks used to isolate carbonaceous residues in the KT boundary samples [12] could be applied to the samples in each of the five studies. Samples are first crushed to increase surface area and hence the rate of chemical demineralization. To avoid contamination from the laboratory setting during preparation for demineralization, samples are wrapped in clean aluminum foil before being crushed. Although small amounts of aluminum are introduced into the sample during this process, this contamination is eliminated during the demineralization process by reaction of the aluminum with acid:



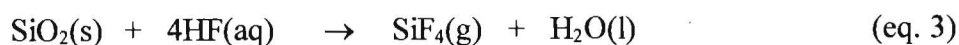
Sample mass needs to be monitored during demineralization. To achieve accuracy, weighing is repeated until masses have stabilized to the fifth decimal place (to 0.01 mg). Repeated weighing of original rock samples for previous studies have shown that a standard error of 0.00009 grams can be assigned to the masses obtained during this weighing process [13]. Only one weighing is required before demineralization because this error is negligible relative to the large sample mass (approximately 2.0 grams). For all other weighing processes, standard deviations for repeated weighings are calculated and assigned as errors. Standard analytical error propagation techniques are used for subsequent calculations.

For the process of demineralization, hydrochloric acid, HCl, readily reacts with carbonate, CO_3^{2-} , from limestone and dolostone (CaCO_3 and MgCO_3 , respectively),

producing carbon dioxide and water:



Silicates in the residue, SiO_4^{4-} , are destroyed with hydrofluoric acid, HF, which attacks the Si-O bonds in a highly exothermic reaction:



Addition of HF to the residue in the presence of calcium or magnesium ions, however, causes the precipitation of calcium or magnesium fluoride (CaF_2 and MgF_2 , respectively), which would contaminate the residue:



To prevent this precipitation, the residues are copiously rinsed with distilled water to minimize Ca^{2+} and Mg^{2+} concentrations in the supernatants after the HCl treatment.

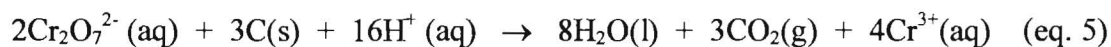
Supernatants are tested with small amounts of HF for precipitation of fluorides. If no precipitation occurs, the residues are considered to be free of Ca^{2+} and Mg^{2+} and are then treated with HF.

Complete demineralization is very difficult because of small amounts of relatively inert minerals such as TiO_2 and the slow reactivity of stable silicates such as quartz. A small fraction of acid-resistant minerals, less than 5 percent of the sample by mass, will not add significant error to the quantification of the carbonaceous residues (the methodology of this quantification has a larger built-in error), and therefore is generally ignored.

Residues remaining following demineralization are primarily carbonaceous and are dark brown or black in color. Since silicates are tan or white, visual examination for absence of minerals can be used to determine when the samples are adequately demineralized. If significant quantities of minerals persist ($> 5\%$ by mass), heavy liquid density separations

can be utilized for removal of these minerals. A detailed description of these separations is given in Appendix 1.

Once demineralization is complete, only carbonaceous residues, including organic carbon, kerogen (complex, fossilized organic matter which has undergone some diagenesis), and elemental carbon theoretically remain in the sample. To separate organic material from elemental carbon (the component of primary interest, since it includes soot), residues are oxidized with $\text{Na}_2\text{Cr}_2\text{O}_7$ in H_2SO_4 at 50 °C, which preferentially destroys organic carbon by converting it to CO_2 :



Reaction progress can be monitored through observation of supernatant color. The $\text{Na}_2\text{Cr}_2\text{O}_7/\text{H}_2\text{SO}_4$ solution is bright orange, while Cr^{3+} is dark green in solution. The $\text{Na}_2\text{Cr}_2\text{O}_7/\text{H}_2\text{SO}_4$ solution is replaced upon visual indication of a color change.

Different forms of carbon oxidize at different rates. The oxidation rate of elemental carbon is much slower [half-life ($t_{1/2}$) > 600 hr] than that of the most resistant kerogen ($t_{1/2}$ < 180 hr) at a constant temperature of 50 °C [12]. Under controlled conditions of a constant temperature of 50 °C and a duration of 600 hours, most organic carbon and kerogen can be destroyed while destruction of elemental carbon is minimized [12]. Approximately half of the soot carbon is oxidized during this process [12]. A division factor of 0.48 is applied to the calculated soot mass as a correction for this loss, and an error of 0.05 is assigned to this correction factor [12]. This correction is as follows:

$$\text{Soot Mass} = (\text{Calculated Soot Mass}) / (0.48 \pm 0.05) \quad (\text{eq. 6})$$

Some glass tubes used during the oxidation process can be leached by the $\text{Na}_2\text{Cr}_2\text{O}_7/\text{H}_2\text{SO}_4$ solution, resulting in negative values for small post-oxidation carbonaceous residue masses. Tubes with manufacturer markings and labeling are most susceptible to this process. The labeling is often removed during the etching process as a result of the elevated temperatures and the effects of the acidic solution. Because visible residue is often present in several samples having these negative values, a correction factor can be applied to all samples in tubes that undergo this leaching. This factor has been determined through examination of the DSDP Core samples [13]. A correction of 0.0048 g is applied, and a maximum error of ten percent is assumed. A detailed explanation of this correction is given in Appendix 2.

Characterization of soot and non-soot portions of the elemental carbonaceous residue is performed using scanning electron microscopy (SEM) imaging. Man-made soot or carbon black has characteristic spheroidal morphology at high magnification, resembling grape bunches [12]. This same morphology is found in KT boundary soot [3]. Other forms of coarse carbon such as coal and charcoal are larger, platy particles, sometimes retaining the imprint of cell walls. This coarse carbon often co-exists with but is easily distinguishable from soot using SEM imaging. A schematic summary of the soot isolation process is given in Figure 7. An SEM micrograph showing classic soot morphology is given in Figure 8.

Figure 7. Isolation of Elemental Carbon from Sediments

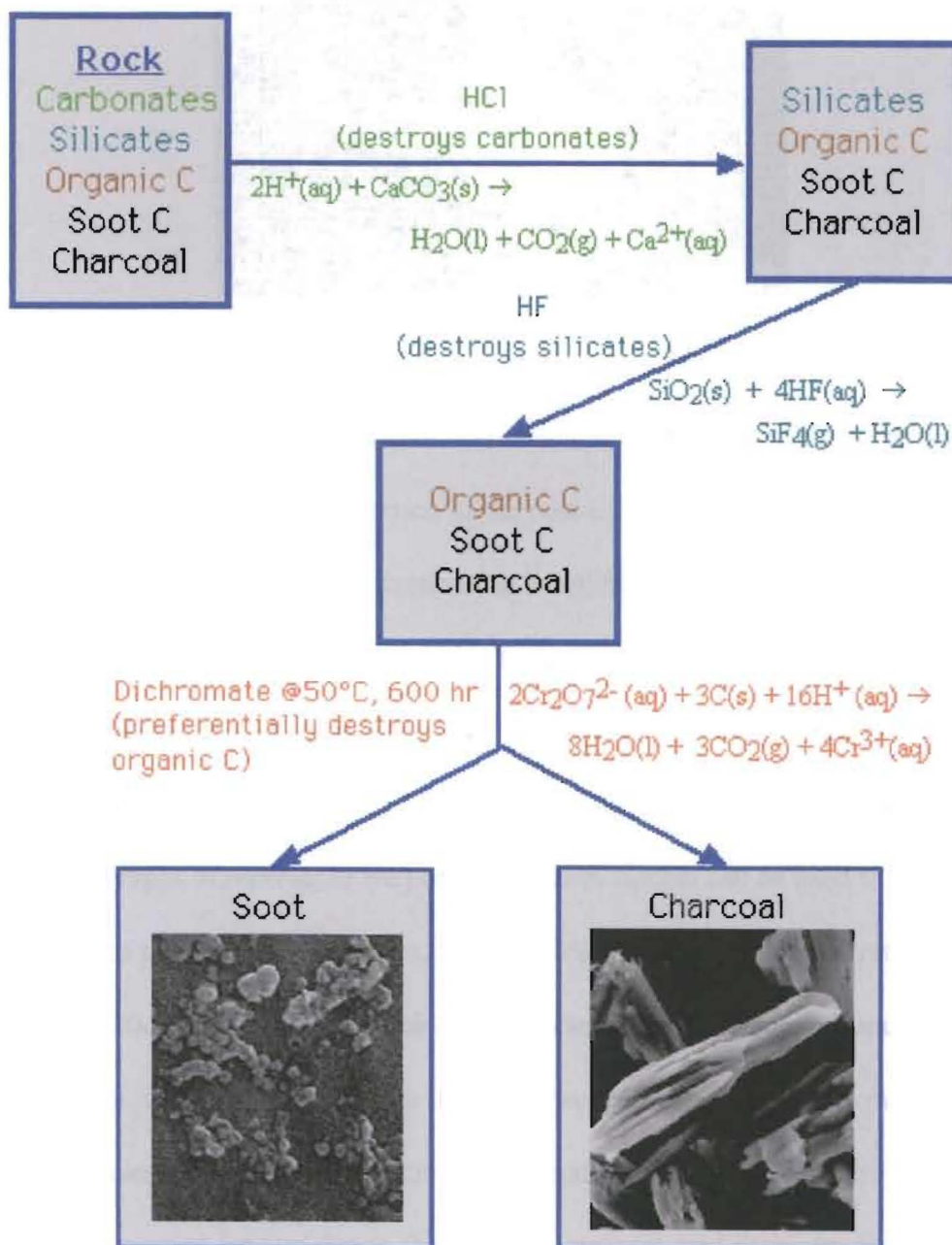
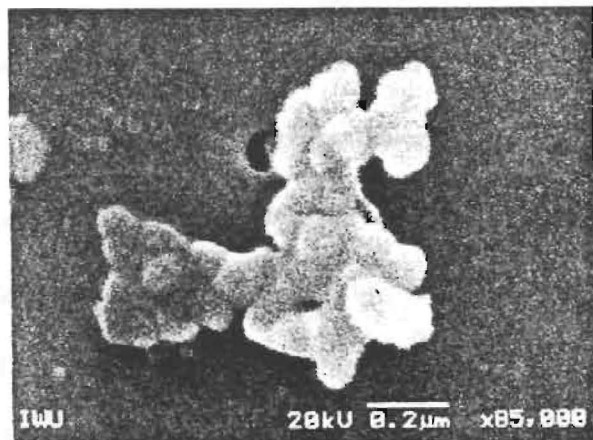


Figure 8. SEM Micrograph of Characteristic Soot Particle



In some cases, persistent minerals that were considered negligible in the pre-oxidation sample are a significant portion of the post-oxidation residue. The methods of visual estimation and SEM characterization can be utilized to determine the percent by volume carbon in the post-oxidation residue. Component densities can then be used to convert this value to percent by mass carbon. Post-oxidation residue weights are adjusted accordingly. A detailed explanation of these conversions is given in Appendix 3.

Micrographs of representative portions of each sample can be used to quantify ratios of soot to non-soot particle areas, which are directly proportional to ratios of soot to non-soot particle masses. By assuming all particles to be spherical in shape and having uniform density, the area ratio raised to the 1.5 power gives the volumetric ratio of soot to non-soot particles. This volumetric ratio is then used to calculate soot mass. The soot mass is then corrected for loss due to the oxidation process, and concentration of soot and non-soot components are calculated. A detailed explanation and derivation of these conversion factors is given in Appendix 4.

Procedure:

The following experimental procedure was used for the Berwind samples:

The samples were individually wrapped in clean aluminum foil (Diamond brand) and crushed with a geological hammer. A crushed, weighed portion (1.4 to 2.9 grams weighed on a Mettler AT261 Delta Range balance) of each sample was placed in a pre-labeled polystyrene graduated conical centrifuge tube (15 mL Fisherbrand). Excess solution of 9.0 M HCl (Fisher Scientific reagent grade) was introduced dropwise. The tubes were covered with parafilm and the samples were mixed thoroughly. The samples remained under acid for 24 hours. They were then centrifuged (International IEC Size 2, Model K Centrifuge) and supernatants were decanted with transfer pipets (polyethylene diSPo plastic). The samples were rinsed thoroughly with distilled water, centrifuged, and supernatants were decanted. This rinsing process was repeated three additional times.

After the third rinse, the supernatants were tested with two drops of an aqueous solution of 15.0 M HF and 1.0 M HCl (Fisher Scientific reagent grades). The supernatants of Berwind 4 formed precipitates during this process. No precipitate formation was observed in the other samples. The rinsing process was repeated once for Berwind 4, and the supernatants were tested with the HF/HCl solution. No precipitates formed. Excess HF/HCl solution was then added dropwise to each sample, each tube was covered with parafilm, and the samples were thoroughly mixed. The samples remained under acid for three days. Subsequent treatments with excess HCl for two days and then HF/HCl for five days were carried out. These subsequent acid treatments were repeated two additional times. Samples were copiously rinsed with distilled water after each acid treatment.

Samples were then treated with excess concentrated (12.0 M Fisher Scientific reagent grade) HCl and heated in a 50 ± 5 °C distilled water bath for six days. Samples were then cooled, rinsed twice with distilled water, and treated with excess HF/HCl solution for 13 days. Samples were treated with concentrated HCl and heated in a 50 ± 5 °C distilled water bath for 24 hours, cooled, and rinsed twice with distilled water. Samples were then treated with concentrated HF (30.0 M Fisher Scientific reagent grade) and heated in a 50 ± 5 °C distilled water bath for four days. Samples were cooled, rinsed twice with distilled water, treated with concentrated HCl, and heated in a 50 ± 5 °C distilled water bath for 24 hours. Samples were then cooled, rinsed twice with distilled water, and treated with the HF/HCl solution for 35 days. Samples were then rinsed twice with distilled water and treated with 9 M HCl for 24 hours.

Due to the chemical resistance of minerals to the acid treatments, heavy liquid density separation with dibromomethane (CH_2Br_2 , Aldrich Brand, 98%) was performed on Berwind 3. The detailed procedure for heavy liquid density separation is given in Appendix 1. Each sample was then transferred to a clean Pyrex beaker and treated with excess acetone (Aldrich Brand, 98%) for removal of excess dibromomethane. Samples were then transferred to clean, labeled polystyrene centrifuge tubes, copiously rinsed with distilled water, and treated with excess 9 M HCl for 24 hours.

The polystyrene centrifuge tube containing Berwind 3 cracked during centrifugation, contaminating a large portion of this sample. The above demineralization procedures (excluding the dibromomethane density separation) were repeated on another representative portion of this sample.

Heavy liquid density separations with a CsCl solution of density 1.6 grams/milliliter were performed on each sample (Appendix 1). It was determined by SEM analysis that complete separation of minerals from Berwind 3 was not achieved during this procedure. This process was repeated with a CsCl solution of density 1.9 grams/milliliter, and the polystyrene centrifuge tube again cracked during centrifugation. Demineralization and density separations were again repeated for Berwind 3.

It was determined through visual examination that all of the samples were sufficiently demineralized. The samples were centrifuged, supernatants were decanted, and the samples were rinsed with distilled water. The samples were then transferred to clean, labeled, weighed, disposable glass centrifuge tubes (10.0 mL Kimble Brand), centrifuged, and the supernatants were decanted. The tubes were covered with aluminum foil, and the samples were dried in an oven (Fisher Scientific Isotemp 500 Series) at 110 °C for approximately 12 hours, cooled in a desiccator (Pyrex), and weighed repeatedly until weights stabilized.

The samples were treated with approximately 1.0 mL of 0.2 M Na₂Cr₂O₇/2.0 M H₂SO₄ (Fisher Scientific reagent grades) and ultrasonicated until thoroughly mixed. The tubes were then filled with additional 0.2 M Na₂Cr₂O₇/2.0 M H₂SO₄ solution and placed in a 50 °C ± 5 °C hot water bath. At the first indication of Cr³⁺ production (green color), samples were taken out of the hot water bath, centrifuged, supernatants were decanted, fresh 0.2 M Na₂Cr₂O₇ and 2.0 M H₂SO₄ solution was added, and the samples were returned to the hot water bath. After 600 hours, the samples were removed from the hot water bath, centrifuged, and supernatants were decanted. The samples were rinsed with distilled water, centrifuged, and supernatants were decanted. This rinsing process was

repeated four additional times. The samples were again covered with aluminum foil and dried at 110 °C. They were then weighed repeatedly until masses stabilized.

The elemental carbonaceous residue was characterized using scanning electron microscope imaging (JEOL 5800 LV). No appreciable soot was detected in Berwind 3 or 4. Soot and non-soot portions of the Berwind 1 and 2 residue were quantified by particle size analysis of SEM micrographs of each sample. Cutouts of the soot and non-soot portions were separated, weighed repeatedly until weights stabilized, and mathematical calculations were used to convert the weights from the two-dimensional areas to equivalent three-dimensional weights (Appendix 4). The percentages of soot and non-soot portions of the elemental carbonaceous residue were calculated and adjusted for loss of soot carbon during the oxidation process. Parts per million of soot and non-soot portions were calculated for each sample.

The following experimental procedure was used for the Madrid samples:

The samples were individually wrapped in clean aluminum foil (Diamond brand) and crushed with a geological hammer. A crushed, weighed portion (0.8 to 1.3 grams weighed on a Mettler AT261 Delta Range balance) of each sample was placed in a pre-labeled polystyrene graduated conical centrifuge tube (15 mL Fisherbrand). Excess solution of 9.0 M HCl (Fisher Scientific reagent grade) was introduced dropwise. The tubes were covered with parafilm and the samples were mixed thoroughly. The samples remained under acid for two days. They were then centrifuged (International IEC Size 2, Model K Centrifuge) and supernatants were decanted with transfer pipets (polyethylene

diSPo plastic). The samples were rinsed thoroughly with distilled water, centrifuged, and supernatants were decanted. This rinsing process was repeated three additional times.

After the third rinse, the supernatants were tested with two drops of an aqueous solution of 15.0 M HF and 1.0 M HCl (Fisher Scientific reagent grades). No precipitate formation was observed. Excess HF/HCl solution was then added dropwise to each sample, each tube was covered with parafilm, and the samples were thoroughly mixed. The samples remained under acid for four days. Subsequent treatments of excess HCl for three days and then HF/HCl for four days were carried out. These subsequent acid treatments were repeated two additional times, with the duration of HCl treatments being seven days and four days, respectively, and the duration of HF/HCl treatments being two days and eight days, respectively. Samples were rinsed copiously with distilled water after each acid treatment.

Samples were then treated with excess concentrated (12.0 M Fisher Scientific reagent grade) HCl and heated in a 50 ± 5 °C distilled water bath for 17 days. Samples were then cooled, rinsed twice with distilled water, treated with excess HF/HCl solution, and heated in a 50 ± 5 °C distilled water bath for 12 days. Samples were then cooled and rinsed twice with distilled water. Samples were treated with concentrated HCl and heated in a 50 ± 5 °C distilled water bath for three days, cooled, and rinsed with distilled water. Samples were then treated with concentrated HF/HCl and heated in a 50 ± 5 °C distilled water bath for four days. Samples were cooled, rinsed with distilled water, treated with concentrated HCl, and heated in a 50 ± 5 °C distilled water bath for three days. Samples were then cooled, rinsed with distilled water, and treated with HF/HCl for 35 days. Samples were then rinsed with distilled water and treated with 9 M HCl for two days.

Due to the resistance of minerals to the acid treatments, heavy liquid density separation with dibromomethane (CH_2Br_2 , Aldrich Brand, 99%) was performed on Madrid 1 (Appendix 1). No separation of minerals was achieved during this process. The sample was transferred to a clean, labeled, weighed, glass disposable centrifuge tube (10.0 mL Kimble Brand) and treated with excess acetone (Aldrich Brand, 98%) for removal of excess dibromomethane. The sample was then rinsed with distilled water.

Heavy liquid density separation with a CsCl solution of density 1.8 grams/milliliter was performed on Madrid 1 (Appendix 1). It was determined by visual analysis that complete separation of minerals from this sample was not achieved during this procedure. This process was repeated with a CsCl solution of density 1.4 grams/milliliter, and again incomplete separation was achieved. This process was repeated with a CsCl solution of density 1.6 grams/milliliter, and complete separation was achieved.

Due to the difficulties faced during the separation processes, a second aliquot of Madrid 1 was demineralized similarly to the above demineralization procedure. Repeated attempts at CsCl density separations with solution densities ranging from 1.4 grams/milliliter to 1.9 grams/milliliter were conducted until complete separation of minerals from carbonaceous material were achieved.

It was determined through visual examination that all of the samples were sufficiently demineralized. The samples were centrifuged, supernatants were decanted, and the samples were rinsed with distilled water. The samples were then transferred to clean, labeled, weighed, glass disposable centrifuge tubes (10.0 mL Kimble Brand), centrifuged, and supernatants were decanted. The tubes were covered with aluminum foil, and the samples were dried in an oven (Fisher Scientific Isotemp 500 Series) at 110 °C for

approximately 4 hours, cooled in a desiccator (Pyrex), and weighed repeatedly until weights stabilized.

The samples were treated with approximately 1.0 mL of 0.2 M Na₂Cr₂O₇/2.0 M H₂SO₄ (Fisher Scientific reagent grades) and ultrasonicated until thoroughly mixed. The tubes were then filled with additional 0.2 M Na₂Cr₂O₇/2.0 M H₂SO₄ solution and placed in a 50 °C ± 5 °C hot water bath. At the first indication of Cr³⁺ production (green color), samples were taken out of the hot water bath, centrifuged, supernatants were decanted, fresh 0.2 M Na₂Cr₂O₇ and 2.0 M H₂SO₄ solution was added, and the samples were returned to the hot water bath. After 600 hours, the samples were removed from the hot water bath, centrifuged, and supernatants were decanted. The samples were rinsed with distilled water, centrifuged, and supernatants were decanted. This rinsing process was repeated four additional times. The samples were again covered with aluminum foil and dried at 110°C. They were then weighed repeatedly until masses stabilized.

The elemental carbonaceous residue was characterized using scanning electron microscope imaging (JEOL 5800 LV). Soot and non-soot portions of the samples were quantified by particle size analysis of SEM micrographs of each sample. Cutouts of the soot and non-soot portions were separated, weighed repeatedly until weights stabilized, and mathematical calculations were used to convert the weights from the two-dimensional areas to equivalent three-dimensional weights (Appendix 4). The percentages of soot and non-soot portions of the elemental carbonaceous residue were calculated and adjusted for loss of soot carbon during the oxidation process. Parts per million of soot and non-soot portions were calculated for each sample.

The following experimental procedure was used for the DSDP Core samples:

The samples were individually crushed with a clean agate mortar and pestle. The mortar and pestle were cleaned thoroughly with acetone and allowed to dry between the crushing of each sample. Crushed, weighed portions (weighed on a Mettler AT261 Delta Range balance) of each sample were placed in a pre-labeled polystyrene graduated conical centrifuge tube (15 mL Fisherbrand). Two tubes were used for each sample, with approximately half of the sample placed into each tube. Excess solution of 9.0 M HCl (Fisher Scientific reagent grade) was introduced dropwise, inducing violent, gas-producing, exothermic reactions. Due to the extreme nature of these reactions, samples were transferred to clean, labeled Pyrex beakers and HCl was added slowly until the reaction subsided. The sample/HCl mixtures were transferred back to the original plastic tubes, the tubes were covered with parafilm, and the samples were mixed thoroughly. The samples remained under acid for 24 hours. They were then centrifuged (International IEC Size 2, Model K Centrifuge) and supernatants were decanted with transfer pipets (polyethylene diSPo plastic). The samples were rinsed thoroughly with distilled water, combined into one polystyrene tube, centrifuged, and supernatants were decanted. The rinsing process was repeated four additional times.

After the fourth rinse, the supernatants were tested with two drops of an aqueous solution of 15.0 M HF and 1.0 M HCl (Fisher Scientific reagent grades). No precipitate formation was observed. Excess HF/HCl solution was then added dropwise to each sample, each tube was covered with parafilm, and the samples were thoroughly mixed. The samples remained under acid for 24 hours. Subsequent treatments of excess HCl for 24 hours and then HF/HCl for four days were carried out. These subsequent acid

treatments were repeated two additional times. Samples were rinsed copiously with distilled water after each acid treatment. Samples were then treated with excess concentrated HCl (Fisher Scientific reagent grade) for two days. The samples were ultrasonicated (Fisher Scientific FS5 ultrasonic bath) for approximately 20 hours during this process, reaching maximum temperatures of 50 °C.

It was determined through visual examination that Cores 1, 2, 4, 5, 6, 7, 9, and 11 were sufficiently demineralized. The samples were centrifuged, supernatants were decanted, and the samples were rinsed twice with distilled water. Cores 3, 8, and 10 were rinsed twice with distilled water and treated with excess HF/HCl for 10 days. These samples were subsequently treated with concentrated HCl for one day. It was determined through visual examination that these samples were sufficiently demineralized. All samples were then transferred to clean, labeled, weighed, disposable glass centrifuge tubes (10.0 mL Kimble or 15 mL Kimble Kimax Brand), centrifuged, and supernatants were decanted. The tubes were covered with aluminum foil, and the samples were dried in an oven (Fisher Scientific Isotemp 500 Series) at 110 °C for approximately 2 hours, cooled in a desiccator (Pyrex), and weighed repeatedly until weights stabilized.

The samples were treated with approximately 1.0 mL of 0.2 M Na₂Cr₂O₇/2.0 M H₂SO₄ (Fisher Scientific reagent grades) and ultrasonicated until thoroughly mixed. The tubes were then filled with additional 0.2 M Na₂Cr₂O₇/2.0 M H₂SO₄ solution and placed in a 50 °C ± 5 °C hot water bath. At the first indication of Cr³⁺ production (green color), samples were taken out of the hot water bath, centrifuged, supernatants were decanted, fresh 0.2 M Na₂Cr₂O₇ and 2.0 M H₂SO₄ solution was added, and the samples were returned to the hot water bath. After 600 hours, the samples were removed from the hot

water bath, centrifuged, and supernatants were decanted. The samples were rinsed with distilled water, centrifuged, and supernatants were decanted. This rinsing process was repeated four additional times. The samples were again covered with aluminum foil and dried at 110°C. They were then weighed repeatedly until masses stabilized.

The elemental carbonaceous residue was characterized using scanning electron microscope imaging (JEOL 5800 LV). Appreciable soot was detected in Core 9 and Core 11. Soot and non-soot portions of these samples were quantified by particle size analysis of SEM micrographs of each sample. Cutouts of the soot and non-soot portions were separated, weighed repeatedly until weights stabilized, and mathematical calculations were used to convert the weights from the two-dimensional areas to equivalent three-dimensional weights (Appendix 4). The percentages of soot and non-soot portions of the elemental carbonaceous residue were calculated and adjusted for loss of soot carbon and leaching of the glass test tubes during the oxidation process (Appendix 2). Parts per million of soot and non-soot portions were calculated for each sample.

The following experimental procedure was used for samples from the Sudbury impact structure:

The samples were individually wrapped in clean aluminum foil (Diamond brand) and crushed with a geological hammer. A crushed, weighed portion (1.8 to 2.0 grams weighed on a Mettler AT261 Delta Range balance) of each sample was placed in a pre-labeled polystyrene graduated conical centrifuge tube (15 mL Fisherbrand). Excess solution of 9.0 M HCl (Fisher Scientific reagent grade) was introduced dropwise. The tubes were covered with parafilm and the samples were mixed thoroughly. The samples

remained under acid for 24 days. They were then centrifuged (International IEC Size 2, Model K Centrifuge) and supernatants were decanted with transfer pipets (polyethylene diSPo plastic). The samples were rinsed thoroughly with distilled water, centrifuged, and supernatants were decanted. This rinsing process was repeated three additional times.

After the third rinse, the supernatants were tested with two drops of an aqueous solution of 15.0 M HF and 1.0 M HCl (Fisher Scientific reagent grades). No precipitate formation was observed. Excess HF/HCl solution was then added dropwise to each sample, each tube was covered with parafilm, and the samples were thoroughly mixed. The samples underwent a highly exothermic reaction during this process. The samples remained under acid for 11 days. Subsequent treatments with excess HCl for 31 days and then HF/HCl for 36 days were carried out. Samples were rinsed copiously with distilled water after each acid treatment. Samples were then rinsed with distilled water twice and treated with excess concentrated HCl (12.0 M, ACS Reagent Grade) for four days.

It was determined through visual examination that all of the samples were sufficiently demineralized. The samples were centrifuged, supernatants were decanted, and the samples were rinsed with distilled water. This rinsing process was repeated two additional times. The samples were then transferred to clean, labeled, weighed, glass disposable centrifuge tubes (10.0 mL Kimble Brand), centrifuged, and supernatants were decanted. The tubes were covered with aluminum foil, and the samples were dried in an oven (Fisher Scientific Isotemp 500 Series) at 110 °C for approximately 3 hours, cooled in a desiccator (Pyrex), and weighed repeatedly until weights stabilized.

The samples were treated with approximately 1.0 mL of 0.2 M Na₂Cr₂O₇/2.0 M H₂SO₄ (Fisher Scientific reagent grades) and ultrasonicated until thoroughly mixed. The

tubes were then filled with additional 0.2 M Na₂Cr₂O₇/2.0 M H₂SO₄ solution and placed in a 50°C ± 5°C hot water bath. At the first indication of Cr³⁺ production (green color), samples were taken out of the hot water bath, centrifuged, supernatants were decanted, fresh 0.2 M Na₂Cr₂O₇ and 2.0 M H₂SO₄ solution was added, and the samples were returned to the hot water bath. After 600 hours, the samples were removed from the hot water bath, centrifuged, and supernatants were decanted. The samples were rinsed with distilled water, centrifuged, and supernatants were decanted. This rinsing process was repeated four additional times. The samples were again covered with aluminum foil and dried at 110°C. They were then weighed repeatedly until masses stabilized.

The elemental carbonaceous residue was characterized using scanning electron microscope imaging (JEOL 5800 LV). Soot and non-soot portions of the samples were quantified by particle size analysis of SEM micrographs of each sample. Cutouts of the soot and non-soot portions were separated, weighed repeatedly until weights stabilized, and mathematical calculations were used to convert the weights from the two-dimensional areas to equivalent three-dimensional weights (Appendix 4). The percentages of soot and non-soot portions of the elemental carbonaceous residue were calculated and adjusted for loss of soot carbon during the oxidation process. Parts per million of soot and non-soot portions were calculated for each sample.

The following experimental procedure was used for the samples from the Gardnos impact structure:

The samples were individually wrapped in clean aluminum foil (Diamond brand) and crushed with a geological hammer. A crushed, weighed portion (approximately 2.0 to 2.5 grams weighed on a Mettler AT261 Delta Range balance) of each sample was placed in a pre-labeled polystyrene graduated conical centrifuge tube (15 mL Fisherbrand). Excess solution of 9.0 M HCl (Fisher Scientific reagent grade) was introduced dropwise. The tubes were covered with parafilm and the samples were mixed thoroughly. The samples remained under acid for 24 hours. They were then centrifuged (International IEC Size 2, Model K Centrifuge) and supernatants were decanted with transfer pipets (polyethylene diSPo plastic). The samples were rinsed thoroughly with distilled water, centrifuged, and supernatants were decanted. This rinsing process was repeated four additional times.

After the fourth rinse, the supernatants were tested with a drop of an aqueous solution of 15.0 M HF and 1.0 M HCl (Fisher Scientific reagent grades). No precipitate formation was observed. Excess HF/HCl solution was then added dropwise, each tube was covered with parafilm, and the samples were thoroughly mixed. The samples remained under acid for four days. Subsequent treatments of excess HCl for three days and then HF/HCl for a week were carried out. Samples were rinsed copiously with distilled water after each acid treatment. The samples were ultrasonicated (Fisher Scientific FS5 ultrasonic bath) for several hours at various times throughout this process, reaching maximum temperatures of 50°C.

After visual examination of the samples, it was concluded that three of the samples (171, 126, 137) were sufficiently demineralized. All of the samples were treated with 9.0 M HCl (Fisher Scientific reagent grade) for two days. The three demineralized samples were centrifuged, supernatants were decanted, and the samples were rinsed with distilled water twice, covered with parafilm to prevent dust contamination, and set aside. The other samples were treated again with the HF/HCl solution for two days, ultrasonicated, and rinsed twice with distilled water. They were then treated with concentrated HCl (12.0 M Fisher Scientific reagent grade), covered with parafilm, and mixed. Visual examination after three days confirmed that these samples were also sufficiently demineralized. The samples were centrifuged, supernatants were decanted, and the samples were rinsed once with distilled water.

All samples were transferred to glass disposable centrifuge tubes (10.0 mL Kimble or 15 mL Kimble Kimax Brand), centrifuged, and supernatants were decanted. The samples were covered with aluminum foil, dried in an oven (Fisher Scientific Isotemp 500 Series) at 110 °C for approximately 12 hours, cooled in a desiccator (Pyrex), and weighed repeatedly until weights stabilized.

The tube containing sample 176 was broken during this process and approximately half of the sample was contaminated. The uncontaminated portion was transferred to a new tube. All further calculations were adjusted for a loss of half the sample (a visual determination), with an assumed error on this correction of 0.00050 g.

The samples were treated with approximately 1.0 mL of 0.2 M Na₂Cr₂O₇/2.0 M H₂SO₄ (Fisher Scientific reagent grades) and ultrasonicated until thoroughly mixed. The tubes were then filled with additional 0.2 M Na₂Cr₂O₇/2.0 M H₂SO₄ solution and placed

in a $50^{\circ}\text{C} \pm 5^{\circ}\text{C}$ hot water bath. At the first indication of Cr^{3+} production (green color), samples were taken out of the hot water bath, centrifuged, supernatants were decanted, fresh 0.2 M $\text{Na}_2\text{Cr}_2\text{O}_7$ and 2.0 M H_2SO_4 solution was added, and the samples were returned to the hot water bath. After 600 hours, the samples were removed from the hot water bath, centrifuged, and supernatants were decanted. The samples were rinsed with distilled water, centrifuged, and supernatants were decanted. This rinsing process was repeated four additional times. The samples were again covered with aluminum foil and dried at 110°C . They were then weighed repeatedly until masses stabilized.

The elemental carbonaceous residue was characterized using scanning electron microscope imaging (JEOL 5800 LV). Post-oxidation elemental carbon residue weights were adjusted for the presence of unreacted minerals by SEM characterization and visual analysis (Appendix 3). Soot and non-soot portions of the residue were then quantified by particle size analysis of SEM micrographs of each sample. Cutouts of the soot and non-soot portions were separated, weighed repeatedly until weights stabilized, and mathematical calculations were used to convert the weights from the two-dimensional areas to equivalent three-dimensional weights (Appendix 4). The percentages of soot and non-soot portions of the elemental carbonaceous residue were calculated and adjusted for loss of soot carbon and leaching of the glass test tubes during the oxidation process (Appendices 2 and 4). Parts per million of soot and non-soot portions were calculated for each sample.

Raw Data:

The raw data for the Berwind samples, Madrid samples, DSDP Core samples, Sudbury samples, and Gardnos samples are presented in Appendices 5-9, respectively.

Calculated Data and Sample Calculations:

The calculated soot concentrations in the Berwind samples, Madrid samples, DSDP Core samples, Sudbury samples, and Gardnos samples are presented in Tables 6 - 10, respectively. Detailed calculated data are presented in Appendices 10-14, respectively. Sample Calculations for these data are presented in Appendix 15.

Although the propagated absolute error for the soot concentrations of the Berwind samples is ± 0 ppm, a ten percent error has been estimated for the SEM analysis and characterization [13]. In many cases, as for the Madrid samples, the propagated error is the appropriate order of magnitude to account for the SEM characterization error. In addition, difficulties in demineralization resulting in heavy liquid density separation add to the error which must be considered in the calculated soot values for affected samples. Therefore, for those samples that have a small error due to propagation alone, a minimum of a ten percent error is automatically assigned to the final calculated values. This additional error correction applies to samples analyzed from all sites included in this study, and should be considered during interpretation of the presented data.

Table 6. Concentration of Soot Carbon in Berwind Samples

Sample	Description	Soot (ppm)	Absolute Error (ppm)
Berwind 1	Post-Impact Sediments	1200	0
Berwind 2	Post-Impact Sediments	520000	0
Berwind 3	Pre-Impact Sediments	2000	0
Berwind 4	KT Boundary Layer	3000	0

Table 7. Concentration of Soot Carbon In Madrid Samples

Sample	Description	Soot (ppm)	Absolute Error (ppm)
Madrid 1	Post-Impact Sediments	3100	300
Madrid 2	Post-Impact Sediments	790000	82000
Madrid 3	KT Boundary Layer	780	90
Madrid 4	Pre-Impact Sediments	67000	7000
Madrid 5	Pre-Impact Sediments	130000	14000

Table 8. Concentration of Soot Carbon In DSDP Core Samples

Sample	Description	Soot (ppm)	Absolute Error (ppm)
Core 1	Pre-Impact Rock	3	3
Core 2	Pre-Impact Rock	4	4
Core 3	Post-Impact Sediments	4	4
Core 4	Post-Impact Sediments	4	4
Core 5	Post-Impact Sediments	7	8
Core 6	Post-Impact Sediments	4	4
Core 7	Post-Impact Sediments	4	4
Core 8	Post-Impact Sediments	4	4
Core 9	Post-Impact Sediments	402	401
Core 10	Post-Impact Sediments	6	6
Core 11	KT Boundary Layer	550	750
Core 12*	KT Boundary Layer	1800	200

*This sample was analyzed in a previous study conducted by Sarah Moecker. Implications of these results are presented in the discussion section of this paper.

Table 9. Concentration of Soot Carbon In Sudbury Samples

Sample	Description	Soot (ppm)	Absolute Error (ppm)
Sudbury 22	Crater Fill Sediments	110	60
Sudbury 20	Crater-Fill Sediments / Contact Unit	760	90
Sudbury 16	Contact Unit	2300	200
Sudbury 12	Contact Unit	3000	300
Sudbury 1	Contact Unit / Basement Rock	2800	300
Sudbury 7	Basement Rock	380	140

Table 10. Concentration of Soot Carbon in Gardnos Samples

Sample	Description	Soot (ppm)	Absolute Error (ppm)
Gardnos 19	Crater Fill Sediments	1	79
Gardnos 20	Crater Fill Sediments	17	17
Gardnos 21	Crater Fill Sediments	15	15
Gardnos 22	Crater Fill Sediments	4451	5484
Gardnos 157	Crater Fill Sediments	16	340
Gardnos 158	Crater Fill Sediments	4	543
Gardnos 159	Crater Fill Sediments	0	16
Gardnos 160a	Crater Fill Sediments	4726	4901
Gardnos 160b	Crater Fill Sediments	10	10
Gardnos 161a	Crater Fill Sediments	1133	273
Gardnos 161b	Crater Fill Sediments	< 1	--
Gardnos 162a	Crater Fill Sediments	17	17
Gardnos 162b	Crater Fill Sediments	10	10
Gardnos 162c	Crater Fill Sediments	10	10
Gardnos 129	Basement Rocks	67	234
Gardnos 126	Basement Rocks	637	6084
Gardnos 120	Basement Rocks	8	9
Gardnos 121	Basement Rocks	8	9
Gardnos 143	Basement Rocks	8	3536
Gardnos 176	Basement Rocks	3	270
Gardnos 172	Contact Unit	< 1	--
Gardnos 179	Contact Unit	27	113
Gardnos 178	Contact Unit	107	7700
Gardnos 133	Contact Unit	10	626
Gardnos 137	Contact Unit	425	4475
Gardnos 175	Contact Unit	1	342
Gardnos 137 B	Contact Unit	97	867
Gardnos 140	Contact Unit	17	17
Gardnos 141	Contact Unit	26	130
Gardnos 142	Contact Unit	16	16
Gardnos 164	Distant Sediments	4982	1667
Gardnos 171	Distant Sediments	6161	4597
Gardnos 170	Distant Sediments	1994	893
Gardnos 169	Distant Sediments	655	988
Gardnos 168	Distant Sediments	10	10
Gardnos 167	Distant Sediments	10	10

Discussion:

The following are the results and implications from Berwind, Colorado, and Madrid, Colorado:

Soot concentrations of 3000 ± 0 ppm and 780 ± 90 ppm, similar to those found in pre-impact samples, were found for the KT boundary layers of the Berwind and Madrid studies, respectively. Assuming a sample thickness of 1.0 ± 0.1 cm for KT boundary samples, these soot concentrations correspond to a soot flux to the Berwind and Madrid sites of 3.0 ± 0.4 mg/cm² and 0.78 ± 0.11 mg/cm², respectively¹. These values give excellent correlation to the calculated global soot concentration of 2.2 ± 0.7 mg/cm² [6]. SEM micrographs of the post-oxidation residue for Berwind 4 and Madrid 3 samples are shown in Figures 9 and 10.

¹ Soot flux is calculated as follows:

$$\begin{aligned}\text{Soot flux} &= \left(\frac{x \text{ grams Soot}}{10^6 \text{ grams Rock}} \right) (\text{Carbonaceous Rock Density}) (\text{Sample Thickness}) \\ &= \left(\frac{\text{ppm Soot}}{10^6 \text{ grams Rock}} \right) \left(\frac{1.0 \text{ grams}}{\text{cm}^3} \right) \left(\frac{10^3 \text{ mg Soot}}{\text{gram Soot}} \right) (1.0 \text{ cm}) \\ &= \left(\frac{3000 \text{ ppm Soot}}{10^6 \text{ gram Rock}} \right) \left(\frac{1.0 \text{ grams}}{\text{cm}^3} \right) \left(\frac{10^3 \text{ mg Soot}}{\text{gram Soot}} \right) (1.0 \text{ cm}) \\ &= 3.0 \text{ mg/cm}^2 \\ \text{Absolute Error} &= (\text{Soot Flux}) \sqrt{\left(\frac{\text{Soot Concentration Error}}{\text{Soot Concentration}} \right)^2 + \left(\frac{\text{Carbonaceous Rock Density Error}}{\text{Carbonaceous Rock Density}} \right)^2 + \left(\frac{\text{Sample Thickness Error}}{\text{Sample Thickness}} \right)^2} \\ &= (3.0 \text{ mg/cm}^2) \sqrt{\left(\frac{0 \text{ ppm}}{3000 \text{ ppm}} \right)^2 + \left(\frac{0.1 \text{ grams}}{1.0 \text{ grams}} \right)^2 + \left(\frac{0.1 \text{ centimeters}}{1.0 \text{ centimeters}} \right)^2} \\ &= 0.4 \text{ mg/cm}^2\end{aligned}$$

Figure 9. SEM Micrograph of Berwind 4 (Berwind, Colorado, KT Boundary)

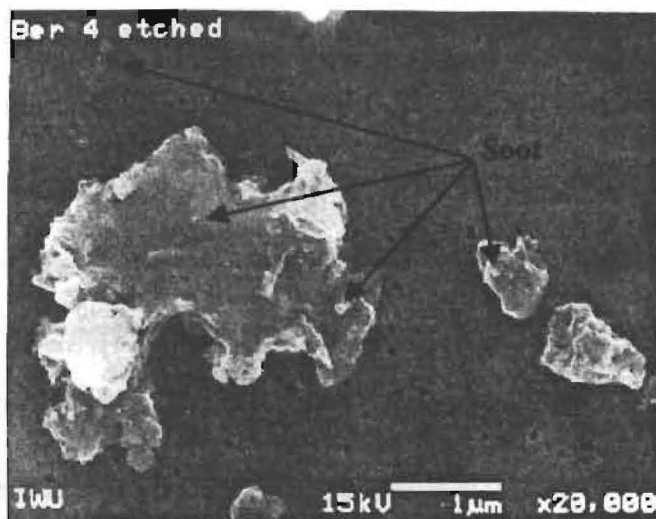
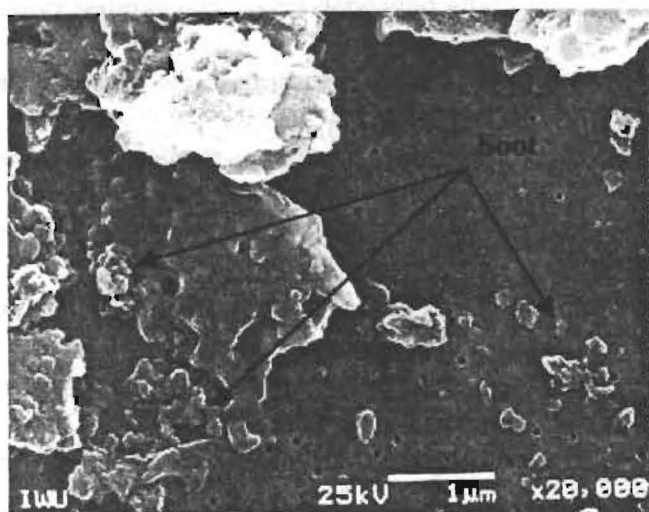


Figure 10. SEM Micrograph of Madrid 3 (Madrid, Colorado, KT Boundary)



Soot concentrations of $520,000 \pm 0$ ppm and $790,000 \pm 82000$ ppm were found for the post-impact Berwind 2 and Madrid 2 samples, respectively. Although much higher than the soot concentrations found in previous KT boundary studies, these concentrations indicate the magnitude of fires triggered near to the impact site. These results offer

support for the results of previous KT boundary studies and to the theory of global wildfires triggered by the impact event. In addition, these results support previously developed models for post-impact soot deposition [3, 4, 5].

Due to the magnitude of the Chicxulub impact event, a large amount of ejecta material would be expected to have been deposited in the KT boundary layer itself (immediately following impact) in locations near the impact site. The close proximity of the Berwind and Madrid sites to the Chicxulub site itself thus indicate that a significant amount of ejecta material should have been deposited in the KT boundary layer at these sites. Because the wildfires which gave rise to the soot are thought to have been triggered by the impact, it is expected that a large portion of the soot deposition would have occurred in post-impact sedimentary layers deposited after (above) the KT boundary layer at these sites. Therefore, soot concentrations in the KT boundary layer would be expected to be lower than those found in post-impact sediments for Western Interior samples, unlike what is observed in KT and related samples farther from the impact site. The results of the Berwind and Madrid studies correlate well with these expectations. In addition, the larger magnitude of the soot concentrations found above the KT boundary in the Western Interior could be attributed to the close proximity of the sites to the impact event itself. The experimental results indicate that the magnitude of the fires on the North American continent might have been much larger than those on other continents.

However, unusual results are also found in pre-impact samples (below the KT boundary) at these sites. In the Madrid study, higher soot concentrations than those found at the KT boundary are found in pre-impact samples (Madrid 4 and 5). Similar soot concentrations are found in Berwind pre-impact sediments and KT boundary sediments.

Although unexpected when considered in the context of traditional oxidative sedimentation processes, these findings can be attributed to the environmental conditions of the Western Interior at the time of the impact. The anaerobic, reducing conditions of the Western Interior favored the preservation of carbonaceous material. Large amounts of coal have been found at several Western Interior sites, and very high concentrations of carbon have been found in most Western Interior samples [8]. Furthermore, since wildfires occur naturally, ignited by lightning, the reducing conditions would preserve soot from smaller, local fires in the Western Interior, unlike in deeper, oxidizing marine environments farther from shore. Due to these factors, the elemental carbon concentrations are elevated in these samples with respect to other KT boundary studies.

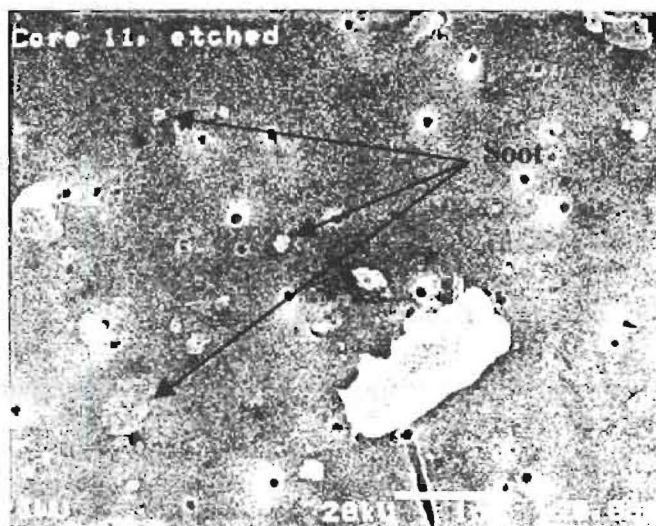
In addition, pre-impact sediments were deposited gradually, at the naturally occurring sedimentation rate of approximately 10 cm/1000 years [1]. It is suspected that the magnitude of the impact event led to a much faster impact and post-impact sedimentation rate (approximately 3 cm/1 year), reducing the amount of non-impact-related sedimentation and preservation of carbonaceous material found in these samples. The main source for elemental carbon in impact and post-impact sites would be ejecta material and post-impact fallout (soot) rather than reduced organic carbon such as coal. Therefore, the pre-impact samples have elevated carbon concentrations not only with respect to other KT boundary studies, but also with respect to the KT boundary and post-impact samples from these sites. Any elevation of carbon concentration leads directly to an elevation of soot concentration. The high soot concentrations found in these samples can therefore be attributed to the reducing environment and the differences in sedimentation rates of these sites. Because the methods of soot determination tend to

result in unnaturally skewed soot concentrations when coal is present, these samples are difficult to use for soot analysis. Therefore, results from these sites are considered to be less conclusive than those from marine sites.

The following are the results and implications from DSDP Core 465-A:

Soot concentrations of 402 ± 401 ppm and 550 ± 750 ppm were found for Core 9 and Core 11, respectively. The soot flux to Core 465-A, based on the soot concentration in the KT boundary sample Core 11, is calculated to be 1.1 ± 1.5 mg/cm², well within the calculated average global soot concentration range. The high error associated with these values can be attributed to the corrections made to sample weights due to the tube leaching process (Appendix 2). However, because this error is the same order of magnitude as the calculated soot concentrations, these concentrations are considered significant. An SEM micrograph of the post-oxidation residue for Core 11 is shown in Figure 11.

Figure 11. SEM Micrograph of Core 11 (DSDP Core 465-A, KT Boundary)



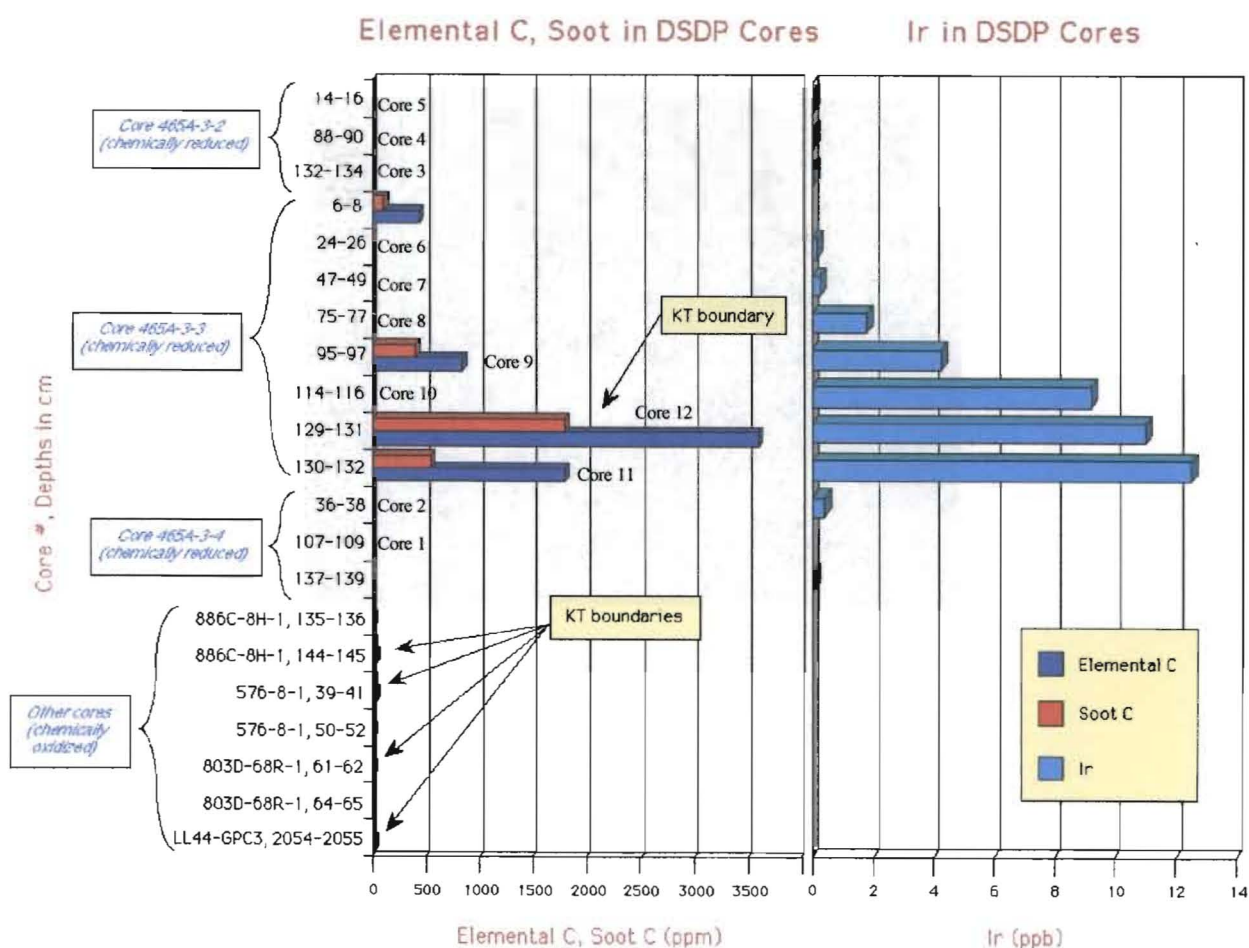
Negligible soot concentrations were found in all other DSDP Core 465-A samples. The location of Core 465-A rules out the possibility of soot deposition from groundwater runoff and indicates that eolian transport is the most probable mechanism for soot deposition. Therefore, the presence of soot in boundary and post-impact sediments in DSDP Core 465-A supports the theory that the KT boundary soot layer is indeed global.

Four other DSDP cores had previously been analyzed for the presence of soot at the KT boundary. In addition, analyses of three samples from Core 465-A (not included in this study) were conducted [13]. All of the cores analyzed, with the exception of Core 465-A, were from oxidizing environments. It was considered possible that soot might not be preserved at these sites. This proved to be correct as no soot or elemental carbon was recovered. Upper limits on soot ranged from <2 to <18 ppm in these samples [6].

However, significant quantities of soot were found in a pure KT boundary clast studied during the Core 465-A analysis. This sample, which shall be referred to as Core 12, contained a soot concentration of 1800 ± 200 ppm [6]. The variation between the soot concentrations in Core 12 and Core 11 can be attributed to the condition of the core and sampling technique. While Core 12 was comprised of pure KT boundary sediments, Core 11 was taken from sediments very near to KT boundary sediments (within approximately 1.0 cm). Because of severe drilling disturbance, it is highly possible that this sample contained small fragments of boundary clay. Therefore, lower soot concentrations in Core 11 with respect to Core 12 can be expected. The presence of soot in both of these samples strongly supports the global wildfire theory.

In addition to analysis for soot, each of the DSDP core samples was analyzed for iridium by Frank T. Kyte at UCLA. In excellent correlation with previous KT boundary studies, a maximum in the iridium concentration was found at the KT boundary. This coincides with the soot concentration patterns observed in these samples, giving further support to the theory of post-impact mixing of soot and meteoritic material, air transport, and eolian deposition. A summary of the soot and iridium concentrations for all samples studied in the DSDP studies, including Core 465-A, is given in Figure 12. Iridium concentrations for the oxidized cores are not presented in this figure.

Figure 12. Soot, Non-Soot, and Iridium Contents in DSDP Core Samples



The following are the results and implications from the Sudbury Impact Structure, Canada:

Significant soot concentrations were found in three of the post-impact, contact unit samples analyzed for the Sudbury structure. These samples, Sudbury 16, Sudbury 12, and Sudbury 1, contained 2300 ± 200 ppm soot, 3000 ± 300 ppm soot, and 2800 ± 300 ppm soot, respectively. SEM micrographs of the post-oxidation residues for these samples are shown in Figures 13, 14, and 15, respectively. A profile of the soot concentrations across the impact structure is given in Figure 16.

Figure 13. SEM Micrograph of Sudbury 12 (Sudbury Impact Structure, Canada, Contact Unit)

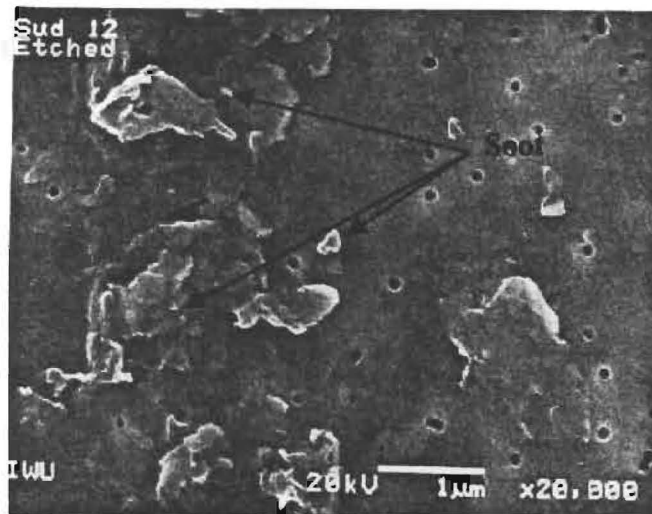


Figure 14. SEM Micrograph of Sudbury 16 (Sudbury Impact Structure, Canada, Contact Unit)

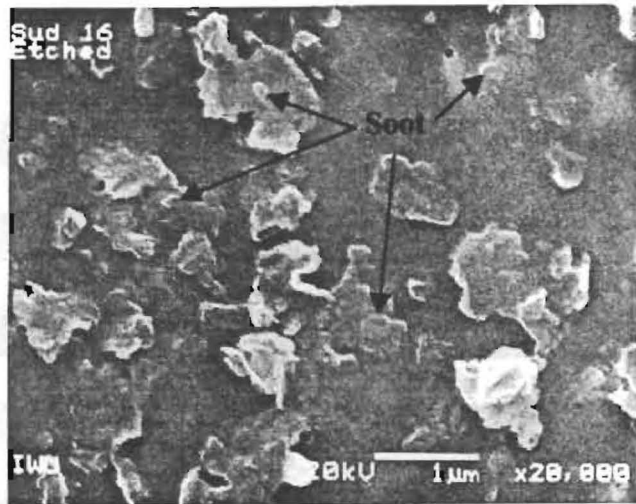


Figure 15. SEM Micrograph of Sudbury 1 (Sudbury Impact Structure, Canada, Contact Unit/Basement Rock)

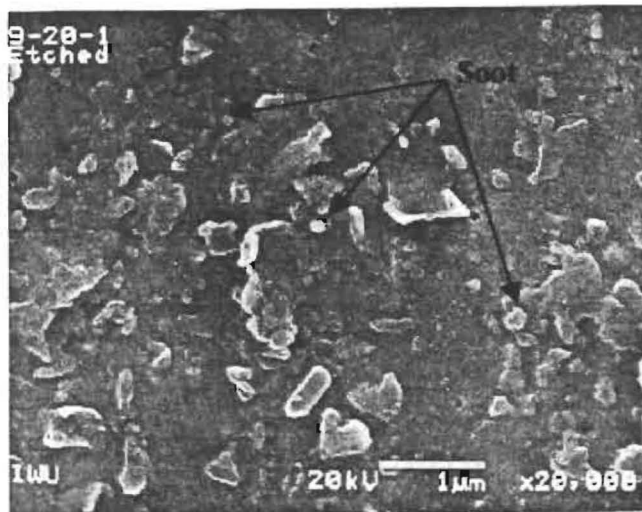
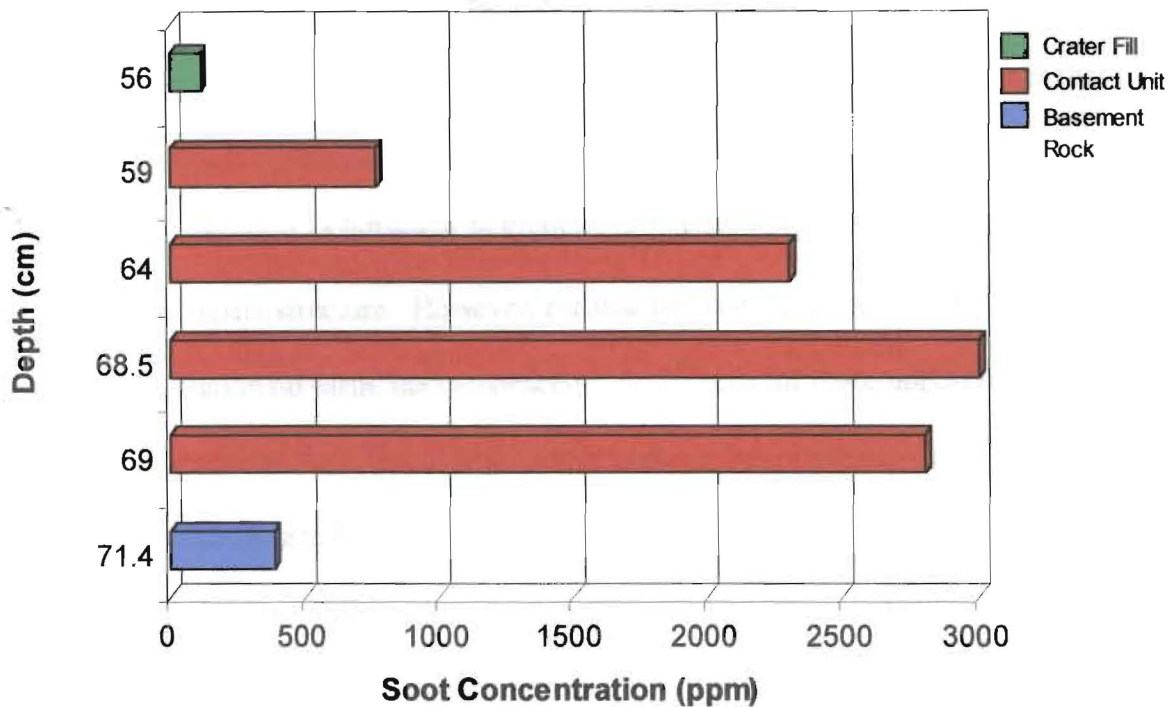


Figure 16. Profile of Soot Carbon Concentrations Across the Sudbury Impact Structure, Canada



These Sudbury soot concentrations and fallout patterns are similar to those found in previous KT boundary studies. The highest concentration of soot is found in Sudbury 12, the post-impact contact unit sample. However, significant soot concentrations are found in the other contact unit sediments, indicating that combustion was triggered immediately by the impact event and continued for some time after the impact. As is shown in Figure 16, soot concentrations gradually taper off to background levels. The crater-fill sediments analyzed, Sudbury 22 and Sudbury 20, contained similar soot concentrations to Sudbury 7, the basement rock sample.

The presence of soot in these samples indicates that combustion of carbonaceous material was indeed triggered by the Sudbury impact event. Elemental carbon in the form of fullerenes, cage-like compounds which are close relatives of soot, has also been detected in the Sudbury structure [16]. Soot is thought to be incomplete fullerenes that continue to wrap in a snowball effect rather than closing to form the cage structure [17]. Therefore, the presence of fullerenes in Sudbury sediments further supports the discovery of soot in this impact structure. However, because the Sudbury event occurred before there was vegetation on earth, the carbonaceous fuel source for this combustion remains unknown. Possibilities for a fuel source include carbonaceous materials in the target rock and carbonaceous materials from the impactor. Future work will include analysis of additional samples across the impact structure to determine a more complete sedimentation profile for combustion products.

The following are the results and implications from the Gardnos Impact Structure, Norway:

Unlike sediments which have been analyzed across the K/T boundary, many of the Gardnos samples contained significant quantities of HF-resistant, slow to dissolve, silicate minerals. In some cases, significant quantities of these undissolved silicates and other minerals were left along with the desired elemental carbon following demineralization and oxidation. Post-oxidation carbon weights were corrected using SEM imaging and particle size analysis of both carbon and silicate fractions (Appendix 3). Most required corrections were large, resulting in associated errors larger in magnitude than the calculated soot concentrations. Therefore, soot contents were not considered significant unless the

amount exceeded the estimated error. None of the Gardnos impactites showed significant soot contents (>1 ppm) after corrections were applied. No detectable combustion products are observed in any of the Gardnos samples directly associated with the impact event.

Surprisingly, significant soot contents were found in three black shale samples not directly related to the Gardnos impact event. A soot concentration of 1133 ± 273 ppm was found in Gardnos 161a, which was collected from post-impact crater-filling sediments within the Gardnos crater. Three samples, Gardnos 164, Gardnos 170 and Gardnos 171, from the pre-impact shale over 100 km east of the crater contained soot concentrations of 4982 ± 1667 ppm, 1944 ± 893 ppm and 6161 ± 4597 ppm, respectively. SEM micrographs of these samples are shown in Figures 17, 18, 19, and 20, respectively.

Figure 17. SEM Micrograph of Gardnos 161a (Gardnos Impact Structure, Norway, Crater Fill Sediments)

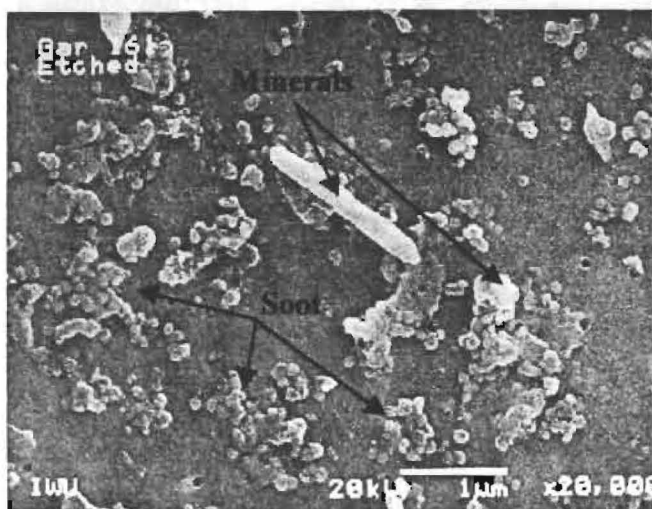


Figure 18. SEM Micrograph of Gardnos 164 (Gardnos Impact Structure, Norway, Distant Sediments)

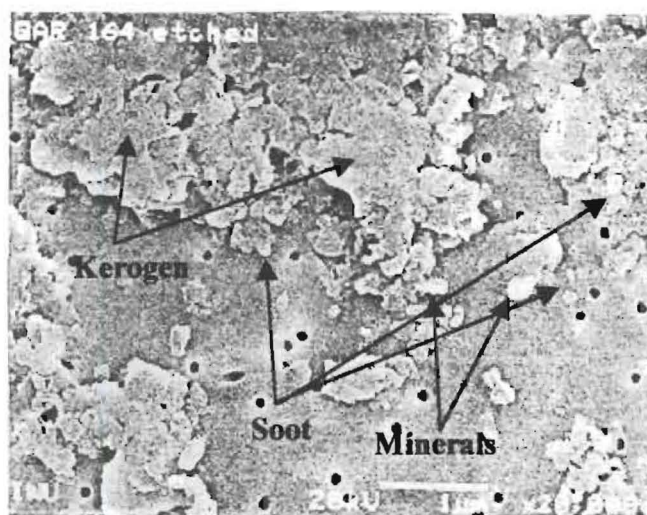
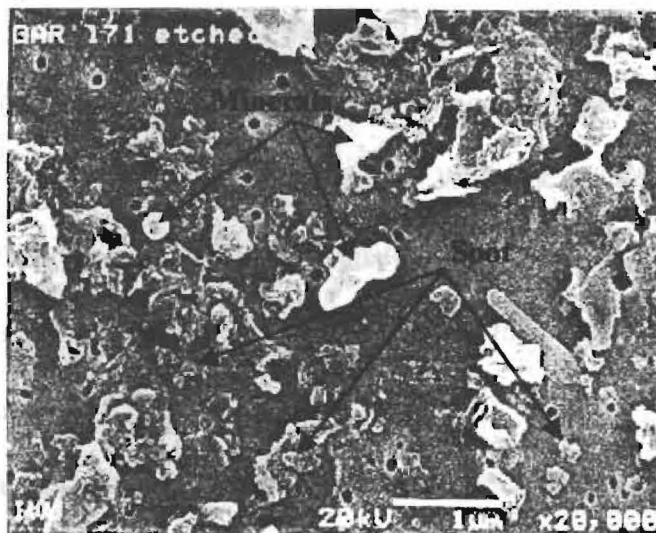


Figure 19. SEM Micrograph of Gardnos 170 (Gardnos Impact Structure, Norway, Distant Sediments)



Figure 20. SEM Micrograph of Gardnos 171 (Gardnos Impact Structure, Norway, Distant Sediments)



It was discovered during post-analysis data interpretation that the background samples collected from distant sediments had been collected from near the surface of a road cut. This road cut had been built through use of dynamite and had been exposed to the byproducts of internal combustion engines for more than 30 years. The large soot concentrations in these samples can therefore be attributed to these modern sources. The detection of soot in these samples, in spite of the difficulties faced in the quantification of soot at Gardnos, indicates the sensitivity of the presented isolation techniques. These findings lend support to the soot concentrations reported for the other studies.

Ongoing and Future Work:

The difficulties faced while demineralizing the Gardnos samples were much more challenging than those dealt with in other studies. However, many of the samples analyzed for these five projects required demineralization techniques more complex than those originally developed for KT boundary studies. While the problems with demineralization of Gardnos samples were ultimately solved, they have brought into question the applicability of the chemical techniques used to isolate and identify elemental carbon in sedimentary rocks in general.

Ongoing studies are being conducted to develop and broaden such techniques so as to be useful for samples of varying ages and compositions. To begin this task, twenty-four carbonaceous shale samples were obtained from The Field Museum of Natural History in Chicago. These shales range from Pre-Cambrian (>570 Ma old) to Carboniferous (~300 Ma old) in age and come from a variety of locations in North America. The carbon composition of these samples ranges from 0.0008 percent to 75.385 percent by mass. A systematic analysis of traditional demineralization and oxidation techniques is being performed on each sample to determine ideal reactants and conditions for elemental carbon isolation. The results will then be correlated with sample and kerogen type. Once this has been established, the results should be generally applicable to any carbon-containing sedimentary rock in which researchers wish to separate land-derived elemental carbon from organic carbon of marine provenance.

Due to the variety of geological conditions under which shale and impact-related sediments are deposited, analysis of each presents a new challenge to established chemical

techniques. Thus, several different projects are currently being pursued with these samples:

1) Demineralization. Many of these samples contain acid resistant minerals. Although extended exposure to the HCl/HF treatment, even at elevated temperatures, will eliminate most silicates², the procedure is time consuming and sometimes completely ineffective. For example, a continuing source of carbon "contamination" is the existence of pyrite in many chemically reduced samples. Because pyrite is acid-resistant, traditional demineralization techniques will not remove it from samples. However, pyrite reacts quite vigorously under oxidizing conditions. The ideal method for removal of pyrite would neither alter carbonaceous components of the samples nor introduce carbon-containing reagents which would contaminate the carbon isotopically. (This method would be of interest to geochemists studying the stable carbon isotopic composition of these samples.)

Some promising demineralization techniques include reaction with inorganic reagents which do not involve boiling acidic conditions, increasing reaction pressures via an acid digestion bomb, and using heavy liquid density separations. Although boiling acidic conditions are effective on resistant silicates, pyrite is unreactive with these reagents. Likewise, acid digestion bomb techniques are limited to non-pyritic mineral removal. Due to the dangers associated with these processes, their use is limited to a small number of samples containing only resistant silicate material. To date, the most

² This technique was utilized for samples from the Berwind, Colorado, and Madrid, Colorado, studies.

successful removal of minerals **has been** achieved through heavy liquid density separations³. The developed techniques for this process are given in Appendix 2.

2) Controlled Oxidation. Acidic dichromate oxidation under controlled temperature conditions was originally performed on carbonaceous components of KT boundary samples using a range of dichromate concentrations and reaction temperatures [12]. The purpose was to determine the kinetics of kerogen and elemental carbon oxidation for KT samples only. From these data, ideal oxidation conditions (0.1 M dichromate; 2 M sulfuric acid; 50 ° Celsius; reaction duration of 600 hours) were determined. These conditions were applied to all samples analyzed in this study.

Because these conditions are known to work on some samples, they have been applied to the twenty-four shale samples. The separation is being assessed using mass loss and infrared spectroscopic data. Once all of the samples have reacted entirely, the kinetic data will be analyzed, and efficiency of the technique will be determined for samples of each age category. If it is found that the procedure is not effective for destroying kerogen of certain types or ages, the oxidation conditions (reagents, concentrations, temperatures) will be altered and the experiment repeated under these new conditions. This process will be continued until ideal oxidation conditions for the isolation of elemental carbon from each sample type have been determined.

Of these twenty-four samples, twenty-three have completed the oxidation process with traditional KT boundary techniques. Many of these samples have undergone

³ This technique was utilized for samples from the Berwind, Colorado, and Madrid, Colorado, studies. In addition, it has been utilized extensively in the shale analysis.

oxidation for much longer periods than those required for complete oxidation during the original KT boundary study (approximately 2000 hours) [12]. The remaining sample has currently undergone oxidation for 4686 hours, and visible carbonaceous sample persists at this time [15]. Oxidation will be continued on this sample until only unreactive material remains (indicated by lack of sample loss) or until complete oxidation has been obtained. Once this process is complete for all samples, the kinetic data will be analyzed to determine the necessity for further studies.

The difficulties posed by the presence of pyrite were not considered until after the oxidation process was begun for these shales. Therefore, several of the shale samples analyzed contained significant amounts of pyrite. The presence of pyrite (even in small quantities) and its reactivity under oxidizing conditions affects the interpretation of carbon oxidation rates. Literature searches have revealed that the nature of this process is highly debated. If pyrite oxidation is diffusion-controlled, the kinetic data for the pyritic portion of each sample can be separated out and subtracted from the kinetic data of the sample as a whole (carbonaceous components plus pyrite). Samples can therefore be oxidized without previous removal of the pyritic portions, as long as the amount of pyrite present is known. However, if pyrite oxidation is not a diffusion controlled, first-order process, but rather a surface area dependent process, mathematical manipulation of the oxidation data becomes quite difficult. The kinetic data for the carbonaceous components then become difficult to resolve.

Kinetic studies on pyrite samples of various particulate sizes were performed [15]. It was found that the oxidation of pyrite under KT boundary conditions is indeed a surface area dependent process with the oxidation rate varying drastically with particle size.

Therefore, removal of the pyritic portion of the shale samples and repeat analysis of those samples containing pyrite became necessary. Heavy liquid density separations were utilized to determine the pyritic mass fraction of each shale sample (Appendix 2). If this fraction was significant (greater than 10 percent of the sample by mass), the oxidation process was repeated with the pure carbonaceous portions of these samples. Thirteen of the shale samples required this repeat analysis. To date, three of the samples have oxidized to completion. The other ten samples have currently undergone oxidation for 1350 hours. Similarly to the original shale samples, oxidation will be continued for these samples until only unreactive material remains (indicated by lack of sample loss) or until complete oxidation has been obtained. Once this process is complete for all samples, the kinetic data will be analyzed to determine the necessity for further studies.

Appendix 1. Heavy Liquid Density Separations

Many impact-related samples contain significant quantities of acid resistant minerals. Although extended exposure to HCl/HF treatment will eliminate most silicates, the procedure is time consuming and often completely ineffective, even at elevated temperatures. Other minerals, such as pyrite (FeS_2), are resistant to such acid treatments.

Heavy liquid density separations achieve separation of mineral components from samples by utilizing the differences between the densities of minerals and carbonaceous components. Small portions (~ 0.5 grams) of the sample are suspended in water by extended ultrasonification. A small amount of high density liquid (1 - 2 mL) is placed in a centrifuge tube and the aqueous sample suspension is gently layered onto this liquid via pipet. After extended centrifugation, the mineral component sinks to the bottom of the high density liquid, while the carbonaceous sample remains at the interface of the two liquids. The sample component is carefully removed and returned to its original centrifuge tube for rinsing and weighing. The mineral component can be stored or discarded.

No separation was achieved using dibromomethane as the high density liquid. However, two successful methods for this type of separation have been developed for the removal of problematic minerals. Aqueous solutions of cesium chloride (CsCl) and sodium metatungstate ($3\text{Na}_2\text{WO}_4 \cdot 9\text{WO}_3 \cdot \text{H}_2\text{O}$, referred to here as SMT) at appropriate densities have been found effective in the separation of silicates and pyrite, respectively, from the bulk sample. Successful separation of silicates has been achieved at CsCl solution densities ranging from 1.6 to 1.9 grams/milliliter. Likewise, successful separation of pyrite has been achieved at SMT solution densities ranging from 2.1 to 2.3 grams/milliliter.

Appendix 2. Correction Factor for Leaching of Glass Tubes

Leaching of 15 mL Kimble Kimax Brand glass centrifuge tubes occurred in the Gardnos project and the DSDP Core project. Because visible sample was present for several samples yielding negative mass, a correction factor was applied to all samples in tubes that underwent this leaching. This factor has been determined through examination of samples from the DSDP Core project [14]. The largest negative value obtained for a tube with visible sample remaining was obtained, and the amount of sample remaining in the tube was estimated. This gave a correction of 6.0 mg. Independently, an average of the negative masses of all tubes with no visible sample remaining was obtained, leading to a correction of 3.6 mg. These corrections were averaged, yielding a value of 4.8 mg, and a maximum error of ten percent was assumed based on visual estimates of carbon present.

Appendix 3. Correction for Significant Minerals in Post-Oxidation Residue

Higher mass number elements appear brighter during SEM characterization than do elements of lower mass number. Minerals contain elements of higher mass number and therefore appear brighter than do carbonaceous components of a sample. The relative brightness of particles is used during SEM characterization to distinguish between carbonaceous and non-carbonaceous portions of the sample. Visual estimates of the carbon and non-carbon fractions of the SEM image area can be used to calculate the percent by area of carbon and non-carbon portions (of the total particle area) as follows:

$$\text{Total Area} = \text{Area}_{\text{carbon}} + \text{Area}_{\text{non-carbon}}$$

$$y = \% \text{ by Area}_{\text{non-carbon}} = \left(\frac{\text{Area}_{\text{non-carbon}}}{\text{Total Area}} \right) (100)$$

$$x = \% \text{ by Area}_{\text{carbon}} = \left(\frac{\text{Area}_{\text{carbon}}}{\text{Total Area}} \right) (100)$$

The mass of the particles is directly proportional to the area of the particles.

Therefore, x/y, the mass ratio, is equal to the area ratio. If one assumes all particles to be spherical, the following conversions can be made:

r = radius of the particle

$$\text{Area} = (\pi)(r)^2$$

$$\left(\frac{x}{y} \right) = \left[\frac{(\pi)(r_{\text{carbon}})^2}{(\pi)(r_{\text{non-carbon}})^2} \right] \Rightarrow \left(\frac{x}{y} \right)^{\frac{1}{2}} = \left(\frac{r_{\text{carbon}}}{r_{\text{non-carbon}}} \right) \Rightarrow r_{\text{non-carbon}} = \frac{r_{\text{carbon}}}{\left(\frac{x}{y} \right)^{\frac{1}{2}}}$$

$$\text{Volume} = \left(\frac{4}{3}\right)(\pi)(r)^3$$

$$\text{Volume}_{\text{carbon}} = \left(\frac{4}{3}\right)(\pi)(r_{\text{carbon}})^3$$

$$\text{Volume}_{\text{non-carbon}} = \left(\frac{4}{3}\right)(\pi)(r_{\text{non-carbon}})^3 = \left(\frac{4}{3}\right)(\pi) \left[\frac{r_{\text{carbon}}}{\left(\frac{x}{y}\right)^{\frac{1}{2}}} \right]^3$$

$$\begin{aligned} \frac{\text{Volume}_{\text{carbon}}}{\text{Volume}_{\text{non-carbon}}} &= \frac{\left(\frac{4}{3}\right)(\pi)(r_{\text{carbon}})^3}{\left(\frac{4}{3}\right)(\pi) \left[\frac{r_{\text{carbon}}}{\left(\frac{x}{y}\right)^{\frac{1}{2}}} \right]^3} = \left(\frac{x}{y}\right)^{\frac{3}{2}} \\ \Rightarrow \text{Volume}_{\text{carbon}} &= \left(\frac{x}{y}\right)^{\frac{3}{2}} \text{Volume}_{\text{non-carbon}} \end{aligned}$$

$$\text{Volume}_{\text{non-carbon}} = \text{Total Volume} - \text{Volume}_{\text{carbon}}$$

$$\Rightarrow \text{Volume}_{\text{carbon}} = \left(\frac{x}{y}\right)^{\frac{3}{2}} (\text{Total Volume} - \text{Volume}_{\text{carbon}})$$

$$\Rightarrow (\text{Volume}_{\text{carbon}}) \left[1 + \left(\frac{x}{y}\right)^{\frac{3}{2}} \right] = \left(\frac{x}{y}\right)^{\frac{3}{2}} (\text{Total Volume})$$

$$\Rightarrow \frac{(\text{Volume}_{\text{carbon}})}{(\text{Total Volume})} = \frac{\left(\frac{x}{y}\right)^{\frac{3}{2}}}{\left[1 + \left(\frac{x}{y}\right)^{\frac{3}{2}} \right]} = \frac{1}{\left(\frac{y}{x}\right)^{\frac{3}{2}} + 1}$$

$$\% \text{ by Volume}_{\text{carbon}} = \frac{100}{\left(\frac{y}{x}\right)^{\frac{3}{2}} + 1}$$

In some cases, the percent by volume carbon can be determined by visual examination of the bulk sample material. Once this value is determined, the percent by mass carbon can be obtained by utilizing the respective component densities as follows:

$$\begin{aligned} \text{Mass}_{\text{non-carbon}} &= (\% \text{ by Volume}_{\text{non-carbon}})(\text{Total Volume})(\text{Mineral Density}) \\ &= (\% \text{ by Volume}_{\text{non-carbon}})(\text{Total Volume})(2.5) \end{aligned}$$

$$\begin{aligned} \text{Mass}_{\text{carbon}} &= (\% \text{ by Volume}_{\text{carbon}})(\text{Total Volume})(\text{Carbon Density}) \\ &= (\% \text{ by Volume}_{\text{carbon}})(\text{Total Volume})(1.0) \end{aligned}$$

$$\begin{aligned} \% \text{ by Mass}_{\text{carbon}} &= \left(\frac{\text{Mass}_{\text{carbon}}}{(\text{Mass}_{\text{carbon}} + \text{Mass}_{\text{non-carbon}})} \right) (100) \\ &= \left(\frac{(\% \text{ by Volume}_{\text{carbon}})(\text{Total Volume})(1.0)}{(\% \text{ by Volume}_{\text{carbon}})(\text{Total Volume})(1.0) + (\% \text{ by Volume}_{\text{non-carbon}})(\text{Total Volume})(2.5)} \right) (100) \\ &= \left(\frac{(\% \text{ by Volume}_{\text{carbon}})}{(\% \text{ by Volume}_{\text{carbon}}) + (\% \text{ by Volume}_{\text{non-carbon}})(2.5)} \right) (100) \end{aligned}$$

Appendix 4. Estimation of Soot Fraction Using SEM Data

After photocopying and enlargement of SEM micrographs, cutouts of soot and non-soot particles are separated and weighed. Let x = Soot Cutout Mass and y = Non-Soot Cutout Mass. The mass of the cutouts is directly proportional to the area of the cutouts. Therefore, x/y , the mass ratio, is equal to the area ratio. If one assumes all particles to be spherical and density to be uniform, the following conversions can be made:

r = radius of the particle

$$\text{Area} = (\pi)(r)^2$$

$$\left(\frac{x}{y}\right) = \left[\frac{(\pi)(r_{\text{soot}})^2}{(\pi)(r_{\text{non-soot}})^2} \right] \Rightarrow \left(\frac{x}{y}\right)^{\frac{1}{2}} = \left(\frac{r_{\text{soot}}}{r_{\text{non-soot}}}\right) \Rightarrow r_{\text{non-soot}} = \frac{r_{\text{soot}}}{\left(\frac{x}{y}\right)^{\frac{1}{2}}}$$

$$\text{Volume} = \left(\frac{4}{3}\right)(\pi)(r)^3$$

$$\text{Volume}_{\text{soot}} = \left(\frac{4}{3}\right)(\pi)(r_{\text{soot}})^3$$

$$\text{Volume}_{\text{non-soot}} = \left(\frac{4}{3}\right)(\pi)(r_{\text{non-soot}})^3 = \left(\frac{4}{3}\right)(\pi) \left[\frac{r_{\text{soot}}}{\left(\frac{x}{y}\right)^{\frac{1}{2}}} \right]^3$$

$$\frac{\text{Volume}_{\text{soot}}}{\text{Volume}_{\text{non-soot}}} = \frac{\left(\frac{4}{3}\right)(\pi)(r_{\text{soot}})^3}{\left(\frac{4}{3}\right)(\pi) \left[\frac{r_{\text{soot}}}{\left(\frac{x}{y}\right)^{\frac{1}{2}}} \right]^3} = \left(\frac{x}{y}\right)^{\frac{3}{2}}$$

$$\frac{\text{Mass}_{\text{soot}}}{\text{Mass}_{\text{non-soot}}} = \left(\frac{x}{y} \right)^{\frac{3}{2}} \Rightarrow \text{Mass}_{\text{soot}} = \left(\frac{x}{y} \right)^{\frac{3}{2}} (\text{Mass}_{\text{non-soot}})$$

Soot and non-soot masses can be calculated from the above equation, with the sum of uncorrected soot mass and non-soot mass being equal to elemental carbon residue mass.

Appendix 5. Raw Data for Berwind, Colorado

Table 11. Initial Sample Masses

Sample	Sample Mass (grams)	Error (grams)
Berwind 1	2.85300	0.00009
Berwind 2	1.39538	0.00009
Berwind 3	2.25714	0.00009
Berwind 4	1.43740	0.00009

Table 12. Empty Tube Masses

Sample	Mass 1 (grams)	Mass 2 (grams)	Mass 3 (grams)	Mass 4 (grams)
Berwind 1	13.68427	13.68428	13.68426	13.68425
Berwind 2	13.01585	13.01588	13.01588	13.01586
Berwind 3	13.24191	13.24189	13.24189	13.24189
Berwind 4	14.14708	14.14709	14.14706	14.14708

Table 13. Pre-Oxidation Tube + Sample Masses

Sample	Mass 1 (grams)	Mass 2 (grams)	Mass 3 (grams)	Mass 4 (grams)
Berwind 1	13.71932	13.71931	13.71933	13.71933
Berwind 2	14.15827	14.15831	14.15828	14.15827
Berwind 3	13.26330	13.26330	13.26330	13.26331
Berwind 4	14.19186	14.19185	14.19181	14.19185

Table 14. Post-Oxidation Tube + Sample Masses

Sample	Mass 1 (grams)	Mass 2 (grams)	Mass 3 (grams)
Berwind 1	13.68824	13.68828	13.68823
Berwind 2	13.88868	13.88867	13.88866
Berwind 3	13.24645	13.24647	13.24647
Berwind 4	14.15172	14.15172	14.15174

Table 15. SEM Soot Particle Cutout Masses

Sample	Mass 1 (grams)	Mass 2 (grams)	Mass 3 (grams)
Berwind 1	0.82279	0.82279	0.82283
Berwind 2	0.51875	0.51866	0.51864

Table 16. SEM Non-Soot Particle Cutout Masses

Sample	Mass 1 (grams)	Mass 2 (grams)	Mass 3 (grams)
Berwind 1	3.20182	3.20173	3.20179
Berwind 2	1.54015	1.54007	1.54009

Table 17. Upper Limit Assumptions for Soot Mass

Sample	Upper Limit (grams)	Absolute Error (grams)
Berwind 3	0.00001	0.00001
Berwind 4	0.00001	0.00001

Appendix 6. Raw Data for Madrid, Colorado

Table 18. Initial Sample Masses

Sample	Sample Mass (grams)	Error (grams)
Madrid 1	0.94995	0.00009
Madrid 2	0.88721	0.00009
Madrid 3	1.31719	0.00009
Madrid 4	0.99755	0.00009
Madrid 5	1.04348	0.00009

Table 19. Empty Tube Masses

Sample	Mass 1 (grams)	Mass 2 (grams)
Madrid 1	13.25326	13.25326
Madrid 2	13.29860	13.29860
Madrid 3	13.31115	13.31117
Madrid 4	13.13437	13.13438
Madrid 5	12.98037	12.98037

Table 20. Pre-Oxidation Tube + Sample Masses

Sample	Mass 1 (grams)	Mass 2 (grams)
Madrid 1	13.28490	13.28490
Madrid 2	13.89715	13.89716
Madrid 3	13.36086	13.36082
Madrid 4	13.42545	13.42543
Madrid 5	13.26153	13.26155

Table 21. Post-Oxidation Tube + Sample Masses

Sample	Mass 1 (grams)	Mass 2 (grams)
Madrid 1	13.25697	13.25697
Madrid 2	13.74323	13.74323
Madrid 3	13.31518	13.31518
Madrid 4	13.25443	13.25442
Madrid 5	13.12766	13.12766

Table 22. SEM Soot Particle Cutout + Beaker Masses

Sample	Mass 1 (grams)	Mass 2 (grams)	Mass 3 (grams)
Madrid 1	104.8585	104.8584	104.8585
Madrid 2	113.9167	113.9167	113.9167
Madrid 3	92.9821	92.9821	92.9820
Madrid 4	104.9852	104.9852	104.9851
Madrid 5	113.0528	113.0528	113.0527

Table 23. SEM Soot Beaker Masses

Sample	Mass 1 (grams)	Mass 2 (grams)	Mass 3 (grams)
Madrid 1	102.9857	102.98	102.9857
Madrid 2	110.7450	110.7451	110.7450
Madrid 3	91.4748	91.4747	91.4748
Madrid 4	104.1175	104.1175	104.1175
Madrid 5	110.7326	110.7327	110.7328

Table 24. SEM Non-Soot Particle Cutout + Beaker Masses

Sample	Mass 1 (grams)	Mass 2 (grams)	Mass 3 (grams)
Madrid 1	113.1690	113.1689	113.1689
Madrid 2	67.5345	67.5345	67.5344
Madrid 3	108.8837	108.8836	108.8835
Madrid 4	105.7296	105.7296	105.7296
Madrid 5	106.6532	106.6532	106.6530

Table 25. SEM Non-Soot Beaker Masses

Sample	Mass 1 (grams)	Mass 2 (grams)	Mass 3 (grams)
Madrid 1	110.6196	110.6195	110.6196
Madrid 2	66.0389	66.0389	66.0389
Madrid 3	103.2885	103.2885	103.2885
Madrid 4	104.0338	104.0337	104.0338
Madrid 5	104.0473	104.0475	104.0475

Appendix 7. Raw Data for DSDP Core 465-A

Table 26. Initial Sample Masses

Sample	Sample Mass 1 (grams)	Error (grams)	Sample Mass 2 (grams)	Error (grams)
Core 1	3.82138	0.00009	3.76358	0.00009
Core 2	3.89096	0.00009	1.74166	0.00009
Core 3	2.70593	0.00009	2.82872	0.00009
Core 4	3.18805	0.00009	1.97232	0.00009
Core 5	2.77826	0.00009	--	0.00009
Core 6	3.01097	0.00009	2.64966	0.00009
Core 7	3.04802	0.00009	2.63980	0.00009
Core 8	2.81280	0.00009	1.90009	0.00009
Core 9	1.82541	0.00009	1.22722	0.00009
Core 10	1.85528	0.00009	1.73221	0.00009
Core 11	1.71779	0.00009	--	0.00009

Table 27. Empty Tube Masses

Sample	Mass 1 (grams)	Mass 2 (grams)	Mass 3 (grams)	Mass 4 (grams)
Core 1	11.12734	11.12736	11.12737	11.12730
Core 2	11.24398	11.24401	11.24405	11.24403
Core 3	11.28402	11.28404	11.28404	11.28409
Core 4	11.27717	11.27719	11.27722	11.27725
Core 5	11.23022	11.23020	11.23019	11.23022
Core 6	11.19974	11.19971	11.19971	11.19968
Core 7	11.29872	11.29869	11.29870	11.29869
Core 8	11.29072	11.29070	11.29072	11.29073
Core 9	11.19589	11.19586	11.19586	11.19588
Core 10	11.20450	11.20448	11.20446	11.20453
Core 11	11.24527	11.24531	11.24528	11.24530

Table 28. Pre-Oxidation Tube + Sample Masses

Sample	Mass 1 (grams)	Mass 2 (grams)	Mass 3 (grams)
Core 1	11.12763	11.12757	11.12757
Core 2	11.24445	11.24447	11.24449
Core 3	11.28408	11.28409	11.28411
Core 4	11.27740	11.27738	11.27737
Core 5	11.23126	11.23127	11.23128
Core 6	11.20110	11.20110	11.20112
Core 7	11.30112	11.30124	11.30121
Core 8	11.29416	11.29413	11.29414
Core 9	11.19862	11.19863	11.19860
Core 10	11.20926	11.20930	11.20927
Core 11	11.25456	11.25455	11.25453

Table 29. Post-Oxidation Tube + Sample Masses

Sample	Mass 1 (grams)	Mass 2 (grams)	Mass 3 (grams)
Core 1	11.12348	11.12344	11.12346
Core 2	11.24060	11.24057	11.24058
Core 3	11.27973	11.27973	11.27972
Core 4	11.27398	11.27399	11.27397
Core 5	11.22620	11.22618	11.22616
Core 6	11.19693	11.19694	11.19694
Core 7	11.29619	11.29618	11.29616
Core 8	11.28775	11.28774	11.28773
Core 9	11.19301	11.19300	11.19298
Core 10	11.20127	11.20148	11.20150
Core 11	11.24282	11.24280	11.24280

Table 30. SEM Soot Particle Cutout + Beaker Masses

Sample	Mass 1 (grams)	Mass 2 (grams)	Mass 3 (grams)
Core 9	50.14348	50.14342	50.14337
Core 11	57.15318	57.15322	57.15321

Table 31. SEM Soot Beaker Masses

Sample	Mass 1 (grams)	Mass 2 (grams)	Mass 3 (grams)
Core 9	49.92030	49.92030	49.92031
Core 11	56.85888	56.85884	56.85888

Table 32. SEM Non-Soot Particle Cutout + Beaker Masses

Sample	Mass 1 (grams)	Mass 2 (grams)	Mass 3 (grams)
Core 9	45.75786	45.75781	45.75778
Core 11	66.79360	66.79360	66.79350

Table 33. SEM Non-Soot Beaker Masses

Sample	Mass 1 (grams)	Mass 2 (grams)	Mass 3 (grams)
Core 9	45.37274	45.37276	45.37280
Core 11	66.03840	66.03840	66.03840

Table 34. Upper Limit Assumptions for Soot Mass

Sample	Upper Limit (grams)	Absolute Error (grams)
Core 1	0.00001	0.00001
Core 2	0.00001	0.00001
Core 3	0.00001	0.00001
Core 4	0.00001	0.00001
Core 5	0.00001	0.00001
Core 6	0.00001	0.00001
Core 7	0.00001	0.00001
Core 8	0.00001	0.00001
Core 10	0.00001	0.00001

Appendix 8. Raw Data for the Sudbury Impact Structure, Canada

Table 35. Initial Sample Masses

Sample	Sample Mass (grams)	Error (grams)
Sudbury 22	1.81346	0.00009
Sudbury 20	1.92985	0.00009
Sudbury 16	1.94528	0.00009
Sudbury 12	1.91319	0.00009
Sudbury 7	1.97381	0.00009
Sudbury 1	1.25153	0.00009

Table 36. Empty Tube Masses

Sample	Mass 1 (grams)	Mass 2 (grams)	Mass 3 (grams)
Sudbury 22	14.15604	14.15604	14.15604
Sudbury 20	21.33408	21.33409	21.33408
Sudbury 16	22.09858	22.09862	22.09858
Sudbury 12	13.04060	13.04061	13.04060
Sudbury 7	13.13434	13.13428	13.13432
Sudbury 1	21.16954	21.16952	21.16951

Table 37. Pre-Oxidation Tube + Sample Masses

Sample	Mass 1 (grams)	Mass 2 (grams)	Mass 3 (grams)
Sudbury 22	14.35625	14.35625	14.35625
Sudbury 20	21.46767	21.46768	21.46766
Sudbury 16	22.18822	22.18822	22.18820
Sudbury 12	13.31980	13.31981	13.31979
Sudbury 7	13.27934	13.27934	13.27935
Sudbury 1	21.18303	21.18303	21.18306

Table 38. Post-Oxidation Tube + Sample Masses

Sample	Mass 1 (grams)	Mass 2 (grams)	Mass 3 (grams)
Sudbury 22	14.29171	14.29171	14.29174
Sudbury 20	21.39078	21.39080	21.39082
Sudbury 16	22.12250	22.12251	22.12252
Sudbury 12	13.20039	13.20038	13.20041
Sudbury 7	13.24453	13.24454	13.24456
Sudbury 1	21.17179	21.17179	21.17179

Table 39. SEM Soot Particle Cutout Masses

Sample	Mass 1 (grams)	Mass 2 (grams)	Mass 3 (grams)
Sudbury 22	0.04714	0.04713	0.04715
Sudbury 20	0.48536	0.48535	0.48537
Sudbury 16	0.74421	0.74418	0.74417
Sudbury 12	0.20925	0.20923	0.20920
Sudbury 7	0.12143	0.12133	0.12126
Sudbury 1	3.89322	3.89319	3.89312

Table 40. SEM Non-Soot Particle Cutout Masses

Sample	Mass 1 (grams)	Mass 2 (grams)	Mass 3 (grams)
Sudbury 22	6.0697	6.0697	6.0696
Sudbury 20	8.9616	8.9617	8.9619
Sudbury 16	3.4784	3.4784	3.4784
Sudbury 12	3.0829	3.0828	3.0828
Sudbury 7	5.5461	5.5461	5.5461
Sudbury 1	1.9515	1.9514	1.9514

Appendix 9. Raw Data for the Gardnos Impact Structure, Norway

Table 41. Initial Sample Masses

Sample	Sample Mass (grams)	Error (grams)
Gardnos 19	1.22335	0.00009
Gardnos 20	1.23980	0.00009
Gardnos 21	1.38572	0.00009
Gardnos 22	1.58972	0.00009
Gardnos 157	1.30216	0.00009
Gardnos 158	1.22597	0.00009
Gardnos 159	1.44966	0.00009
Gardnos 160a	2.38759	0.00009
Gardnos 160b	2.14910	0.00009
Gardnos 161a	1.26088	0.00009
Gardnos 161b	2.12160	0.00009
Gardnos 162a	1.22015	0.00009
Gardnos 162b	2.05165	0.00009
Gardnos 162c	2.05893	0.00009
Gardnos 129	2.35474	0.00009
Gardnos 126	2.52514	0.00009
Gardnos 120	2.45246	0.00009
Gardnos 121	2.54749	0.00009
Gardnos 143	2.03032	0.00009
Gardnos 176*	2.45272	0.00009
Gardnos 172	1.34700	0.00009
Gardnos 179	2.48521	0.00009
Gardnos 178	2.46650	0.00009
Gardnos 133	2.37714	0.00009
Gardnos 137	2.26706	0.00009
Gardnos 175	2.50408	0.00009
Gardnos 137 B	1.32379	0.00009
Gardnos 140	1.23762	0.00009
Gardnos 141	1.28982	0.00009
Gardnos 142	1.32847	0.00009
Gardnos 164	2.56444	0.00009
Gardnos 171	2.42848	0.00009
Gardnos 170	2.24192	0.00009
Gardnos 169	2.25117	0.00009
Gardnos 168	2.17210	0.00009
Gardnos 167	2.17748	0.00009

*Sample was dropped on floor and part was lost. All masses from Table 81 to Table 97 are based only on 0.5000 +/- 0.0005 of the original sample mass. This correction is accounted for in Table 98.

Table 42. Empty Tube Masses

Sample	Mass 1 (grams)	Mass 2 (grams)	Mass 3 (grams)
Gardnos 19	21.76025	21.76023	21.76027
Gardnos 20	13.99987	13.99986	13.99986
Gardnos 21	13.72154	13.72154	13.72154
Gardnos 22	13.12929	13.12927	13.12927
Gardnos 157	12.98882	12.98881	12.98879
Gardnos 158	13.15504	13.15506	13.15503
Gardnos 159	21.31807	21.31806	21.31806
Gardnos 160a	12.97191	12.97187	12.97190
Gardnos 160b	11.64304	11.64305	11.64309
Gardnos 161a	13.31803	13.31809	13.31806
Gardnos 161b	11.62317	11.62317	11.62319
Gardnos 162a	22.09143	22.09141	22.09142
Gardnos 162b	11.63055	11.63054	11.63053
Gardnos 162c	11.90774	11.90776	11.90774
Gardnos 129	11.21884	11.21882	11.21881
Gardnos 126	11.35232	11.35232	11.35232
Gardnos 120	11.31079	11.31078	11.31078
Gardnos 121	11.31650	11.31649	11.31648
Gardnos 143	11.21410	11.21409	11.21409
Gardnos 176	14.13588	14.13586	14.13589
Gardnos 172	13.10256	13.10254	13.10253
Gardnos 179	13.04689	13.04688	13.04687
Gardnos 178	11.21391	11.21390	11.21390
Gardnos 133	13.24232	13.24235	13.24235
Gardnos 137	13.66128	13.66129	13.66127
Gardnos 175	11.21674	11.21672	11.21674
Gardnos 137 B	21.46242	21.46240	21.46241
Gardnos 140	21.82319	21.82319	21.82319
Gardnos 141	13.11208	13.11205	13.11207
Gardnos 142	13.68548	13.68548	13.68547
Gardnos 164	11.14044	11.14042	11.14043
Gardnos 171	11.31256	11.31258	11.31257
Gardnos 170	11.26469	11.26467	11.26466
Gardnos 169	11.26499	11.26496	11.26498
Gardnos 168	11.88990	11.88993	11.88996
Gardnos 167	11.71678	11.71678	11.71676

Table 43. Pre-Oxidation Tube + Sample Masses

Sample	Mass 1 (grams)	Mass 2 (grams)	Mass 3 (grams)
Gardnos 19	21.76384	21.76382	21.76380
Gardnos 20	14.00723	14.00722	14.00723
Gardnos 21	13.73641	13.73643	13.73640
Gardnos 22	13.18425	13.18423	13.18425
Gardnos 157	12.99305	12.99305	12.99307
Gardnos 158	13.16657	13.16655	13.16653
Gardnos 159	21.32223	21.32222	21.32220
Gardnos 160a	13.09782	13.09781	13.09785
Gardnos 160b	11.69110	11.69110	11.69110
Gardnos 161a	13.38020	13.38018	13.38017
Gardnos 161b	11.66585	11.66582	11.66587
Gardnos 162a	22.13722	22.13721	22.13720
Gardnos 162b	11.67552	11.67550	11.67553
Gardnos 162c	11.95716	11.95715	11.95711
Gardnos 129	11.22439	11.22440	11.22438
Gardnos 126	11.59187	11.59190	11.59190
Gardnos 120	11.31952	11.31951	11.31953
Gardnos 121	11.34928	11.34925	11.34926
Gardnos 143	11.21620	11.21619	11.21621
Gardnos 176	14.14061	14.14060	14.14060
Gardnos 172	13.10648	13.10646	13.10647
Gardnos 179	13.04963	13.04964	13.04964
Gardnos 178	11.24418	11.24416	11.24417
Gardnos133	13.25770	13.25771	13.25770
Gardnos 137	13.74623	13.74621	13.74621
Gardnos 175	11.24675	11.24672	11.24676
Gardnos 137 B	21.47403	21.47400	21.47405
Gardnos 140	21.82523	21.82525	21.82527
Gardnos 141	13.11301	13.11300	13.11299
Gardnos 142	13.69379	13.69379	13.69377
Gardnos 164	11.34572	11.34572	11.34572
Gardnos 171	11.51234	11.51233	11.51235
Gardnos 170	11.31343	11.31345	11.31346
Gardnos 169	11.33050	11.33051	11.33053
Gardnos 168	11.89175	11.89175	11.89175
Gardnos 167	11.71659	11.71656	11.71657

Table 44. Post-Oxidation Tube + Sample Masses

Sample	Mass 1 (grams)	Mass 2 (grams)	Mass 3 (grams)
Gardnos 19	21.76356	21.76355	21.76356
Gardnos 20	14.00449	14.00449	14.00450
Gardnos 21	13.72774	13.72774	13.72773
Gardnos 22	13.16049	13.16048	13.16050
Gardnos 157	12.99034	12.99035	12.99034
Gardnos 158	13.15731	13.15732	13.15731
Gardnos 159	21.31884	21.31886	21.31884
Gardnos 160a	13.02185	13.02183	13.02181
Gardnos 160b	11.64571	11.64570	11.64573
Gardnos 161a	13.33244	13.33242	13.33242
Gardnos 161b	11.62385	11.62384	11.62387
Gardnos 162a	22.10381	22.10382	22.10383
Gardnos 162b	11.63424	11.63428	11.63425
Gardnos 162c	11.91371	11.91373	11.91375
Gardnos 129	11.21610	11.21611	11.21612
Gardnos 126	11.40018	11.40019	11.40020
Gardnos 120	11.31389	11.31392	11.31389
Gardnos 121	11.31557	11.31557	11.31557
Gardnos 143	11.21040	11.21042	11.21039
Gardnos 176	14.13697	14.13701	14.13699
Gardnos 172	13.10246	13.10245	13.10247
Gardnos 179	13.04789	13.04792	13.04791
Gardnos 178	11.27355	11.27357	11.27355
Gardnos 133	13.24742	13.24740	13.24740
Gardnos 137	13.69630	13.69633	13.69632
Gardnos 175	11.21219	11.21219	11.21217
Gardnos 137 B	21.46632	21.46632	21.46634
Gardnos 140	21.82358	21.82363	21.82360
Gardnos 141	13.11264	13.11266	13.11268
Gardnos 142	13.68865	13.68863	13.68867
Gardnos 164	11.26883	11.26883	11.26886
Gardnos 171	11.35351	11.35351	11.35352
Gardnos 170	11.26724	11.26723	11.26725
Gardnos 169	11.27002	11.27002	11.27003
Gardnos 168	11.89170	11.89169	11.89170
Gardnos 167	11.71642	11.71640	11.71642

Table 45. Percent Carbon* by Volume of Post-Oxidation Residue

Sample	%Carbon (by volume)
Gardnos 19	1.0
Gardnos 20	3.0
Gardnos 21	15
Gardnos 22	98
Gardnos 157	30
Gardnos 158	25
Gardnos 159	1.0
Gardnos 160b	2.0
Gardnos 161a	15
Gardnos 161b	3.0
Gardnos 162a	1.0
Gardnos 162b	2.0
Gardnos 162c	2.0
Gardnos 172	87
Gardnos 137 B	98
Gardnos 140	60
Gardnos 141	50
Gardnos 142	95
Gardnos 168	1.0
Gardnos 167	1.0

*Based on visual estimates

Table 46. Carbon and Non-Carbon Fraction of SEM Image Area of Post-Oxidation Residue

Sample	Carbon Fraction	Non-Carbon Fraction
Gardnos 160a	0.050	0.063
Gardnos 129	0.056	0.111
Gardnos 126	0.375	0.143
Gardnos 120	0.083	0.125
Gardnos 121	0.024	0.100
Gardnos 143	0.083	0.036
Gardnos 176	0.063	0.167
Gardnos 179	0.040	0.056
Gardnos 178	0.167	0.050
Gardnos133	0.063	0.050
Gardnos 137	0.083	0.063
Gardnos 175	0.100	0.042
Gardnos 164	0.800	0.040
Gardnos 171	0.111	0.083
Gardnos 170	0.200	0.063
Gardnos 169	0.083	0.167

*Based on visual SEM estimates

Table 47. SEM Soot Particle Cutout Masses*

Sample	Mass 1 (grams)	Mass 2 (grams)	Mass 3 (grams)
Gardnos 19	0.04652	0.04651	0.04656
Gardnos 22	0.24599	0.24591	0.24594
Gardnos 157	0.36578	0.36580	0.36578
Gardnos 158	0.04635	0.04631	0.04639
Gardnos 159	0.12034	0.12027	0.12027
Gardnos 161a	2.72823	2.72816	2.72815
Gardnos 161b	0.13594	0.13604	0.13603
Gardnos 172	1.18157	1.18149	1.18141
Gardnos 137 B	0.20414	0.20408	0.20406
Gardnos 141	0.66166	0.66165	0.66168

Table 48. SEM Non-Soot Particle Cutout Masses*

Sample	Mass 1 (grams)	Mass 2 (grams)	Mass 3 (grams)
Gardnos 19	0.54806	0.54803	0.54798
Gardnos 22	0.96274	0.96260	0.96262
Gardnos 157	2.78500	2.78494	2.78504
Gardnos 158	1.07802	1.07808	1.07798
Gardnos 159	1.27713	1.27706	1.27696
Gardnos 161a	1.43465	1.43442	1.43434
Gardnos 161b	0.99858	0.99846	0.99847
Gardnos 172	3.98886	3.98880	3.98879
Gardnos 137 B	3.11541	3.11537	3.11539
Gardnos 141	3.01453	3.01460	3.01460

*These masses were obtained by direct measurement, differing from those presented in the calculated data section that were calculated from the difference between the cutout + beaker mass and the beaker mass.

Table 49. SEM Soot Particle Cutout + Beaker Masses

Sample	Mass 1 (grams)	Mass 2 (grams)	Mass 3 (grams)
Gardnos 160a	111.5687	111.5685	111.5685
Gardnos 129	111.1014	111.1014	111.1014
Gardnos 126	103.8217	103.8217	103.8216
Gardnos 143	108.1054	108.1054	108.1054
Gardnos 176	110.8030	110.8031	110.8029
Gardnos 179	104.9464	104.9464	104.9463
Gardnos 178	56.8975	56.8975	56.8975
Gardnos 133	98.5461	98.5461	98.5459
Gardnos 137	104.6487	104.6486	104.6486
Gardnos 175	66.5134	66.5135	66.5134
Gardnos 164	104.4525	104.4524	104.4524
Gardnos 171	113.0569	113.0569	113.0569
Gardnos 170	109.3799	109.3799	109.3798
Gardnos 169	109.5517	109.5517	109.5517

Table 50. SEM Soot Beaker Masses

Sample	Mass 1 (grams)	Mass 2 (grams)	Mass 3 (grams)
Gardnos 160a	109.9028	109.9029	109.9028
Gardnos 129	110.8037	110.8037	110.8037
Gardnos 126	103.5144	103.5143	103.5143
Gardnos 143	107.9389	107.9390	107.9388
Gardnos 176	110.7255	110.7256	110.7256
Gardnos 179	104.1179	104.1179	104.1179
Gardnos 178	56.8585	56.8584	56.8585
Gardnos133	98.5181	98.5182	98.5180
Gardnos 137	104.3581	104.3581	104.3580
Gardnos 175	66.1378	66.1377	66.1377
Gardnos 164	104.0177	104.0176	104.0177
Gardnos 171	111.7866	111.7866	111.7866
Gardnos 170	108.5262	108.5260	108.5260
Gardnos 169	108.0474	108.0473	108.0473

Table 51. SEM Non-Soot Particle Cutout + Beaker Masses

Sample	Mass 1 (grams)	Mass 2 (grams)	Mass 3 (grams)
Gardnos 160a	102.1764	102.1764	102.1764
Gardnos 129	107.6932	107.6931	107.6932
Gardnos 126	109.3111	109.3112	109.3112
Gardnos 143	106.1040	106.1040	106.1040
Gardnos 176	99.1585	99.1583	99.1583
Gardnos 179	106.8304	106.8303	106.8305
Gardnos 178	102.2618	102.2617	102.2616
Gardnos133	102.3546	102.3544	102.3544
Gardnos 137	104.6787	104.6787	104.6787
Gardnos 175	114.0352	114.0353	114.0353
Gardnos 164	114.0352	114.0353	114.0353
Gardnos 171	106.2794	106.2794	106.2794
Gardnos 170	104.4545	104.4544	104.4546
Gardnos 169	92.7497	92.7496	92.7495

Table 52. SEM Non-Soot Beaker Masses

Sample	Mass 1 (grams)	Mass 2 (grams)	Mass 3 (grams)
Gardnos 160a	100.5007	100.5006	100.5006
Gardnos 129	107.1647	107.1647	107.1647
Gardnos 126	105.6295	105.6295	105.6295
Gardnos 143	105.1781	105.1780	105.1780
Gardnos 176	98.0234	98.0233	98.0233
Gardnos 179	104.3310	104.3309	104.3309
Gardnos 178	100.2821	100.2822	100.2821
Gardnos 133	101.5539	101.5538	101.5537
Gardnos 137	102.0163	102.0163	102.0164
Gardnos 175	102.7842	102.7842	102.7842
Gardnos 164	110.8228	110.8228	110.8227
Gardnos 171	104.6787	104.6787	104.6787
Gardnos 170	103.3973	103.3971	103.3972
Gardnos 169	91.5742	91.5742	91.5742

Table 53. Upper Limit Assumptions for Soot Mass

Sample	Upper Limit (grams)	Absolute Error (grams)
Gardnos 20	0.00001	0.00001
Gardnos 21	0.00001	0.00001
Gardnos 160b	0.00001	0.00001
Gardnos 162a	0.00001	0.00001
Gardnos 162b	0.00001	0.00001
Gardnos 162c	0.00001	0.00001
Gardnos 120	0.00001	0.00001
Gardnos 121	0.00001	0.00001
Gardnos 140	0.00001	0.00001
Gardnos 142	0.00001	0.00001
Gardnos 168	0.00001	0.00001
Gardnos 167	0.00001	0.00001

Appendix 10. Calculated Data for Berwind, Colorado

Table 54. Mean Empty Tube Mass and Standard Deviation

Sample	Mean Mass (grams)	Standard Deviation (grams)
Berwind 1	13.68427	0.00001
Berwind 2	13.01587	0.00002
Berwind 3	13.24190	0.00001
Berwind 4	14.14708	0.00001

Table 55. Mean Tube + Pre-Oxidation Sample Mass and Standard Deviation

Sample	Mean Mass (grams)	Standard Deviation (grams)
Berwind 1	13.71932	0.00001
Berwind 2	14.15828	0.00002
Berwind 3	13.26330	0.00001
Berwind 4	14.19184	0.00002

Table 56. Mean Tube + Post-Oxidation Sample Mass and Standard Deviation

Sample	Mean Mass (grams)	Standard Deviation (grams)
Berwind 1	13.68825	0.00003
Berwind 2	13.88867	0.00001
Berwind 3	13.24646	0.00001
Berwind 4	14.15173	0.00001

Table 57. Pre-Oxidation Sample Mass and Absolute Error

Sample	Sample Mass (grams)	Absolute Error (grams)
Berwind 1	0.03506	0.00002
Berwind 2	1.14242	0.00002
Berwind 3	0.02141	0.00001
Berwind 4	0.04476	0.00003

Table 58. Post-Oxidation Sample Mass and Absolute Error

Sample	Sample Mass (grams)	Absolute Error (grams)
Berwind 1	0.00399	0.00003
Berwind 2	0.87280	0.00002
Berwind 3	0.00457	0.00002
Berwind 4	0.00465	0.00002

Table 59. Mean SEM Particle Cutout Masses and Standard Deviations

Sample	Mean Soot Mass (grams)	Standard Deviation (grams)	Mean Non-Soot Mass (grams)	St.
Berwind 1	3.20178	0.00005	3.20178	
Berwind 2	1.54010	0.00004	1.54010	0.

Table 60. Soot to Non-Soot Area Ratio, Volumetric Ratio, and Corresponding

Sample	Area Ratio	Absolute Error	Volumetric Ratio	Absolute Er.
Berwind 1	0.25698	0.00001	0.13027	0.00001
Berwind 2	0.33678	0.00004	0.19545	0.00005

Table 61. Soot Mass, Non-Soot Mass, Corrected Soot Mass, and Corresponding Absolute

Sample	Soot Mass (grams)	Absolute Error (grams)	Non-Soot Mass (grams)	Absolute Error (grams)	Corr Mass
Berwind 1	0.00353	0.00003	0.00046	0.00004	0.06
Berwind 2	0.73011	0.00017	0.14270	0.00017	0.297
Berwind 3	0.00456	0.00002	0.00001	0.00001	0.00002
Berwind 4	0.00464	0.00002	0.00001	0.00001	0.00002

Table 62. Concentration of Soot and Absolute Error

Sample	Soot (ppm)	Absolute Error (ppm)
Berwind 1	1200	0
Berwind 2	520000	0
Berwind 3	2000	0
Berwind 4	3000	0

Appendix 11. Calculated Data for Madrid, Colorado

Table 63. Mean Empty Tube Mass and Standard Deviation

Sample	Mean Mass (grams)	Standard Deviation (grams)
Madrid 1	13.25326	0.00000
Madrid 2	13.29860	0.00000
Madrid 3	13.31116	0.00001
Madrid 4	13.13438	0.00001
Madrid 5	12.98037	0.00000

Table 64. Mean Tube + Pre-Oxidation Sample Mass and Standard Deviation

Sample	Mean Mass (grams)	Standard Deviation (grams)
Madrid 1	13.28490	0.00000
Madrid 2	13.89716	0.00001
Madrid 3	13.36084	0.00003
Madrid 4	13.42544	0.00001
Madrid 5	13.26154	0.00001

Table 65. Mean Tube + Post-Oxidation Sample Mass and Standard Deviation

Sample	Mean Mass (grams)	Standard Deviation (grams)
Madrid 1	13.25697	0.00000
Madrid 2	13.74323	0.00000
Madrid 3	13.31518	0.00000
Madrid 4	13.25443	0.00001
Madrid 5	13.12766	0.00000

Table 66. Pre-Oxidation Sample Mass and Absolute Error

Sample	Sample Mass (grams)	Absolute Error (grams)
Madrid 1	0.03164	0.00000
Madrid 2	0.59855	0.00001
Madrid 3	0.04968	0.00003
Madrid 4	0.29107	0.00002
Madrid 5	0.28117	0.00001

Table 67. Post-Oxidation Sample Mass and Absolute Error

Sample	Sample Mass (grams)	Absolute Error (grams)
Madrid 1	0.00371	0.00000
Madrid 2	0.44463	0.00000
Madrid 3	0.00402	0.00001
Madrid 4	0.12005	0.00001
Madrid 5	0.14729	0.00000

Table 68. Mean SEM Particle Cutout + Beaker Masses and Standard Deviations

Sample	Mean Soot Mass (grams)	Standard Deviation (grams)	Mean Non-Soot Mass (grams)	Standard Deviation (grams)
Madrid 1	104.8585	0.0001	113.1689	0.0001
Madrid 2	113.9167	0.0000	67.5345	0.0001
Madrid 3	92.9821	0.0001	108.8836	0.0001
Madrid 4	104.9852	0.0001	105.7296	0.0000
Madrid 5	113.0528	0.0001	106.6531	0.0001

Table 69. Mean SEM Beaker Masses and Standard Deviations

Sample	Mean Soot Beaker Mass (grams)	Standard Deviation (grams)	Mean Non-Soot Beaker Mass (grams)	Standard Deviation (grams)
Madrid 1	102.9857	0.0000	110.6196	0.0001
Madrid 2	110.7450	0.0001	66.0389	0.0000
Madrid 3	91.4748	0.0001	103.2885	0.0000
Madrid 4	104.1175	0.0000	104.0338	0.0001
Madrid 5	110.7327	0.0001	104.0474	0.0001

Table 70. SEM Cutout Masses and Standard Deviations

Sample	Soot Mass (grams)	Standard Deviation (grams)	Non-Soot Mass (grams)	Standard Deviation (grams)
Madrid 1	1.8728	0.0001	2.5494	0.0001
Madrid 2	3.1717	0.0001	1.4956	0.0001
Madrid 3	1.5073	0.0001	5.5951	0.0001
Madrid 4	0.8677	0.0001	1.6958	0.0001
Madrid 5	2.3201	0.0001	2.6057	0.0002

Table 71. Soot to Non-Soot Area Ratio, Volumetric Ratio, and Corresponding Absolute Errors

Sample	Area Ratio	Absolute Error	Volumetric Ratio	Absolute Error
Madrid 1	0.73460	0.00003	0.62962	0.00006
Madrid 2	2.12071	0.00009	3.08832	0.00026
Madrid 3	0.26940	0.00002	0.13983	0.00002
Madrid 4	0.51165	0.00004	0.36598	0.00005
Madrid 5	0.89038	0.00007	0.84016	0.00013

Table 72. Soot Mass, Non-Soot Mass, Corrected Soot Mass, and Corresponding Absolute Errors

Sample	Soot Mass (grams)	Absolute Error (grams)	Non-Soot Mass (grams)	Absolute Error (grams)	Corrected Soot Mass (grams)	Absolute Error (grams)
Madrid 1	0.0014	0.0000	0.0023	0.0000	0.0030	0.0003
Madrid 2	0.3359	0.0000	0.1088	0.0000	0.6997	0.0729
Madrid 3	0.0005	0.0000	0.0035	0.0000	0.0010	0.0001
Madrid 4	0.0322	0.0000	0.0879	0.0000	0.0670	0.0070
Madrid 5	0.0672	0.0000	0.0800	0.0000	0.1401	0.0146

Table 73. Concentration Soot and Absolute Error

Sample	Soot (ppm)	Absolute Error (ppm)
Madrid 1	3100	300
Madrid 2	790000	82000
Madrid 3	780	90
Madrid 4	67000	7000
Madrid 5	130000	14000

Appendix 12. Calculated Data for DSDP Core 465-A

Table 74. Total Initial Sample Mass and Absolute Error

Sample	Rock Mass (grams)	Absolute Error (grams)
Core 1	7.58496	0.00013
Core 2	5.63262	0.00013
Core 3	5.53465	0.00013
Core 4	5.16037	0.00013
Core 5	2.77826	0.00013
Core 6	5.66063	0.00013
Core 7	5.68782	0.00013
Core 8	4.71289	0.00013
Core 9	3.05263	0.00013
Core 10	3.58749	0.00013
Core 11	1.71779	0.00013

Table 75. Mean Empty Tube Mass and Standard Deviation

Sample	Mean Mass (grams)	Standard Deviation (grams)
Core 1	11.12734	0.00003
Core 2	11.24402	0.00003
Core 3	11.28405	0.00003
Core 4	11.27721	0.00003
Core 5	11.23021	0.00002
Core 6	11.19971	0.00002
Core 7	11.29870	0.00001
Core 8	11.29072	0.00001
Core 9	11.19587	0.00001
Core 10	11.20449	0.00003
Core 11	11.24529	0.00002

Table 76. Mean Tube + Pre-Oxidation Sample Mass and Standard Deviation

Sample	Mean Mass (grams)	Standard Deviation (grams)
Core 1	11.12759	0.00003
Core 2	11.24447	0.00002
Core 3	11.28409	0.00002
Core 4	11.27738	0.00002
Core 5	11.23127	0.00001
Core 6	11.20111	0.00001
Core 7	11.30119	0.00006
Core 8	11.29414	0.00002
Core 9	11.19862	0.00002
Core 10	11.20928	0.00002
Core 11	11.25455	0.00002

Table 77. Mean Tube + Post-Oxidation Sample Mass and Standard Deviation

Sample	Mean Mass (grams)	Standard Deviation (grams)
Core 1	11.12346	0.00002
Core 2	11.24058	0.00002
Core 3	11.27973	0.00001
Core 4	11.27398	0.00001
Core 5	11.22618	0.00002
Core 6	11.19694	0.00001
Core 7	11.29618	0.00002
Core 8	11.28774	0.00001
Core 9	11.19300	0.00002
Core 10	11.20142	0.00013
Core 11	11.24281	0.00001

Table 78. Pre-Oxidation Sample Mass and Absolute Error

Sample	Sample Mass (grams)	Absolute Error (grams)
Core 1	0.00025	0.00005
Core 2	0.00045	0.00004
Core 3	0.00005	0.00003
Core 4	0.00018	0.00004
Core 5	0.00106	0.00002
Core 6	0.00140	0.00003
Core 7	0.00249	0.00006
Core 8	0.00343	0.00002
Core 9	0.00274	0.00002
Core 10	0.00478	0.00004
Core 11	0.00926	0.00002

Table 79. Post-Oxidation Sample Mass, Corrected* Post-Oxidation Sample Mass, and Absolute Errors

Sample	Sample Mass (grams)	Absolute Error (grams)	Corrected* Sample Mass (grams)	Absolute Error (grams)
Core 1	-0.00388	0.00004	0.00000	0.00000
Core 2	-0.00343	0.00003	0.00000	0.00000
Core 3	-0.00432	0.00003	0.00000	0.00000
Core 4	-0.00323	0.00004	0.00000	0.00000
Core 5	-0.00403	0.00003	0.00000	0.00000
Core 6	-0.00277	0.00003	0.00000	0.00000
Core 7	-0.00252	0.00002	0.00000	0.00000
Core 8	-0.00298	0.00002	0.00000	0.00000
Core 9	-0.00288	0.00002	0.00192	0.00048
Core 10	-0.00308	0.00013	0.00172	0.00050
Core 11	-0.00248	0.00002	0.00232	0.00048

*Those samples for which a mass of 0.00000 +/- 0.00000 grams is shown were assigned this mass because no visual sample was present.

Table 80. Mean SEM Particle Cutout + Beaker Masses and Standard Deviations

Sample	Mean Soot Mass (grams)	Standard Deviation (grams)	Mean Non-Soot Mass (grams)	Standard Deviation (grams)
Core 9	50.14342	0.00006	45.75782	0.00004
Core 11	57.15320	0.00002	66.79357	0.00006

Table 81. Mean SEM Beaker Masses and Standard Deviations

Sample	Mean Soot Beaker Mass (grams)	Standard Deviation (grams)	Mean Non-Soot Beaker Mass (grams)	Standard Deviation (grams)
Core 9	49.92030	0.00001	45.37277	0.00003
Core 11	56.85887	0.00002	66.03840	0.00000

Table 82. Mean SEM Cutout Masses and Standard Deviations

Sample	Soot Mass (grams)	Standard Deviation (grams)	Non-Soot Mass (grams)	Standard Deviation (grams)
Core 9	0.22312	0.00006	0.38505	0.00005
Core 11	0.29434	0.00003	0.75517	0.00006

Table 83. Soot to Non-Soot Area Ratio, Volumetric Ratio, and Corresponding Absolute Errors

Sample	Area Ratio	Absolute Error	Volumetric Ratio	Absolute Error
Core 9	0.57946	0.00016	0.44109	0.00019
Core 11	0.38976	0.00005	0.24333	0.00005

Table 84. Soot Mass, Non-Soot Mass, Corrected Soot Mass, and Corresponding Absolute Errors

Sample	Soot Mass (grams)	Absolute Error (grams)	Non-Soot Mass (grams)	Absolute Error (grams)	Corrected Soot Mass (grams)	Absolute Error (grams)
Core 1	0.00001	0.00001	0.00000	0.00001	0.00002	0.00002
Core 2	0.00001	0.00001	0.00000	0.00001	0.00002	0.00002
Core 3	0.00001	0.00001	0.00000	0.00001	0.00002	0.00002
Core 4	0.00001	0.00001	0.00000	0.00001	0.00002	0.00002
Core 5	0.00001	0.00001	0.00000	0.00001	0.00002	0.00002
Core 6	0.00001	0.00001	0.00000	0.00001	0.00002	0.00002
Core 7	0.00001	0.00001	0.00000	0.00001	0.00002	0.00002
Core 8	0.00001	0.00001	0.00000	0.00001	0.00002	0.00002
Core 9	0.00059	0.00058	0.00134	0.00033	0.00123	0.00122
Core 10	0.00001	0.00001	0.00000	0.00001	0.00002	0.00002
Core 11	0.00045	0.00062	0.00186	0.00039	0.00094	0.00129

Table 85. Concentration Soot and Absolute Error

Sample	Soot (ppm)	Absolute Error (ppm)
Core 1	3	3
Core 2	4	4
Core 3	4	4
Core 4	4	4
Core 5	7	8
Core 6	4	4
Core 7	4	4
Core 8	4	4
Core 9	402	401
Core 10	6	6
Core 11	550	750

Appendix 13. Calculated Data for the Sudbury Impact Structure, Canada

Table 86. Mean Empty Tube Mass and Standard Deviation

Sample	Mean Mass (grams)	Standard Deviation (grams)
Sudbury 22	14.15604	0.00000
Sudbury 20	21.33408	0.00001
Sudbury 16	22.09859	0.00002
Sudbury 12	13.04060	0.00000
Sudbury 7	13.13431	0.00003
Sudbury 1	21.16952	0.00002

Table 87. Mean Tube + Pre-Oxidation Sample Mass and Standard Deviation

Sample	Mean Mass (grams)	Standard Deviation (grams)
Sudbury 22	14.35625	0.00000
Sudbury 20	21.46767	0.00001
Sudbury 16	22.18821	0.00001
Sudbury 12	13.31980	0.00001
Sudbury 7	13.27934	0.00001
Sudbury 1	21.18304	0.00002

Table 88. Mean Tube + Post-Oxidation Sample Mass and Standard Deviation

Sample	Mean Mass (grams)	Standard Deviation (grams)
Sudbury 22	14.29172	0.00002
Sudbury 20	21.39080	0.00002
Sudbury 16	22.12251	0.00001
Sudbury 12	13.20039	0.00002
Sudbury 7	13.24454	0.00002
Sudbury 1	21.17179	0.00000

Table 89. Pre-Oxidation Sample Mass and Absolute Error

Sample	Sample Mass (grams)	Absolute Error (grams)
Sudbury 22	0.20021	0.00000
Sudbury 20	0.13359	0.00001
Sudbury 16	0.08962	0.00003
Sudbury 12	0.27920	0.00001
Sudbury 7	0.14503	0.00003
Sudbury 1	0.01352	0.00002

Table 90. Post-Oxidation Sample Mass and Absolute Error

Sample	Sample Mass (grams)	Absolute Error (grams)
Sudbury 22	0.13568	0.00002
Sudbury 20	0.05672	0.00002
Sudbury 16	0.02392	0.00003
Sudbury 12	0.15979	0.00002
Sudbury 7	0.11023	0.00003
Sudbury 1	0.00227	0.00002

Table 91. Mean SEM Particle Cutout Masses and Standard Deviations

Sample	Mean Soot Mass (grams)	Standard Deviation (grams)	Mean Non-Soot Mass (grams)	Standard Deviation (grams)
Sudbury 22	0.04714	0.00001	6.06967	0.00003
Sudbury 20	0.48536	0.00001	8.96174	0.00015
Sudbury 16	0.74419	0.00002	3.47839	0.00002
Sudbury 12	0.20923	0.00003	3.08282	0.00003
Sudbury 7	0.12134	0.00009	5.54609	0.00003
Sudbury 1	3.89318	0.00005	1.95143	0.00003

Table 92. Soot to Non-Soot Area Ratio, Volumetric Ratio, and Corresponding Absolute Errors

Sample	Area Ratio	Absolute Error	Volumetric Ratio	Absolute Error
Sudbury 22	0.00777	0.00000	0.00068	0.00000
Sudbury 20	0.05416	0.00000	0.01260	0.00000
Sudbury 16	0.21395	0.00001	0.09896	0.00000
Sudbury 12	0.06787	0.00001	0.01768	0.00000
Sudbury 7	0.02188	0.00002	0.00324	0.00000
Sudbury 1	1.99503	0.00004	2.81790	0.00009

Table 93. Soot Mass, Non-Soot Mass, Corrected Soot Mass, and Corresponding Absolute Errors

Sample	Soot Mass (grams)	Absolute Error (grams)	Non-Soot Mass (grams)	Absolute Error (grams)	Corrected Soot Mass (grams)	Absolute Error (grams)
Sudbury 22	0.00009	0.00005	0.13559	0.00005	0.00019	0.00011
Sudbury 20	0.00071	0.00003	0.05601	0.00002	0.00147	0.00016
Sudbury 16	0.00215	0.00003	0.02176	0.00002	0.00449	0.00047
Sudbury 12	0.00278	0.00004	0.15701	0.00003	0.00578	0.00061
Sudbury 7	0.00036	0.00013	0.10987	0.00012	0.00074	0.00027
Sudbury 1	0.00167	0.00002	0.00059	0.00000	0.00349	0.00036

Table 94. Concentration of Soot and Absolute Error

Sample	Soot (ppm)	Absolute Error (ppm)
Sudbury 22	110	60
Sudbury 20	760	90
Sudbury 16	2300	200
Sudbury 12	3000	300
Sudbury 7	380	140
Sudbury 1	2800	300

Appendix 14. Calculated Data for the Gardnos Impact Structure, Norway

Table 95. Mean Empty Tube Mass and Standard Deviation

Sample	Mean Mass (grams)	Standard Deviation (grams)
Gardnos 19	21.76025	0.00002
Gardnos 20	13.99986	0.00001
Gardnos 21	13.72154	0.00000
Gardnos 22	13.12928	0.00001
Gardnos 157	12.98881	0.00002
Gardnos 158	13.15504	0.00002
Gardnos 159	21.31806	0.00001
Gardnos 160a	12.97189	0.00002
Gardnos 160b	11.64306	0.00003
Gardnos 161a	13.31806	0.00003
Gardnos 161b	11.62318	0.00001
Gardnos 162a	22.09142	0.00001
Gardnos 162b	11.63054	0.00001
Gardnos 162c	11.90775	0.00001
Gardnos 129	11.21882	0.00002
Gardnos 126	11.35232	0.00000
Gardnos 120	11.31078	0.00001
Gardnos 121	11.31649	0.00001
Gardnos 143	11.21409	0.00001
Gardnos 176	14.13588	0.00002
Gardnos 172	13.10254	0.00002
Gardnos 179	13.04688	0.00001
Gardnos 178	11.21390	0.00001
Gardnos 133	13.24234	0.00002
Gardnos 137	13.66128	0.00001
Gardnos 175	11.21673	0.00001
Gardnos 137 B	21.46241	0.00001
Gardnos 140	21.82319	0.00000
Gardnos 141	13.11207	0.00002
Gardnos 142	13.68548	0.00001
Gardnos 164	11.14043	0.00001
Gardnos 171	11.31257	0.00001
Gardnos 170	11.26467	0.00002
Gardnos 169	11.26498	0.00002
Gardnos 168	11.88993	0.00003
Gardnos 167	11.71677	0.00001

Table 96. Mean Tube + Pre-Oxidation Sample Mass and Standard Deviation

Sample	Mean Mass (grams)	Standard Deviation (grams)
Gardnos 19	21.76382	0.00002
Gardnos 20	14.00723	0.00001
Gardnos 21	13.73641	0.00002
Gardnos 22	13.18424	0.00001
Gardnos 157	12.99306	0.00001
Gardnos 158	13.16655	0.00002
Gardnos 159	21.32222	0.00002
Gardnos 160a	13.09783	0.00002
Gardnos 160b	11.69110	0.00000
Gardnos 161a	13.38018	0.00002
Gardnos 161b	11.66585	0.00003
Gardnos 162a	22.13721	0.00001
Gardnos 162b	11.67552	0.00002
Gardnos 162c	11.95714	0.00003
Gardnos 129	11.22439	0.00001
Gardnos 126	11.59189	0.00002
Gardnos 120	11.31952	0.00001
Gardnos 121	11.34926	0.00002
Gardnos 143	11.21620	0.00001
Gardnos 176	14.14060	0.00001
Gardnos 172	13.10647	0.00001
Gardnos 179	13.04964	0.00001
Gardnos 178	11.24417	0.00001
Gardnos 133	13.25770	0.00001
Gardnos 137	13.74622	0.00001
Gardnos 175	11.24674	0.00002
Gardnos 137 B	21.47403	0.00003
Gardnos 140	21.82525	0.00002
Gardnos 141	13.11300	0.00001
Gardnos 142	13.69378	0.00001
Gardnos 164	11.34572	0.00000
Gardnos 171	11.51234	0.00001
Gardnos 170	11.31345	0.00002
Gardnos 169	11.33051	0.00002
Gardnos 168	11.71657	0.00002
Gardnos 167	11.89175	0.00000

Table 97. Mean Tube + Post-Oxidation Sample Mass and Standard Deviation

Sample	Mean Mass (grams)	Standard Deviation (grams)
Gardnos 19	21.76356	0.00001
Gardnos 20	14.00449	0.00001
Gardnos 21	13.72774	0.00001
Gardnos 22	13.16049	0.00001
Gardnos 157	12.99034	0.00001
Gardnos 158	13.15731	0.00001
Gardnos 159	21.31885	0.00001
Gardnos 160a	13.02183	0.00002
Gardnos 160b	11.64571	0.00002
Gardnos 161a	13.33243	0.00001
Gardnos 161b	11.62385	0.00002
Gardnos 162a	22.10382	0.00001
Gardnos 162b	11.63426	0.00002
Gardnos 162c	11.91373	0.00002
Gardnos 129	11.21611	0.00001
Gardnos 126	11.40019	0.00001
Gardnos 120	11.31390	0.00002
Gardnos 121	11.31557	0.00000
Gardnos 143	11.21040	0.00002
Gardnos 176	14.13699	0.00002
Gardnos 172	13.10246	0.00001
Gardnos 179	13.04791	0.00002
Gardnos 178	11.27356	0.00001
Gardnos 133	13.24741	0.00001
Gardnos 137	13.69632	0.00002
Gardnos 175	11.21218	0.00001
Gardnos 137 B	21.46633	0.00001
Gardnos 140	21.82360	0.00003
Gardnos 141	13.11266	0.00002
Gardnos 142	13.68865	0.00002
Gardnos 164	11.26884	0.00002
Gardnos 171	11.35351	0.00001
Gardnos 170	11.26724	0.00001
Gardnos 169	11.27002	0.00001
Gardnos 168	11.89170	0.00001
Gardnos 167	11.71641	0.00001

Table 98. Pre-Oxidation Sample Mass and Absolute Error

Sample	Sample Mass (grams)	Absolute Error (grams)
Gardnos 19	0.00357	0.00003
Gardnos 20	0.00736	0.00001
Gardnos 21	0.01487	0.00002
Gardnos 22	0.05497	0.00002
Gardnos 157	0.00425	0.00002
Gardnos 158	0.01151	0.00003
Gardnos 159	0.00415	0.00002
Gardnos 160a	0.12593	0.00003
Gardnos 160b	0.04804	0.00003
Gardnos 161a	0.06212	0.00003
Gardnos 161b	0.04267	0.00003
Gardnos 162a	0.04579	0.00001
Gardnos 162b	0.04498	0.00002
Gardnos 162c	0.04939	0.00003
Gardnos 129	0.00557	0.00002
Gardnos 126	0.23957	0.00002
Gardnos 120	0.00874	0.00001
Gardnos 121	0.03277	0.00002
Gardnos 143	0.00211	0.00001
Gardnos 176	0.00473	0.00002
Gardnos 172	0.00393	0.00002
Gardnos 179	0.00276	0.00001
Gardnos 178	0.03027	0.00001
Gardnos 133	0.01536	0.00002
Gardnos 137	0.08494	0.00002
Gardnos 175	0.03001	0.00002
Gardnos 137 B	0.01162	0.00003
Gardnos 140	0.00206	0.00002
Gardnos 141	0.00093	0.00002
Gardnos 142	0.00831	0.00001
Gardnos 164	0.20529	0.00001
Gardnos 171	0.19977	0.00001
Gardnos 170	0.04877	0.00002
Gardnos 169	0.06554	0.00002
Gardnos 168	0.00182	0.00003
Gardnos 167	-0.00020	0.00002

Table 99. Post-Oxidation Sample Mass, Corrected Post-Oxidation Sample Mass, and Absolute Errors

Sample	Sample Mass (grams)	Absolute Error (grams)	Corrected Sample Mass (grams)	Absolute Error (grams)
Gardnos 19	0.00331	0.00002	--	--
Gardnos 20	0.00463	0.00001	--	--
Gardnos 21	0.00620	0.00002	--	--
Gardnos 22	0.03121	0.00002	--	--
Gardnos 157	0.00154	0.00001	--	--
Gardnos 158	0.00227	0.00002	--	--
Gardnos 159	0.00078	0.00002	--	--
Gardnos 160a	0.04994	0.00003	--	--
Gardnos 160b	0.00265	0.00003	--	--
Gardnos 161a	0.01437	0.00002	--	--
Gardnos 161b	0.00068	0.00002	--	--
Gardnos 162a	0.01240	0.00001	--	--
Gardnos 162b	0.00372	0.00002	--	--
Gardnos 162c	0.00598	0.00002	--	--
Gardnos 129	-0.00271	0.00002	0.00209	0.00048
Gardnos 126	0.04787	0.00001	0.05267	0.00048
Gardnos 120	0.00312	0.00002	0.00792	0.00048
Gardnos 121	-0.00092	0.00001	0.00388	0.00048
Gardnos 143	-0.00369	0.00002	0.00111	0.00048
Gardnos 176	0.00111	0.00003	--	--
Gardnos 172	-0.00008	0.00001	--	--
Gardnos 179	0.00103	0.00002	--	--
Gardnos 178	0.05965	0.00001	0.06445	0.00048
Gardnos 133	0.00507	0.00002	--	--
Gardnos 137	0.03504	0.00002	--	--
Gardnos 175	-0.00455	0.00002	0.00025	0.00048
Gardnos 137 B	0.00392	0.00003	--	--
Gardnos 140	0.00041	0.00003	--	--
Gardnos 141	0.00059	0.00002	--	--
Gardnos 142	0.00317	0.00002	--	--
Gardnos 164	0.12841	0.00002	0.13321	0.00048
Gardnos 171	0.04094	0.00001	0.04574	0.00048
Gardnos 170	0.00257	0.00002	0.00737	0.00048
Gardnos 169	0.00505	0.00002	0.00985	0.00048
Gardnos 168	0.00177	0.00003	--	--
Gardnos 167	-0.00036	0.00002	--	--

Table 100. Further Correction* to Post-Oxidation Sample Mass and Absolute Error

Sample	Corrected Mass (grams)	Absolute Error (grams)
Gardnos 176	0.00223	0.00050

*Correction based on visual estimate of amount of sample lost. See raw data for explanation of sample loss.

Table 101. Percent Non-Carbon by Area*, Percent Carbon by Area*, and Percent Carbon by Volume for Post-Oxidation Residue

Sample	% Non-Carbon (by area)	% Carbon (by area)	% Carbon (by volume)
Gardnos 19	--	--	--
Gardnos 20	--	--	--
Gardnos 21	--	--	--
Gardnos 22	--	--	--
Gardnos 157	--	--	--
Gardnos 158	--	--	--
Gardnos 159	--	--	--
Gardnos 160a	56	44	41.1
Gardnos 160b	--	--	--
Gardnos 161a	--	--	--
Gardnos 161b	--	--	--
Gardnos 162a	--	--	--
Gardnos 162b	--	--	--
Gardnos 162c	--	--	--
Gardnos 129	67	33	25.7
Gardnos 126	28	72	80.5
Gardnos 120	60	40	35.3
Gardnos 121	81	19	10.2
Gardnos 143	70	30	21.9
Gardnos 176	73	27	18.4
Gardnos 172	--	--	--
Gardnos 179	58	42	38.1
Gardnos 178	23	77	86.0
Gardnos 133	44	56	59.0
Gardnos 137	43	57	60.4
Gardnos 175	29	71	79.3
Gardnos 137 B	--	--	--
Gardnos 140	--	--	--
Gardnos 141	--	--	--
Gardnos 142	--	--	--
Gardnos 164	5	95	98.8
Gardnos 171	43	57	60.4
Gardnos 170	24	76	84.9
Gardnos 169	67	33	25.7
Gardnos 168	--	--	--
Gardnos 167	--	--	--

*Based on visual SEM estimates of post-oxidation residue.

Table 102. Percent Carbon by Mass*, Post-Etch Carbon Residue Mass, and Errors

Sample	% Carbon (by mass)	Assigned Error (%)	Post-Etch Carbon Residue Mass (grams)	Absolute Error (grams)
Gardnos 19	0.402	1.000	0.00001	0.00003
Gardnos 20	1.22	1.00	0.00006	0.00005
Gardnos 21	6.59	1.00	0.00041	0.00006
Gardnos 22	95.1	10.0	0.02970	0.00312
Gardnos 157	14.6	10.0	0.00022	0.00015
Gardnos 158	11.8	10.0	0.00027	0.00023
Gardnos 159	0.402	1.000	0.00000	0.00001
Gardnos 160a	21.8	10.0	0.01088	0.00499
Gardnos 160b	0.810	1.000	0.00002	0.00003
Gardnos 161a	6.59	1.00	0.00095	0.00014
Gardnos 161b	1.22	1.00	0.00001	0.00001
Gardnos 162a	0.402	1.000	0.00005	0.00012
Gardnos 162b	0.810	1.000	0.00003	0.00004
Gardnos 162c	0.810	1.000	0.00005	0.00006
Gardnos 129	12.2	10.0	0.00025	0.00022
Gardnos 126	62.3	10.0	0.03279	0.00528
Gardnos 120	17.9	10.0	0.00142	0.00080
Gardnos 121	4.350	10.000	0.00017	0.00039
Gardnos 143	10.09	10.00	0.00011	0.00012
Gardnos 176	8.250	10.000	0.00018	0.00023
Gardnos 172	72.8	10.0	-0.00006	-0.00001
Gardnos 179	19.8	10.0	0.00020	0.00010
Gardnos 178	71.0	10.0	0.04577	0.00645
Gardnos 133	36.5	10.0	0.00185	0.00051
Gardnos 137	37.9	10.0	0.01328	0.00350
Gardnos 175	60.5	10.0	0.00015	0.00029
Gardnos 137 B	95.2	10.0	0.00373	0.00039
Gardnos 140	37.5	10.0	0.00016	0.00004
Gardnos 141	28.6	10.0	0.00017	0.00006
Gardnos 142	88.4	10.0	0.00280	0.00032
Gardnos 164	97.1	1.0	0.12931	0.00141
Gardnos 171	37.9	10.0	0.01734	0.00458
Gardnos 170	69.3	10.0	0.00510	0.00081
Gardnos 169	12.2	10.0	0.00120	0.00099
Gardnos 168	0.402	1.000	0.00001	0.00002
Gardnos 167	0.402	1.000	0.00000	0.00000

Table 103. Mean SEM Particle Cutout Masses and Standard Deviations

Sample	Mean Soot Mass (grams)	Standard Deviation (grams)	Mean Non-Soot Mass (grams)	Standard Deviation (grams)
Gardnos 19	0.04653	0.00003	0.54802	0.00004
Gardnos 22	0.24595	0.00004	0.96265	0.00008
Gardnos 157	0.36579	0.00001	2.78499	0.00005
Gardnos 158	0.04635	0.00004	1.07803	0.00005
Gardnos 159	0.12029	0.00004	1.27705	0.00009
Gardnos 161a	2.72818	0.00004	1.43447	0.00016
Gardnos 161b	0.13600	0.00006	0.99850	0.00007
Gardnos 172	1.18149	0.00008	3.98882	0.00004
Gardnos 137 B	0.20409	0.00004	3.11539	0.00002
Gardnos 141	0.66166	0.00002	3.01458	0.00004

Table 104. Mean SEM Particle Cutout + Beaker Masses and Standard Deviations

Sample	Mean Soot Mass (grams)	Standard Deviation (grams)	Mean Non-Soot Mass (grams)	Standard Deviation (grams)
Gardnos 160a	111.5686	0.0001	102.1764	0.0000
Gardnos 129	111.1014	0.0000	107.6932	0.0001
Gardnos 126	103.8217	0.0001	109.3112	0.0001
Gardnos 143	108.1054	0.0000	106.1040	0.0000
Gardnos 176	110.8030	0.0001	99.1584	0.0001
Gardnos 179	104.9464	0.0001	106.8304	0.0001
Gardnos 178	56.8975	0.0000	102.2617	0.0001
Gardnos 133	98.5460	0.0001	102.3545	0.0001
Gardnos 137	104.6486	0.0001	104.6787	0.0000
Gardnos 175	66.5134	0.0001	114.0353	0.0001
Gardnos 164	104.4524	0.0001	114.0353	0.0001
Gardnos 171	113.0569	0.0000	106.2794	0.0000
Gardnos 170	109.3799	0.0001	104.4545	0.0001
Gardnos 169	109.5517	0.0000	92.7496	0.0001

Table 105. Mean SEM Beaker Masses and Standard Deviations

Sample	Mean Soot Beaker Mass (grams)	Standard Deviation (grams)	Mean Non-Soot Beaker Mass (grams)	Standard Deviation (grams)
Gardnos 160a	109.9028	0.0001	100.5006	0.0001
Gardnos 129	110.8037	0.0000	107.1647	0.0000
Gardnos 126	103.5143	0.0001	105.6295	0.0000
Gardnos 143	107.9389	0.0001	105.1780	0.0001
Gardnos 176	110.7256	0.0001	98.0233	0.0001
Gardnos 179	104.1179	0.0000	104.3309	0.0001
Gardnos 178	56.8585	0.0001	100.2821	0.0001
Gardnos133	98.5181	0.0001	101.5538	0.0001
Gardnos 137	104.3581	0.0001	102.0163	0.0001
Gardnos 175	66.1377	0.0001	102.7842	0.0000
Gardnos 164	104.0177	0.0001	110.8228	0.0001
Gardnos 171	111.7866	0.0000	104.6787	0.0000
Gardnos 170	108.5261	0.0001	103.3972	0.0001
Gardnos 169	108.0473	0.0001	91.5742	0.0000

Table 106. SEM Cutout Masses and Absolute Errors

Sample	Soot Mass (grams)	Absolute Error (grams)	Non-Soot Mass (grams)	Absolute Error (grams)
Gardnos 160a	1.6657	0.0001	1.6758	0.0001
Gardnos 129	0.2977	0.0000	0.5285	0.0001
Gardnos 126	0.3073	0.0001	3.6817	0.0001
Gardnos 143	0.1665	0.0001	0.9260	0.0001
Gardnos 176	0.0774	0.0001	1.1350	0.0001
Gardnos 179	0.8285	0.0001	2.4995	0.0001
Gardnos 178	0.0390	0.0001	1.9796	0.0001
Gardnos 133	0.0279	0.0002	0.8007	0.0002
Gardnos 137	0.2906	0.0001	2.6624	0.0001
Gardnos 175	0.3757	0.0001	11.2511	0.0001
Gardnos 164	0.4348	0.0001	3.2125	0.0001
Gardnos 171	1.2703	0.0000	1.6007	0.0000
Gardnos 170	0.8538	0.0001	1.0573	0.0001
Gardnos 169	1.5044	0.0001	1.1754	0.0001

Table 107. Soot to Non-Soot Area Ratio, Volumetric Ratio, and Corresponding Absolute Errors

Sample	Area Ratio	Absolute Error	Volumetric Ratio	Absolute Error
Gardnos 19	0.08491	0.00005	0.02474	0.00002
Gardnos 22	0.25549	0.00005	0.12914	0.00004
Gardnos 157	0.13134	0.00000	0.04760	0.00000
Gardnos 158	0.04300	0.00004	0.00892	0.00001
Gardnos 159	0.09420	0.00003	0.02891	0.00001
Gardnos 160a	0.9940	0.0001	0.9910	0.0001
Gardnos 161a	1.90187	0.00022	2.62284	0.00045
Gardnos 161b	0.13621	0.00006	0.05027	0.00003
Gardnos 129	0.5633	0.0001	0.4228	0.0001
Gardnos 126	0.0835	0.0000	0.0241	0.0000
Gardnos 143	0.1798	0.0001	0.0762	0.0001
Gardnos 176	0.0682	0.0001	0.0178	0.0000
Gardnos 172	0.29620	0.00002	0.16121	0.00002
Gardnos 179	0.3315	0.0000	0.1908	0.0000
Gardnos 178	0.0197	0.0000	0.0028	0.0000
Gardnos 133	0.0349	0.0002	0.0065	0.0001
Gardnos 137	0.1091	0.0000	0.0361	0.0000
Gardnos 175	0.0334	0.0000	0.0061	0.0000
Gardnos 137 B	0.06551	0.00001	0.01677	0.00001
Gardnos 141	0.21949	0.00001	0.10283	0.00000
Gardnos 164	0.1353	0.0000	0.0498	0.0000
Gardnos 171	0.7936	0.0000	0.7070	0.0000
Gardnos 170	0.8075	0.0002	0.7257	0.0002
Gardnos 169	1.2799	0.0001	1.4479	0.0002

Table 108. Soot Mass, Non-Soot Mass, Corrected Soot Mass, and Corresponding Absolute Errors

Sample	Soot Mass (grams)	Absolute Error (grams)	Non-Soot Mass (grams)	Absolute Error (grams)	Corrected Soot Mass (grams)	Absolute Error (grams)
Gardnos 19	0.00000	0.00005	0.00001	0.00003	0.00000	0.00010
Gardnos 20	0.00001	0.00001	0.00005	0.00005	0.00002	0.00002
Gardnos 21	0.00001	0.00001	0.00040	0.00006	0.00002	0.00002
Gardnos 22	0.00340	0.00417	0.02630	0.00276	0.00708	0.00872
Gardnos 157	0.00001	0.00021	0.00021	0.00015	0.00002	0.00044
Gardnos 158	0.00000	0.00032	0.00026	0.00023	0.00000	0.00067
Gardnos 159	0.00000	0.00001	0.00000	0.00001	0.00000	0.00002
Gardnos 160a	0.0054	0.0056	0.0055	0.0025	0.0113	0.0117
Gardnos 160b	0.00001	0.00001	0.00001	0.00003	0.00002	0.00002
Gardnos 161a	0.00069	0.00015	0.00026	0.00004	0.00143	0.00034
Gardnos 161b	0.00000	0.00001	0.00001	0.00001	0.00000	0.00002
Gardnos 162a	0.00001	0.00001	0.00004	0.00012	0.00002	0.00002
Gardnos 162b	0.00001	0.00001	0.00002	0.00004	0.00002	0.00002
Gardnos 162c	0.00001	0.00001	0.00004	0.00006	0.00002	0.00002
Gardnos 129	0.0001	0.0003	0.0002	0.0002	0.0002	0.0006
Gardnos 126	0.0008	0.0074	0.0320	0.0052	0.0016	0.0154
Gardnos 120	0.00001	0.00001	0.00141	0.00080	0.00002	0.00002
Gardnos 121	0.00001	0.00001	0.00016	0.00039	0.00002	0.00002
Gardnos 143	0.0000	0.0002	0.0001	0.0001	0.0000	0.0072
Gardnos 176	0.0000	0.0003	0.0002	0.0002	0.0000	0.0007
Gardnos 172	-0.00001	0.00002	-0.00005	-0.00001	-0.00002	-0.00004
Gardnos 179	0.0000	0.0001	0.0002	0.0001	0.0001	0.0003
Gardnos 178	0.0001	0.0091	0.0456	0.0064	0.0003	0.0190
Gardnos 133	0.0000	0.0007	0.0018	0.0005	0.0000	0.0015
Gardnos 137	0.0005	0.0049	0.0128	0.0034	0.0010	0.0101
Gardnos 175	0.0000	0.0004	0.0002	0.0003	0.0000	0.0009
Gardnos 137 B	0.00006	0.00055	0.00367	0.00039	0.00013	0.00115
Gardnos 140	0.00001	0.00001	0.00015	0.00004	0.00002	0.00002
Gardnos 141	0.00002	0.00008	0.00015	0.00005	0.00003	0.00017
Gardnos 142	0.00001	0.00001	0.00279	0.00032	0.00002	0.00002
Gardnos 164	0.0061	0.0019	0.1232	0.0013	0.0128	0.0043
Gardnos 171	0.0072	0.0053	0.0102	0.0027	0.0150	0.0112
Gardnos 170	0.0021	0.0009	0.0030	0.0005	0.0045	0.0020
Gardnos 169	0.0007	0.0011	0.0005	0.0004	0.0015	0.0022
Gardnos 168	0.00001	0.00001	0.00000	0.00002	0.00002	0.00002
Gardnos 167	0.00001	0.00001	-0.00001	0.00001	0.00002	0.00002

Table 109. Concentration Soot and Absolute Error

Sample	Soot (ppm)	Absolute Error (ppm)
Gardnos 19	1	79
Gardnos 20	17	17
Gardnos 21	15	15
Gardnos 22	4451	5484
Gardnos 157	16	340
Gardnos 158	4	543
Gardnos 159	0	16
Gardnos 160a	4726	4901
Gardnos 160b	10	10
Gardnos 161a	1133	273
Gardnos 161b	< 1	--
Gardnos 162a	17	17
Gardnos 162b	10	10
Gardnos 162c	10	10
Gardnos 129	67	234
Gardnos 126	637	6084
Gardnos 120	8	9
Gardnos 121	8	9
Gardnos 143	8	3536
Gardnos 176	3	270
Gardnos 172	< 1	--
Gardnos 179	27	113
Gardnos 178	107	7700
Gardnos 133	10	626
Gardnos 137	425	4475
Gardnos 175	1	342
Gardnos 137 B	97	867
Gardnos 140	17	17
Gardnos 141	26	130
Gardnos 142	16	16
Gardnos 164	4982	1667
Gardnos 171	6161	4597
Gardnos 170	1994	893
Gardnos 169	655	988
Gardnos 168	10	10
Gardnos 167	10	10

Sample Calculations:

The following sample calculations pertain to DSDP Core 465-A samples. Data from Core 1 is utilized:

$$\text{Total Initial Sample Mass} = \text{Sample Mass 1} + \text{Sample Mass 2}$$

$$= 3.82138 \text{ grams} + 3.76358 \text{ grams}$$

$$= 7.58496 \text{ grams}$$

$$\begin{aligned} \text{Total Initial Sample Mass Absolute Error} &= \sqrt{(\text{Sample Mass 1 Absolute Error})^2 + (\text{Sample Mass 2 Absolute Error})^2} \\ &= \sqrt{(0.00009 \text{ grams})^2 + (0.00009 \text{ grams})^2} \\ &= 0.00013 \text{ grams} \end{aligned}$$

The following sample calculations pertain to all samples analyzed involving these types of calculations. Data from Gardnos 19 is utilized:

$$\begin{aligned} \text{Mean Empty Tube Mass} &= \frac{\sum \text{Empty Tube Masses}}{\text{Number of Weighings}} \\ &= \frac{21.76025 \text{ grams} + 21.76023 \text{ grams} + 21.76027 \text{ grams}}{3} \\ &= 21.76025 \text{ grams} \end{aligned}$$

Standard Deviation

$$\begin{aligned} \text{of Mean Empty Tube Mass} &= \sqrt{\frac{\sum (\text{Empty Tube Mass} - \text{Mean Empty Tube Mass})^2}{(\text{Number of Weighings} - 1)}} \\ &= \sqrt{\frac{((21.76025 \text{ grams} - 21.76025 \text{ grams})^2 + (21.76023 \text{ grams} - 21.76025 \text{ grams})^2 + (21.76027 \text{ grams} - 21.76025 \text{ grams})^2)}{(3 - 1)}} \\ &= 0.00002 \text{ grams} \end{aligned}$$

$$\begin{aligned}
 \text{Mean Tube + Pre - Oxidation Sample Mass} &= \frac{\sum \text{Tube + Pre - Oxidation Sample Masses}}{\text{Number of Weighings}} \\
 &= \frac{21.76384 \text{ grams} + 21.76382 \text{ grams} + 21.76380 \text{ grams}}{3} \\
 &= 21.76382 \text{ grams}
 \end{aligned}$$

Standard Deviation

$$\begin{aligned}
 \text{of Mean Tube + Pre - Oxidation Sample Mass} &= \sqrt{\frac{\sum \left(\left(\frac{\text{Tube + Pre - Oxidation}}{\text{Sample Mass}} \right) - \left(\frac{\text{Mean Tube + Pre - Oxidation}}{\text{Sample Mass}} \right) \right)^2}{(\text{Number of Weighings} - 1)}} \\
 &= \sqrt{\frac{\left((21.76384 \text{ grams} - 21.76382 \text{ grams})^2 + (21.76382 \text{ grams} - 21.76382 \text{ grams})^2 + (21.76380 \text{ grams} - 21.76382 \text{ grams})^2 \right)}{(3 - 1)}} \\
 &= 0.00002 \text{ grams}
 \end{aligned}$$

$$\begin{aligned}
 \text{Mean Tube + Post - Oxidation Sample Mass} &= \frac{\sum \text{Tube + Post - Oxidation Sample Masses}}{\text{Number of Weighings}} \\
 &= \frac{21.76356 \text{ grams} + 21.76355 \text{ grams} + 21.76356 \text{ grams}}{3} \\
 &= 21.76356 \text{ grams}
 \end{aligned}$$

Standard Deviation

$$\begin{aligned}
 \text{of Mean Tube + Post - Oxidation Sample Mass} &= \sqrt{\frac{\sum \left(\left(\frac{\text{Tube + Post - Oxidation}}{\text{Sample Mass}} \right) - \left(\frac{\text{Mean Tube + Post - Oxidation}}{\text{Sample Mass}} \right) \right)^2}{(\text{Number of Weighings} - 1)}} \\
 &= \sqrt{\frac{\left((21.76356 \text{ grams} - 21.76356 \text{ grams})^2 + (21.76355 \text{ grams} - 21.76356 \text{ grams})^2 + (21.76356 \text{ grams} - 21.76356 \text{ grams})^2 \right)}{(3 - 1)}} \\
 &= 0.00001 \text{ grams}
 \end{aligned}$$

$$\begin{aligned}
\text{Pre - Oxidation Sample Mass} &= (\text{Mean Tube + Pre - Oxidation Sample Mass}) - (\text{Mean Empty Tube Mass}) \\
&= (21.76328 \text{ grams}) - (21.76025 \text{ grams}) \\
&= 0.00357 \text{ grams}
\end{aligned}$$

$$\begin{aligned}
\text{Pre - Oxidation Sample Mass Absolute Error} &= \sqrt{(\text{Mean Tube + Pre - Oxidation Sample Mass Standard Deviation})^2 + (\text{Mean Empty Tube Mass Standard Deviation})^2} \\
&= \sqrt{(0.00002 \text{ grams})^2 + (0.00002 \text{ grams})^2} \\
&= 0.00003 \text{ grams}
\end{aligned}$$

$$\begin{aligned}
\text{Post - Oxidation Sample Mass} &= (\text{Mean Tube + Post - Oxidation Sample Mass}) - (\text{Mean Empty Tube Mass}) \\
&= (21.76356 \text{ grams}) - (21.76025 \text{ grams}) \\
&= 0.00331 \text{ grams}
\end{aligned}$$

$$\begin{aligned}
\text{Post - Oxidation Sample Mass Absolute Error} &= \sqrt{(\text{Mean Tube + Post - Oxidation Sample Mass Standard Deviation})^2 + (\text{Mean Empty Tube Mass Standard Deviation})^2} \\
&= \sqrt{(0.00001 \text{ grams})^2 + (0.00002 \text{ grams})^2} \\
&= 0.00002 \text{ grams}
\end{aligned}$$

The following sample calculations pertain to all samples analyzed involving corrections due to the leaching of the glass tubes during oxidation from the Gardnos and DSDP Core 465-A study. Data from Gardnos 129 is utilized:

$$\begin{aligned}
\text{Corrected Post - Oxidation Sample Mass} &= (\text{Post - Oxidation Sample Mass}) + (0.0048 \text{ grams}) \\
&= (-0.00271 \text{ grams}) + (0.0048 \text{ grams}) \\
&= 0.00209 \text{ grams}
\end{aligned}$$

$$\begin{aligned}
\text{Corrected Post - Oxidation Sample Mass Absolute Error} &= \sqrt{(\text{Post - Oxidation Sample Mass Standard Deviation})^2 + (0.00048 \text{ grams})^2} \\
&= \sqrt{(0.00002 \text{ grams})^2 + (0.00048 \text{ grams})^2} \\
&= 0.00048 \text{ grams}
\end{aligned}$$

The following sample calculations pertain only to Gardnos 176:

$$\begin{aligned}\text{Further Correction to Post - Oxidation Sample Mass} &= (0.5000)(\text{Corrected Post - Oxidation Sample Mass}) \\ &= (0.5000)(0.00111 \text{ grams}) \\ &= 0.00223 \text{ grams}\end{aligned}$$

Further Correction to Post - Oxidation

$$\begin{aligned}\text{Sample Mass Absolute Error} &= \left(\frac{\text{Further Correction to Post - Oxidation Sample Mass}}{\text{Corrected Post - Oxidation Sample Mass}} \right) \sqrt{\left(\frac{\text{Corrected Post - Oxidation Sample Mass Standard Deviation}}{\text{Corrected Post - Oxidation Sample Mass}} \right)^2 + \left(\frac{0.0005}{0.5000} \right)^2} \\ &= (0.00223 \text{ grams}) \sqrt{\left(\frac{0.00003 \text{ grams}}{0.00111 \text{ grams}} \right)^2 + \left(\frac{0.0005}{0.5000} \right)^2} \\ &= 0.00050 \text{ grams}\end{aligned}$$

The following sample calculations pertain only to Gardnos samples corrected for the presence of minerals in post-oxidation residue by SEM visual estimates of carbon and non-carbon fractions. Data from Gardnos 160a is utilized:

$$x = \% \text{ by Area}_{\text{carbon}} = \left(\frac{\text{Area}_{\text{carbon}}}{\text{Total Area}} \right) (100) = \left(\frac{0.050}{0.050 + 0.063} \right) (100) = 44\%$$

$$y = \% \text{ by Area}_{\text{non-carbon}} = \left(\frac{\text{Area}_{\text{non-carbon}}}{\text{Total Area}} \right) (100) = \left(\frac{0.063}{0.050 + 0.063} \right) (100) = 56\%$$

$$\% \text{ by Volume}_{\text{carbon}} = \frac{100}{\left(\frac{y}{x} \right)^{\frac{3}{2}} + 1} = \frac{100}{\left(\frac{56}{44} \right)^{\frac{3}{2}} + 1} = 41.1\%$$

$$\begin{aligned}
 \% \text{ by Mass}_{\text{carbon}} &= \left(\frac{(\% \text{ by Volume}_{\text{carbon}})}{(\% \text{ by Volume}_{\text{carbon}}) + (\% \text{ by Volume}_{\text{non-carbon}})(2.5)} \right) (100) \\
 &= \left(\frac{(41.1\%)}{(41.1\%) + (58.9\%)(2.5)} \right) (100) \\
 &= 21.8\% \text{ Carbon by mass}
 \end{aligned}$$

The following sample calculations pertain only to Gardnos samples corrected for the presence of minerals in post-oxidation residue. Data from Gardnos 19 is utilized:

$$\begin{aligned}
 \text{Post - Oxidation Carbon Residue Mass} &= (\% \text{ by Mass}_{\text{Carbon}})(\text{Corrected Post - Oxidation Sample Mass}) \\
 &= (0.402\%)(0.00331 \text{ grams}) \\
 &= 0.00001 \text{ grams}
 \end{aligned}$$

$$\begin{aligned}
 \text{Post - Oxidation Carbon Residue Mass Absolute Error} &= (\text{Post - Oxidation Carbon Residue Mass}) * \\
 &\quad \sqrt{\left(\frac{\text{Corrected Post - Oxidation Sample Mass Absolute Error}}{\text{Corrected Post - Oxidation Sample Mass}} \right)^2 + \left(\frac{\% \text{ by Mass}_{\text{Carbon}} \text{ Assigned Error}}{\% \text{ by Mass}_{\text{Carbon}}} \right)^2} \\
 &= (0.00001 \text{ grams}) \sqrt{\left(\frac{0.00002 \text{ grams}}{0.00331 \text{ grams}} \right)^2 + \left(\frac{1\%}{0.402\%} \right)^2} \\
 &= 0.00003 \text{ grams}
 \end{aligned}$$

The following sample calculations pertain only to samples for which the SEM particle cutout masses were measured directly. Data from Gardnos 19 is utilized:

$$\begin{aligned}
 \text{Mean SEM Soot Particle Cutout Mass} &= \frac{\sum \text{SEM Soot Particle Cutout Masses}}{\text{Number of Weighings}} \\
 &= \frac{0.04652 \text{ grams} + 0.04651 \text{ grams} + 0.04656 \text{ grams}}{3} \\
 &= 0.04653 \text{ grams}
 \end{aligned}$$

Standard Deviation

$$\begin{aligned} \text{of Mean SEM Soot Particle Cutout Mass} &= \sqrt{\frac{\sum (\text{SEM Soot Particle Cutout Mass} - \text{Mean SEM Soot Particle Cutout Mass})^2}{(\text{Number of Weighings} - 1)}} \\ &= \sqrt{\frac{((0.04652 \text{ grams} - 0.04653 \text{ grams})^2 + (0.04651 \text{ grams} - 0.04653 \text{ grams})^2 + (0.04656 \text{ grams} - 0.04653 \text{ grams})^2)}{(3 - 1)}} \\ &= 0.00003 \text{ grams} \end{aligned}$$

$$\begin{aligned} \text{Mean SEM Non - Soot Particle Cutout Mass} &= \frac{\sum \text{SEM Non - Soot Particle Cutout Masses}}{\text{Number of Weighings}} \\ &= \frac{0.54806 \text{ grams} + 0.54803 \text{ grams} + 0.54798 \text{ grams}}{3} \\ &= 0.54802 \text{ grams} \end{aligned}$$

Standard Deviation of Mean SEM

$$\begin{aligned} \text{Non - Soot Particle Cutout Mass} &= \sqrt{\frac{\sum \left(\left(\frac{\text{SEM Non - Soot Particle Cutout Mass}}{\text{Particle Cutout Mass}} - \left(\frac{\text{Mean SEM Non - Soot Particle Cutout Mass}}{\text{Particle Cutout Mass}} \right) \right)^2}{(\text{Number of Weighings} - 1)}} \\ &= \sqrt{\frac{((0.54806 \text{ grams} - 0.54802 \text{ grams})^2 + (0.54803 \text{ grams} - 0.54802 \text{ grams})^2 + (0.54798 \text{ grams} - 0.54802 \text{ grams})^2)}{(3 - 1)}} \\ &= 0.00004 \text{ grams} \end{aligned}$$

$$\text{Area Ratio} = \frac{\text{Mean SEM Soot Particle Cutout Mass}}{\text{Mean SEM Non - Soot Particle Cutout Mass}} = \left(\frac{0.04653 \text{ grams}}{0.54802 \text{ grams}} \right) = 0.08491$$

Area Ratio Absolute Error = (Area Ratio) *

$$\begin{aligned} &\sqrt{\left(\frac{\text{Mean SEM Soot Particle Cutout Mass Absolute Error}}{\text{Mean SEM Soot Particle Cutout Mass}} \right)^2 + \left(\frac{\text{Mean SEM Non - Soot Particle Cutout Mass Absolute Error}}{\text{Mean SEM Non - Soot Particle Cutout Mass}} \right)^2} \\ &= (0.08491) \sqrt{\left(\frac{0.00003 \text{ grams}}{0.04653 \text{ grams}} \right)^2 + \left(\frac{0.00004 \text{ grams}}{0.54802 \text{ grams}} \right)^2} \\ &= 0.00002 \end{aligned}$$

The following sample calculations pertain only to samples for which the SEM particle cutout masses were determined by the difference between the empty beaker mass and the beaker plus cutout mass. Data from Gardnos 160a is utilized:

$$\begin{aligned}\text{Mean SEM Soot Particle Cutout + Beaker Mass} &= \frac{\sum \text{SEM Soot Particle Cutout + Beaker Masses}}{\text{Number of Weighings}} \\ &= \frac{111.5687 \text{ grams} + 111.5685 \text{ grams} + 111.5685 \text{ grams}}{3} \\ &= 111.5686 \text{ grams}\end{aligned}$$

Standard Deviation of Mean

$$\begin{aligned}\text{SEM Soot Particle Cutout + Beaker Mass} &= \sqrt{\frac{\sum \left(\left(\begin{array}{c} \text{SEM Soot Particle Cutout} \\ + \text{Beaker Mass} \end{array} \right) - \left(\begin{array}{c} \text{Mean SEM Soot Particle} \\ \text{Cutout + Beaker Mass} \end{array} \right) \right)^2}{(\text{Number of Weighings} - 1)}} \\ &= \sqrt{\frac{((111.5687 \text{ grams} - 111.5686 \text{ grams})^2 + (111.5685 \text{ grams} - 111.5686 \text{ grams})^2 + (111.5685 \text{ grams} - 111.5686 \text{ grams})^2)}{(3 - 1)}} \\ &= 0.00001 \text{ grams}\end{aligned}$$

$$\begin{aligned}\text{Mean SEM Non - Soot Particle Cutout + Beaker Mass} &= \frac{\sum \text{SEM Non - Soot Particle Cutout + Beaker Masses}}{\text{Number of Weighings}} \\ &= \frac{102.1764 \text{ grams} + 102.1764 \text{ grams} + 102.1764 \text{ grams}}{3} \\ &= 102.1764 \text{ grams}\end{aligned}$$

Standard Deviation of Mean SEM

$$\begin{aligned} \text{Non - Soot Particle Cutout + Beaker Mass} &= \sqrt{\frac{\sum \left(\left(\text{SEM Non - Soot Particle Cutout + Beaker Mass} \right) - \left(\text{Mean SEM Non - Soot Particle Cutout + Beaker Mass} \right) \right)^2}{(\text{Number of Weighings} - 1)}} \\ &= \sqrt{\frac{((102.1764 \text{ grams} - 102.1764 \text{ grams})^2 + (102.1764 \text{ grams} - 102.1764 \text{ grams})^2 + (102.1764 \text{ grams} - 102.1764 \text{ grams})^2)}{(3 - 1)}} \\ &= 0.0000 \text{ grams} \end{aligned}$$

$$\begin{aligned} \text{Mean SEM Soot Beaker Mass} &= \frac{\sum \text{SEM Soot Beaker Masses}}{\text{Number of Weighings}} \\ &= \frac{109.9028 \text{ grams} + 109.9029 \text{ grams} + 109.9028 \text{ grams}}{3} \\ &= 109.9028 \text{ grams} \end{aligned}$$

Standard Deviation

$$\begin{aligned} \text{of Mean SEM Soot Beaker Mass} &= \sqrt{\frac{\sum (\text{SEM Soot Beaker Mass} - \text{Mean SEM Soot Beaker Mass})^2}{(\text{Number of Weighings} - 1)}} \\ &= \sqrt{\frac{((109.9028 \text{ grams} - 109.9028 \text{ grams})^2 + (109.9029 \text{ grams} - 109.9028 \text{ grams})^2 + (109.9028 \text{ grams} - 109.9028 \text{ grams})^2)}{(3 - 1)}} \\ &= 0.0001 \text{ grams} \end{aligned}$$

$$\begin{aligned} \text{Mean SEM Non - Soot Beaker Mass} &= \frac{\sum \text{SEM Non - Soot Beaker Masses}}{\text{Number of Weighings}} \\ &= \frac{100.5007 \text{ grams} + 100.5006 \text{ grams} + 100.5006 \text{ grams}}{3} \\ &= 100.5006 \text{ grams} \end{aligned}$$

Standard Deviation

$$\text{of Mean SEM Non - Soot Beaker Mass} = \sqrt{\frac{\sum (\text{SEM Non - Soot Beaker Mass} - \text{Mean SEM Non - Soot Beaker Mass})^2}{(\text{Number of Weighings} - 1)}}$$

$$= \sqrt{\frac{((100.5007 \text{ grams} - 100.5006 \text{ grams})^2 + (100.5006 \text{ grams} - 100.5006 \text{ grams})^2 + (100.5006 \text{ grams} - 100.5006 \text{ grams})^2)}{(3-1)}}$$

$$= 0.0001 \text{ grams}$$

$$\text{SEM Soot Particle Cutout Mass} = (\text{Mean SEM Soot Cutout} + \text{Beaker Mass}) - (\text{Mean SEM Soot Beaker Mass})$$

$$= (111.5686 \text{ grams}) - (109.9028 \text{ grams})$$

$$= 1.6657 \text{ grams}$$

$$\text{SEM Soot Particle Cutout Mass Absolute Error} = \sqrt{(\text{Mean SEM Soot Cutout} + \text{Beaker Mass Standard Deviation})^2 + (\text{Mean SEM Soot Beaker Standard Deviation})^2}$$

$$= \sqrt{(0.0001 \text{ grams})^2 + (0.0001 \text{ grams})^2}$$

$$= 0.00001 \text{ grams}$$

$$\text{SEM Non - Soot Particle Cutout Mass} = (\text{Mean SEM Non - Soot Cutout} + \text{Beaker Mass}) - (\text{Mean SEM Non - Soot Beaker Mass})$$

$$= (102.1764 \text{ grams}) - (100.5006 \text{ grams})$$

$$= 1.6758 \text{ grams}$$

$$\text{SEM Non - Soot Particle Cutout Mass Absolute Error} = \sqrt{(\text{Mean SEM Non - Soot Cutout} + \text{Beaker Mass Standard Deviation})^2 + (\text{Mean SEM Non - Soot Beaker Standard Deviation})^2}$$

$$= \sqrt{(0.0000 \text{ grams})^2 + (0.0001 \text{ grams})^2}$$

$$= 0.00001 \text{ grams}$$

$$\text{Area Ratio} = \frac{\text{SEM Soot Particle Cutout Mass}}{\text{SEM Non - Soot Particle Cutout Mass}} = \left(\frac{1.6657 \text{ grams}}{1.6758 \text{ grams}} \right) = 0.9940$$

$$\text{Area Ratio Absolute Error} = (\text{Area Ratio})^*$$

$$\sqrt{\left(\frac{\text{SEM Soot Particle Cutout Mass Absolute Error}}{\text{SEM Soot Particle Cutout Mass}}\right)^2 + \left(\frac{\text{SEM Non - Soot Particle Cutout Mass Absolute Error}}{\text{SEM Non - Soot Particle Cutout Mass}}\right)^2}$$

$$= (0.9940) \sqrt{\left(\frac{0.0001 \text{ grams}}{1.6657 \text{ grams}}\right)^2 + \left(\frac{0.0001 \text{ grams}}{1.6758 \text{ grams}}\right)^2}$$

$$= 0.0001$$

The following sample calculations pertain to all samples analyzed. For those calculations involving the Post-Oxidation Carbon Residue Mass, this value should be replaced with the Post-Oxidation Sample Mass for all non-Gardnos samples. Data from the Gardnos 19 sample is utilized:

$$\text{Volumetric Ratio} = (\text{Area Ratio})^{\frac{3}{2}} = (0.08491)^{\frac{3}{2}} = 0.02474$$

$$\text{Volumetric Ratio Absolute Error} = (\text{Volumetric Ratio}) \left(\frac{3}{2}\right) \left(\frac{\text{Area Ratio Absolute Error}}{\text{Area Ratio}}\right)$$

$$= (0.02474) \left(\frac{3}{2}\right) \left(\frac{0.00005}{0.08491}\right)$$

$$= 0.00002$$

$$\text{Non - Soot Mass} = \left(\frac{\text{Post - Oxidation Carbon Residue Mass}}{1 + \text{Volumetric Ratio}}\right) = \left(\frac{0.00001 \text{ grams}}{1 + 0.02474}\right) = 0.00001 \text{ grams}$$

$$\text{Non - Soot Mass Absolute Error} = (\text{Non - Soot Mass}) \cdot$$

$$\sqrt{\left(\frac{\text{Post - Oxidation Carbon Residue Mass Absolute Error}}{\text{Post - Oxidation Carbon Residue Mass}}\right)^2 + \left(\frac{\text{Volumetric Ratio Absolute Error}}{\text{Volumetric Ratio}}\right)^2}$$

$$= (0.00001 \text{ grams}) \sqrt{\left(\frac{0.00003 \text{ grams}}{0.00001 \text{ grams}}\right)^2 + \left(\frac{0.00002}{0.02474}\right)^2}$$

$$= 0.00003 \text{ grams}$$

$$\text{Soot Mass} = (\text{Post - Oxidation Carbon Residue Mass}) - (\text{Non - Soot Mass})$$

$$= (0.00001 \text{ grams}) - (0.00001 \text{ grams}) = 0.00000 \text{ grams}$$

$$\text{Soot Mass Absolute Error} = \sqrt{(\text{Non - Soot Mass Absolute Error})^2 + (\text{Post - Oxidation Carbon Residue Mass Absolute Error})^2}$$

$$= \sqrt{(0.00003 \text{ grams})^2 + (0.00003 \text{ grams})^2}$$

$$= 0.00005 \text{ grams}$$

$$\text{Corrected Soot Mass} = \frac{\text{Soot Mass}}{0.48} = \frac{0.00000 \text{ grams}}{0.48} = 0.00000067 \text{ grams}$$

Note: This value was rounded off to the fifth decimal place in the calculated data table. It is shown here to significant figures. This value is below the minimum value measurable with the presented experimental techniques and is therefore not presented to significant figures in the data tables for this reason.

$$\text{Corrected Soot Mass Absolute Error} = (\text{Corrected Soot Mass}) \cdot$$

$$\sqrt{\left(\frac{\text{Soot Mass Absolute Error}}{\text{Soot Mass}}\right)^2 + \left(\frac{0.05}{0.48}\right)^2}$$

$$= (0.00000067 \text{ grams}) \cdot \sqrt{\left(\frac{0.00005 \text{ grams}}{0.00000 \text{ grams}}\right)^2 + \left(\frac{0.05}{0.48}\right)^2}$$

$$= 0.00010 \text{ grams}$$

$$\begin{aligned}
 \text{Concentration Soot} &= \left(\frac{\text{Corrected Soot Mass}}{\text{Initial Sample Mass}} \right) (10^6) \\
 &= \left(\frac{0.00000067 \text{ grams}}{1.22335 \text{ grams}} \right) (10^6) \\
 &= 0.55 \text{ parts per million (ppm)}
 \end{aligned}$$

$$\begin{aligned}
 \text{Concentration Soot Absolute Error} &= (\text{Concentration Soot}) \sqrt{\left(\frac{\text{Corrected Soot Mass Absolute Error}}{\text{Corrected Soot Mass}} \right)^2 + \left(\frac{\text{Initial Sample Mass Absolute Error}}{\text{Initial Sample Mass}} \right)^2} \\
 &= (0.55 \text{ ppm}) \sqrt{\left(\frac{0.00010 \text{ grams}}{0.00000067 \text{ grams}} \right)^2 + \left(\frac{0.00009 \text{ grams}}{1.22335 \text{ grams}} \right)^2} \\
 &= 78.68 \text{ ppm}
 \end{aligned}$$

Acknowledgements:

This research has been supported in part by an Illinois Wesleyan University ASD Grant, the American Chemical Society Petroleum Research Fund Grant, and the 1999 Eugene M. Shoemaker Impact Cratering Award.

I wish to gratefully acknowledge Dr. Wolbach for her guidance, assistance, and support throughout the progress of this study and the preparation of this thesis. In addition, I thank her for the opportunity to participate in her research group and for the experience I have gained through this research. I also thank her for allowing me to continue this research after her move to DePaul University.

I also wish to gratefully acknowledge Dr. Rebecca Roesner for her assistance throughout the preparation of this thesis. In addition, I thank her for her support as an advisor during the final stages of these projects after Dr. Wolbach's move to DePaul University.

I wish to thank Sarah Moecker, Benjamin Nelson, and Kathryn Eissfeldt for their support as fellow members of Dr. Wolbach's research group and for their collaboration and work on these projects. I also thank Dr. Will Jaeckle for his assistance in the SEM analysis of these samples.

I wish to thank Dr. Ted Bunch, Dr. Frank Kyte, and Dr. Bevan French for the collection of the Western Interior and Sudbury samples, DSDP Core samples, and Gardnos samples, respectively. In addition, I would like to thank these geologists for their collaboration and support of these projects. I also thank The Field Museum of Natural History, Chicago, for the supply of the carbonaceous shale samples.

I wish to thank the Illinois Wesleyan University Chemistry Department for allowing me to continue this research after Dr. Wolbach's move to DePaul University. In addition, I thank Cindy Honegger of the Illinois Wesleyan University Chemistry Department Stockroom for her assistance with the supplies for these projects. I also thank her for the support and training offered in maintenance and supply of laboratory supplies and equipment after Dr. Wolbach's move to DePaul University.

I wish to thank my honors committee members: Dr. Wendy Wolbach, Dr. Rebecca Roesner, Dr. Ram Mohan, and Dr. Brian Hatcher.

Lastly, I wish to thank Steven Ward and my parents, Paul and Sue Widicus, for their support during this thesis project.

References:

1. Alvarez L. W., Alvarez W., Asaro, F., and Michel, H. V. (1980) *Science* **208**, 1095-1107.
2. Hildebrand, A. R., Penfield, G. T., and Kring, D. A. (1991) *Geology* **19**, 867-71.
3. Wolbach W. S., Lewis R. S., and Anders E. (1985) *Science* **230**, 167-170.
4. Wolbach W. S., Gilmour I., Anders E., Orth C. J., and Brooks R. R. (1988) *Nature* **334**, 665-669.
5. Wolbach W. S., Gilmour I., and Anders E. (1990) In: Global Catastrophes in Earth History (eds. V. L. Sharpton and P. Ward). Geological Society America Special Paper 247, 391-400.
6. Wolbach, W. S., Widicus, S., Moecker, S., and Kyte, F. T., In: Lunar and Planetary Science XXIX, Abstract #1309.
7. Kyte, F.T., Bostwick, J. A., and Zhou L., In: The Cretaceous-Tertiary Event and Other Catastrophes in Earth History (eds. G. Ryder, D. Fatovsky, and S. Gartner) Geological Society America Special Paper 307, 389-401.
8. Wolbach W. S., Widicus, S., Moecker, S., Nelson, B., and Bunch, T. E. (1997-1999) unpublished data.
9. Bunch, T. E., Becker, L., Des Marais, D., Schultz, P. H. Wolbach, W. S., Widicus, S., Glavin, D. P., Brinton, K. L., and Bada, J. L. In press, Geological Society America Special Paper.
10. Wolbach, W. S., Widicus, S., and French, B. M., In: *Lunar and Planetary Science* XXX, Abstract #1043.
11. French B. M., Koeberl C., Gilmour I., Shirey S. B., Dons J. A., and Naterstad J. (1997) *Geochim. Cosmochim. Acta* **61**, 873-904.
12. Wolbach W. S. and Anders E. (1989) *Geochim. Cosmochim. Acta* **53**, 1637-1647.
13. Wolbach W. S. and Moecker S. (1996) Unpublished Data.
14. Wolbach W. S. and Widicus S. (1997) Unpublished Data.

15. Wolbach W. S., Widicus S., Nelson B., and Eissfeldt K. (1998-2000) Unpublished Data.
16. Becker L., Bada J. L., Winans R. E., Hunt J. E., Bunch T. E., and French B. M. (1994) *Science* **265**, 642-644.
17. Kroto H. (1988) *Science* **242**, 1139-1145.